Abstracts

International Conference on Cohesive Sediment Transport Processes

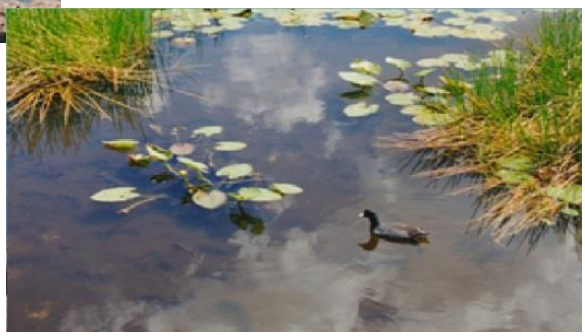

INTERCOH 2013

October 21 – 24, 2013

Hilton Conference Center

Gainesville, Florida

Directional effects on wave predictions over muddy bottoms: Central chenier plain coast, western Louisiana shelf, USA

Ying-Po Liao[1], Ilgar Safak[2], James Kaihatu[1], and Alex Sheremet[3]

[1]Zachry Department of Civil Engineering, Texas A&M University, 3136 TAMU, College Station, TX, 77843-3136. Email: lrobin@neo.tamu.edu (Liao – corresponding author); jkaihatu@tamu.edu (Kaihatu)
[2]United States Geological Survey, Woods Hole Science Center, 384 Woods Hole Rd, Quissett Campus, Woods Hole, MA 02543-1598. Email: isafak@usgs.gov
[3]Department of Civil and Coastal Engineering, University of Florida, P.O. Box 116580, Gainesville, FL, 32611-6580. Email: alex@coastal.ufl.edu

It is known that the presence of mud on the bottom of the coastal ocean has very strong damping effects on both linear wave propagation characteristics (shoaling etc.) and nonlinear wave dynamics (inter-frequency energy exchange within a spectrum). There are several wave models which contain both nonlinear wave-wave interaction effects and mud damping. Validation of these models with data, however, has generally been limited to laboratory measurements. Recently, verification of a one-dimensional wave model with field data from the central chenier plain coast, western Louisiana shelf, USA (Safak et al. 2013 Ocean Modelling) showed that this model was able to replicate the evolution of wave spectra over muddy bottoms given estimates (via inversion) of the appropriate mud parameters. However, the directionality of the wave field was not accounted for in either the data analysis or the modeling effort in that study.

In this study, we investigate the effect of wave directionality by using a phase-resolved parabolic nonlinear wave model which accounts for mud damping and the western Louisiana Shelf data used in the prior study; extraction of both free surface elevations and directional estimates are possible. Wave directions from both the PUV measurements, and a phase-averaged wave model (SWAN) run over the Louisiana Shelf, will be incorporated into the model, and the results compared to nearshore measurements of waves over the muddy bottom. In addition to comparisons of wave energy, free surface elevations from the model will be inspected to determine the effect of the viscous mud on wave shape statistics.

Mechanics of water waves over a muddy seabed

Chiang C. Mei

Department of Civil & Environmental Engineering, Massachusetts Institute of Technology

Fluid mud is a mixture of water and highly cohesive clay particles often transported from inland rivers into the estuary and then deposited along the coast. Its motion changes the seabed, affects the wave climate and shapes the coastline in the long run. The mechanics of wave-mud interaction has military applications in littoral warfare and mine burial. The crudest theoretical analyses have been based on a two-layered model in which water and mud are assumed to be Newtonian fluids with vastly different viscosities.

Owing to the importance of fluid mud in river hydraulics, abundant data exist for *steady flow* conditions under which mud rheology is essentially Bingham plastic. Earlier theories of transient waves are also based on the assumption that fluid mud is either Newtonian (Dalrymple & Liu 1978) or Bingham plastic (Liu & Mei 1989). Existing experimental data for mud in *periodic or transient* motion have however shown that the stress-strain relation for simple harmonic motion to be distinctly viscoelastic.

In this talk, we shall describe the effects of mud on waves. Based on the measured rheology of fluid mud from two field sites, we study the interaction of water waves and fluid mud by a two-layered model in which the water above is assumed to be inviscid and the mud below is viscoelastic. As the fluid-mud layer in shallow seas is usually much thinner than the water layer above, the sharp contrast of scales enables an approximate analytical theory for the interaction between fluid mud and small- amplitude waves with a narrow frequency band. In the first part of the talk, emphasis is on waves of intermediate length in water of finite and constant depth. It is shown that at the leading order and within a short distance of a few wavelengths, wave pressure from above forces mud motion below. Over a much longer distance, waves are modified by the accumulative dissipation in mud. At the next order, infragravity waves owing to convective inertia (or radiation stresses) are affected indirectly by mud motion through the slow modulation of the short waves.

In the second half of the talk we analyze theoretically the interaction between long waves and a thin layer of fluid-mud near a sloping beach. Weakly nonlinear and dispersive effects in water are considered. The fluid-mud is modeled as a thin layer of viscoelastic continuum. The effects of attenuation on harmonic evolution of surface waves are compared for two muds with distinct rheological properties. In general mud dissipation is found to damp out surface waves before they reach the shore, as is known in past observations. Similar to the Eulerian current in an oscillatory boundary layer in a Newtonian fluid, a mean displacement in mud is predicted which may lead to local rise of the sea bottom.

Impact of human interventions on estuarine dynamics

Johan C. Winterwerp[1,2,*)] and Zheng Bing Wang[1,2,3)]

[1)]Delft University of Technology, Faculty of Civil Engineering and Geosciences, The Netherlands
[2)]Deltares, The Netherlands
[3)]East China Normal Institute, SKLEC, Shanghai, China
[*)]corresponding author: j.c.winterwerp@tudelft.nl

Many estuarine rivers in Europe, such as the Ems, the Loire, the Elbe, the Ouse, the Seine, the Weser, and the Scheldt River, have been engineered for more than hundred years. In many cases, these interventions have led to unfavorable amplification of the tide, lowering of low waters, excessive salinity intrusion, and sometimes hyper-turbid conditions characterized by an impoverished ecosystem. In this presentation, historical tidal data (sometimes back to 1900) are analyzed.

Assessing effect-cause relations, we developed a simple linear model, solving the one- dimensional shallow water equations, accounting for the effects of intertidal areas, reduced hydraulic friction and reflections against weirs. This model contains a number of non- dimensional parameters, allowing intercomparison of rivers, and was used to show how canalization (loss of intertidal area) and deepening of four rivers, e.g. Elbe, Ems, Loire and Scheldt may lead to a positive feed-back between tidal characteristics and sediment dynamics, autonomously leading to hyper-turbid conditions. The measured amplification of the tide over years in the Ems estuary is shown as an example in Fig. 1. Fig. 2 shows the dramatic decrease in effective hydraulic drag as a result of enhanced up-estuary tidal pumping of mud, as established from the data, using the linear model.

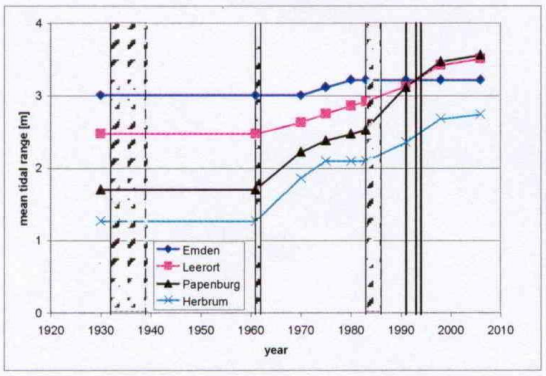

Fig. 1: Measured increase in tidal range along Ems River; vertical bars represents periods of river deepening.

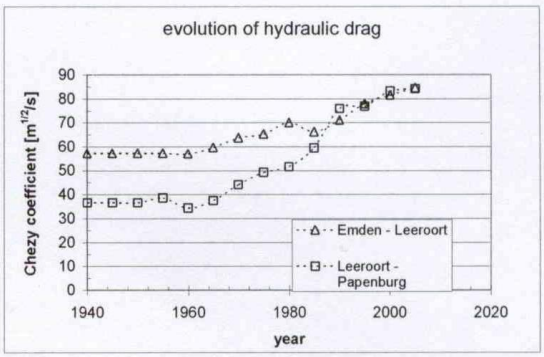

Fig. 2: Computed increase in effective Chézy coefficient induced by large suspended sediment concentrations, as a result of enhanced tidal asymmetry.

In our paper, we present the results for all four rivers. Our general conclusion is that the resilience of many European rivers has decreased dramatically around the end of the 19th and beginning of the 20th century by rectifications, embankments and reclamations. As a result, ongoing deepening to accommodate ever larger ships induced a highly unfavorable response in hydro-sedimentary conditions within these rivers; unfavorable from a water quality and ecological point of view; also maintenance dredging volumes increased to problematic levels. We conclude that the Ems and Loire Rivers have passed a critical point (tipping), and we present an explanation on the physical processes that led to the current hyper-concentrated conditions. The data are not conclusive on whether or not the Elbe and Scheldt are near or beyond such a critical point, but there are certainly risks, as the evolution of the tide is very similar to those during the earlier developments in Ems and Loire.

Vertical sediment dispersion due to Langmuir circulation in a shallow sub-tropical estuary during a tropical s torm

David C. Fugate

Associate Professor of Marine Science, Department of Marine and Ecological Sciences, Florida Gulf Coast University, 10501 FGCU Blvd. South, Fort Myers, FL 33965

Langmuir circulations (LCs), and their cell structure and development have been studied extensively in deep water and coastal environments, but few studies have investigated their dynamics in very shallow estuaries. Furthermore, although LCs were demonstrated to have a significant impact on sediment dynamics by Gargett et al. (2004), few studies have pursued more detailed quantification of their interaction with sediment dynamics. Tropical Storm Isaac passed over the Caloosahatchee River, a shallow subtropical estuary in southwest Florida, USA, in August of 2012. Results from acoustic and optical instruments placed in the river at that time show that vertical dispersion of suspended sediment from LCs were often of the same order of magnitude as vertical sediment flux from turbulent eddies and asymmetrical wave orbits combined. The flux is quantified as a dispersion mixing coefficient that can be implemented in numerical models of sediment transport.

Fine sediment siltation in deep navigation channel

Qing He, Chao Guo, Lei Zhu, Jie Zhao, Dai Zhang

State Key Lab of Estuarine and Coastal Research, East China Normal University, Shanghai 200062, P. R. China,
qinghe@sklec.ecnu.edu.cn

The Yangtze Estuary is one of the largest and most turbid estuaries in the world. As a natural estuary evolvement, sediment transport processes is already a complex and still poorly understood for researchers. It is even more complicated when we have to consider the human impact such as the sharp decrease of sediment supply after Three Georges Dam (TGD) project upstream and the incredible increase of fine sediment siltation after the Deep Navigation Channel (DNC) project in the North Passage of the estuary (Fig.1). Figure 2 shows the amount of dredging required to maintain the DNC. As a result, maintenance dredging increased from less than 20 million m^3 yr^{-1} before 2004 to about 100 million m^3 yr^{-1} at present (Fig.2). The main objective of this study is to investigate physical mechanisms of fine sediment siltation in the DNC and to analyze the source of siltation sediment based on field data.

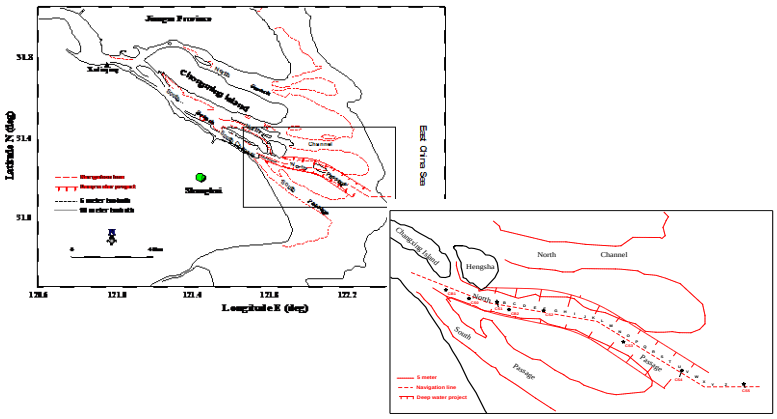

Figure 1 Sketch map of Yangtze Estuary and Deep Navigation Channel project.

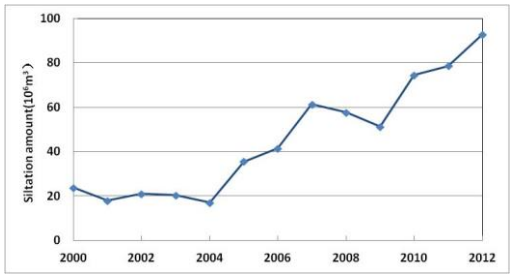

Figure 2 Annual dredging amount in Deep Navigation Channel.

A practical model for drag modulation by suspended sediment with application to the Scheldt estuary

Erik A. Toorman & Qilong Bi

Hydraulics Laboratory, Dept. of Civil Engineering, KU Leuven, Belgium
erik.toorman@bwk.kuleuven.be – qilong.bi@bwk.kuleuven.be

High suspended sediment concentrations near the bottom are inevitable due to the laminar and transitional boundary layer. Usually this layer is very thin, but when sufficient energy is available in the flow and high suspended loads are present, an accumulation of sediment in this inner layer generates special conditions where the flow energy is consumed by additional processes that are negligible in dilute conditions (volumetric concentrations < 0.1%).

For non-cohesive sediments one obtains sheet flow conditions where additional suspension mechanics are provided by turbulence generated in the wake of particles and interparticle collisions. This explains the apparent increase in bottom friction, since additional energy is consumed by these processes.

Generalized Mixing-length theory

This can be modeled in a simple way using the new Generalized Mixing-length (GML) theory (Toorman, 2011). It is based on the vertical stress balance where three stresses are distinguished: the viscous stress, the Reynolds stress (from shear turbulence) and the subgrid scale turbulence stress at the bottom due to roughness and in the water column due to vortex separation in the wake of particles due to inertia induced relative motion. In this stress balance equation, the eddy viscosity (in the Reynolds stress term) is approximated by the parabolic profile for steady open-channel flow, multiplied with a semi-empirical low-Reynolds damping function.

Experimental flume data can very well be modeled by this theory and shows that the extra dissipation stress corresponding to relative motion and particle drift is proportional to the SPM concentration. It may then seem surprising that for cohesive sediments the opposite is observed: high SPM concentrations lead to drag reduction. In order to explain this, one faces the problem that no suitable dataset is available to test the proposed theory and therefore remains hypothetical. The physical explanation for drag reduction by cohesive sediment is as follows.

The GML theory shows that the (vertical) velocity gradient at the bed decreases with increasing concentration. It has to be remembered now that cohesive particles are flocs, such that one should not focus on mass concentrations, but effective volume concentrations. Due to the decrease in shear rate, it is expected that the floc size distribution over the vertical will vary.

Since the floc density is low, the particle inertia will be small and therefore the generation of particle wake turbulence insignificant. At the other hand, the bulk suspension viscosity can be expected to be high due to the large effective volume occupied by the particles. The much smaller free space between cohesive particles moreover will hinder the development of turbulent coherent structures. Subsequently one obtains low velocity gradients, low shear turbulence production and high viscous stresses. This can be illustrated with the GML model, combined with a simple flocculation model assuming equilibrium. One obtains a non-linear set of coupled equations which can be solved iteratively.

Application to the Scheldt estuary

Drag modulation, based on the GML theory, can be implemented even in a 2DH model by computing the drag coefficient from the depth-averaged velocity, obtained by integration of the velocity gradient in the GML theory. In order to keep the bottom friction model running under all conditions, not only the quadratic turbulent drag law, but also the linear laminar drag is considered and added using a damping

function from low-Reynolds modeling theory to be applied to the turbulent stress (Toorman & Bi, 2012). This has the important additional benefit that no inundation threshold is required any more for intertidal areas.

The new friction model has been implemented in the KU Leuven Télémac Scheldt model. Various simulations show that the sediment fluxes in particular are very much influenced by drag modulation. Compared to a constant Chézy roughness model, much lower sediment fluxes are obtained under the same hydrodynamic conditions.

Acknowledgments
This research has been partially funded by the EU FP7 projects Field_AC and THESEUS.

Reference

Toorman, E.A. (2011). Low-Reynolds modelling of high-concentrated near-bottom suspended sediment transport. IAHR Symposium on *Two-phase Modelling for Sediment Dynamics in Geophysical Flows* (THESIS-2011, Paris, April 26-28, 2011), Abstract, 4 pp.

Bed exchange paradigms in cohesive sediment transport

Joseph Vincent Letter, Jr.

U.S. Army Engineer Engineering Research and Development Center, Vicksburg, MS 39180

A critical issue in cohesive sediment transport is whether the decades old paradigm of exclusive erosion or deposition in estuarine flows has legitimacy in physics. The exclusive paradigm assumes that sediment exchange at the bed-water interface is either erosion, deposition or neither, but never both. In contrast, more recent simultaneous exchange paradigm admits the possibility of erosion and deposition occurring at the same time. The exclusive paradigm is the result of attempts to understand cohesive sediment transport based on inferred data in laboratory flumes averaged over time and space. The time-scale of averaging is longer than the time-scale of turbulence and the spatial dimension is scaled by water depth in the flume. Bed sediment exchange has been deduced from the increase or reduction in suspended sediment concentration, rather than from difficult to record observations of particle movement very close to the bed surface. The net result of averaging is positive, negative or zero sediment flux at the bed surface, but not both positive and negative.

With the inclusion of details in mathematical models such as particle size distributions and flocculation sub-models, the bed exchange algorithms have required revision. Modelers have found the need to use the simultaneous approach to replicate observed sedimentation rates in the field environment. The numerical sediment transport tool developed for this study has been shown to be capable of simulating bed exchange processes including flocculation, probabilistic effects in bed exchange and flocculation, hindered settling, depositional or erosional equilibrium concentrations at a fixed shear stress, and floc spectra from field experimentation. Observations from application of the numerical tool are as follows:

- The effects of a probabilistic treatment of the key variables are more pronounced for erosion than for deposition. These variables include current velocity, bottom shear stress, floc shear strength, critical shear stresses for erosion and deposition, internal shear and settling velocity.
- Probabilistic effects are amplified through the flocculation model over effects through bed exchange alone.
- At a given shear stress the flocculation model tends toward an equilibrium distribution of particle sizes.
- The floc distribution spectrum is broader than occurs with use of mean-valued variables.
- Deposition or erosion are initiated sooner and transition from one to the other more gradual in response to changing shear stress in probabilistic treatment compared to mean-valued treatment. The differential timing is a function of the standard deviations of the probabilistic variables and the rate of change of shear stress.
- Use of the exclusive paradigm with a floc size distribution can perform as well as a simultaneous treatment with a single particle size.
- A simulation was performed of a flume test designed to evaluate the exclusive versus simultaneous paradigm by diluting the concentration of a flume suspension that had achieved an equilibrium concentration from bed erosion. If the exclusive paradigm was valid, the concentration at the end of dilution would have remained constant. If the concentration began to rise after dilution was ceased, then the simultaneous paradigm would be an explanation. The flume concentration did rise after the dilution stopped, but at a very low rate of erosion. The numerical model was able to replicate the flume behavior with the correct rate of rise after the end of dilution by using the exclusive paradigm with a probabilistic treatment of the variables.
- The appropriate use of either the exclusive or continuous paradigm appears to be dictated by the level of temporal and spatial averaging used in the development of empirical data and in the formulation of the variables in the analysis. Empirical coefficients for mean- valued analysis may require adjustment when used in a probabilistic treatment.

Sediment transport under wave-current interaction during storm in Yangtze Estuary

Jianbo Ren [1], Qing He [1*], Keqi Zhang [2, 3], Jiyu Chen [1]

[1] State Key Laboratory of Estuarine and Coastal Research, East China Normal University, Shanghai, P.R.China.
qinghe@sklec.ecnu.edu.cn
[2] Department of Earth and Environment, Florida International University, USA
[3] International Hurricane Research Center, Florida International University, USA

Introduction

Many studies have been conducted to investigate the sediment transport under wave-current interaction, most of their observations occur in normal weather conditions, However, data collected during extreme conditions like storm events is comparatively rate, and it is very important of sediment transport during extreme weather conditions. The present study observed wave-current dynamics and sediment transport data during storm Sanba, the strongest tropical cyclone worldwide in 2012, by deployed several instruments near the bed boundary in Hengsha shoal in Yangtze Estuary, sediment transport under wave-current interaction during extreme condition then has been discussed.

Methodology and Weather Conditions

In order to observe near-bed sediment transport under combined wave and current conditions in shallow water areas in tidal flat, an observation system was deployed in Hengsha shoal in September 2012, the in-situ water depth is about 6 m with a mean tidal range of 2.68 m. Two instruments were equipped on the system at heights of 0.7 and 0.5 m above the sea bed, respectively, with an up-looking RDI Acoustic Doppler Current Profilers for measuring current and wave with a frequency of 1.2 MHz and an Optical Backscattering Sensor (OBS-3A) for turbidity, meanwhile in-situ water SSC samples were obtained for calibrating OBS-3A. Also, time series of water level near the observation station has been collected.

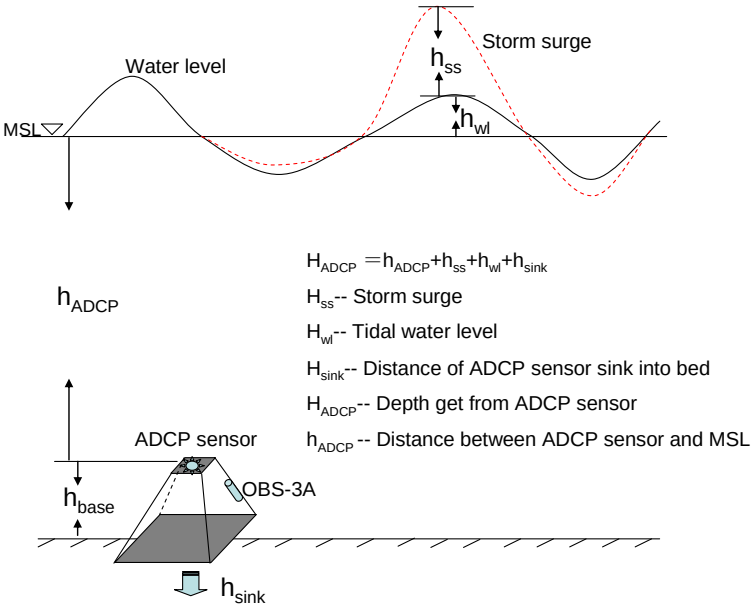

Fig. 1. Layout of observation system and relationship between water depth, storm surge and the distance from ADCP sensor to water level.

During the observation period, a storm named Sanba passed through the study area, Sanba formed as a tropical depression east of The Philippines, and soon developed into a typhoon on September 12, later that day, it reached peak intensity with maximum sustained winds of 57 m/s and a barometric pressure of 900 hPa. Finally the storm caused huge effect to Yangtze Estuary; meanwhile the observation system has sunk for over 2 meters due to frequently near-bed sediments activities, so there came the question that what caused the submergence of the whole system on earth and how?

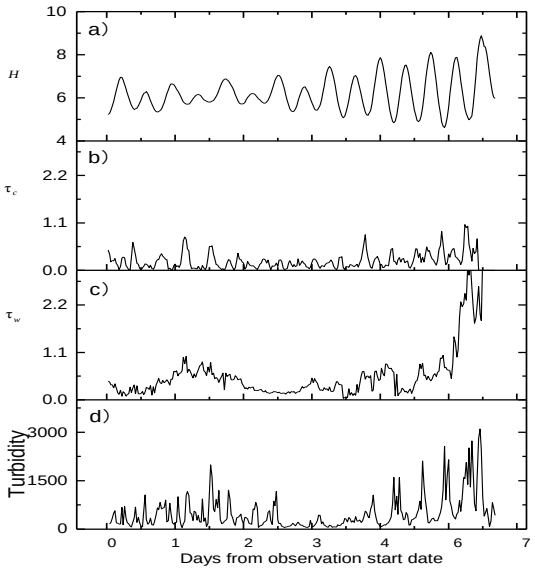

Fig 2. Times series of data observed during Sep.2012 in Yangtze Estuary:(a) Water depth from ADCP sensor to water level(m), (b)Current shear stress(N/m2), (c) Wave shear stress (N/m2), (d) turbidity (NTU)

Results and Conclusions

Generally, the bed shear stress closely associated with sediment transport can be divided into two parts: current-induced and wave-induced stress, the former can be calculated from the quadratic drag law: $\tau_c = \rho u_*^2$ where ρ is water density, u_* is critical shear velocity. Wave-induced shear stress can be calculated as follows: $\tau_w = {}^1\!/_2\, \rho f_w u_w^2$ where f_w is wave friction factor, u_w is the near-bed wave orbit velocity. Normally, simply comparisons between the sum of τ_c τ_w and sediment dynamics thresholds stress $\left(\tau_{sus}^* \tau_{sil}^*\right)$ will be done to determine whether the sediment will suspense or siltation.

However, many studies have been shown that wave-current motion cannot be calculated separately and then superpose; the nonlinear interaction will enhance the total shear stress by times. But until now there is not a valid formula to computer the combined stress, thus additionally, a numeric model has been setup for predicting the total combined shear stress under wave-current interaction.

This paper focuses on the interactions of near-bed flow field, sediment transport as well as wave current. It is concluded that wave performs as the main factor causing sediment transport under storm.

References

[1] Michael Z.Li., Carl L.Amos, David E.Heffler, 1997, Boundary layer dynamics and sediment transport under storm and non-storm conditions on the Scotian Shelf, Marine Geology, 157－181.

[2] William D.Grant, Albert J.Williams, 1983, Bottom Stress Estimates and their Prediction on the Northern California Continental Shelf during CODE-1:The Importance of Wave-Current Interaction, Volume 14.

[3] Ivan Caceres, Jose M.Alsina, 2012, A detailed event-by-event analysis of suspended sediment concentration in the swash zone, Continental Shelf Research, 61－76.

[4] L. Xie, L. J. Pietrafesa, and K. Wu, 2003, A numerical study of wave-current interaction through surface and bottom stresses: Coastal ocean response to Hurricane F ran of 1996, Journal of Geophysical Research, VOL. 108, NO. C2, 3049.

[5] William D.Grant, 1979, Combined Wave and Current Interaction With a Rough bottom, Journal of Geophysical Research, VOL. 84, NO. C4.

Liquefaction of cohesive sediments by waves, laboratory experiments

Francisco Pedocchi, Rodrigo Mosquera, and Valentina Groposo

Instituto de Mecánica de los Fluidos e Ingeniería Ambiental, Facultad de Ingeniería,, Universidad de la República, Montevideo, Uruguay; *rmosquer@fing.edu.uy, vgroposo@fing.edu.uy, kiko@fing.edu.uy*

1. Introduction

During liquefaction the effective stresses among the sediment grains vanish due to the build-up of pore water pressure. In this state, the soil behaves as a fluid and reduces its bearing capacity resulting on serious problems on supported structures, it also becomes available to be transported by currents affecting navigation and increasing the need for maintenance dredging. Previous works on bed liquefaction induced by waves, both in the laboratory and in the field, include the ones by de Wit (1992), Sumer and Fredsøe (2002), and Winterwerp et al. (2006) among many others.

In this abstract we describe preliminary results from a project we have recently carried out to study the behavior of a cohesive sediment bed under regular surface water waves. For this project an existing flume was modified adding a false bottom. The measurements of the bed state were performed using an ultrasonic velocity profiler (UVP Duo by Met-Flow, Switzerland) and several pressure sensors. The pressure sensors were placed inside the bed and the UVP was placed in the water column pointing to the bed. The UVP signal could penetrate into the mud bed allowing us to look at the kinematics of the first three centimeters of mud bed.

2. Experimental set up

A false bottom was installed in an existing wave flume (14 m long, 0.5 m wide) leaving a 0.15 m deep and 1.8 m long depression in the middle of the flume. This depression was filed with a mixture of fresh water and kaolinite. Before each experiment the sediment was dispersed in the water column and then it was let to settle between 4 and 10 days. All the experiments presented here were performed with a water depth of 17.6 cm and with regular waves of 11 cm height and 1.48 s period. The density of the top centimeters of the mud bed was measured at the beginning of each experiment, by taking a small sample.

The pore pressure measurements were performed at seven points inside the sediment bed using PVC tubing and seven pressure sensors. The end of each tube was tightly attached to a supporting frame to avoid movement of the end of the tube. In addition, a filter was placed on the tube end to avoid any sediment getting into the tube, while assuring an easy communication of the water pressure.

Velocity measurements over the top 3 cm of the mud bed were performed using the UVP, working with a 2 MHz transducer. The UVP transducer was placed 27cm above the mudline forming a 35 deg. angle with the vertical and pointing into the bed. This configuration allowed registering both the water and mud motion.

3. Experiment Results

In this abstract the results of three representative experiments are shown. As mentioned before the only difference among these three experiments was the previous consolidation of the bed, with bed densities equal to a) ρ_b=1738 kg/m^3, b) ρ_b=1548 kg/m^3, and c) ρ_b=1608 kg/m^3. Experiments b) and c) were performed on a self-weight consolidated bed that has been in repose for 10 and 4 days, respectively. Experiment a) was performed on a bed that had been mobilized by the same wave condition on the day before.

These three experiments showed clearly different bed behavior:

a) **No motion** of the bed. Even after more than one hundred waves had passed over the sediment bed, no increment of the pore water pressure was detected, and no motion of the mud was registered by the UVP as showed in Figure 1a).

b) **Bed erosion** due to the shear efforts imposed by the oscillatory water motion on the top layer of the sediment bed. This shear stress failure began on the upper layers near the water-mud interface (mudline) as soon as the first waves passed over the sediment bed. Gradually, the lower layers were eroded and mud/water motion was recorded at increasing depths. Figure 1b) shows the velocity profile and pore pressure measured at two depths inside the mud bed.

c) **Liquefaction** of the sediment bed and sudden movement of the whole bed due to a progressive increase of the pore water pressure. A gradually build-up of pore water pressure was measured, but no fluid mud motion was recorded by the UVP. After tens of waves had passed over the bed, all the measurable depths of

mud got abruptly into motion and the pore water pressure started to decrease. Figure 1c) shows the bed velocity and pore pressure recorded before and after the liquefaction had occurred.

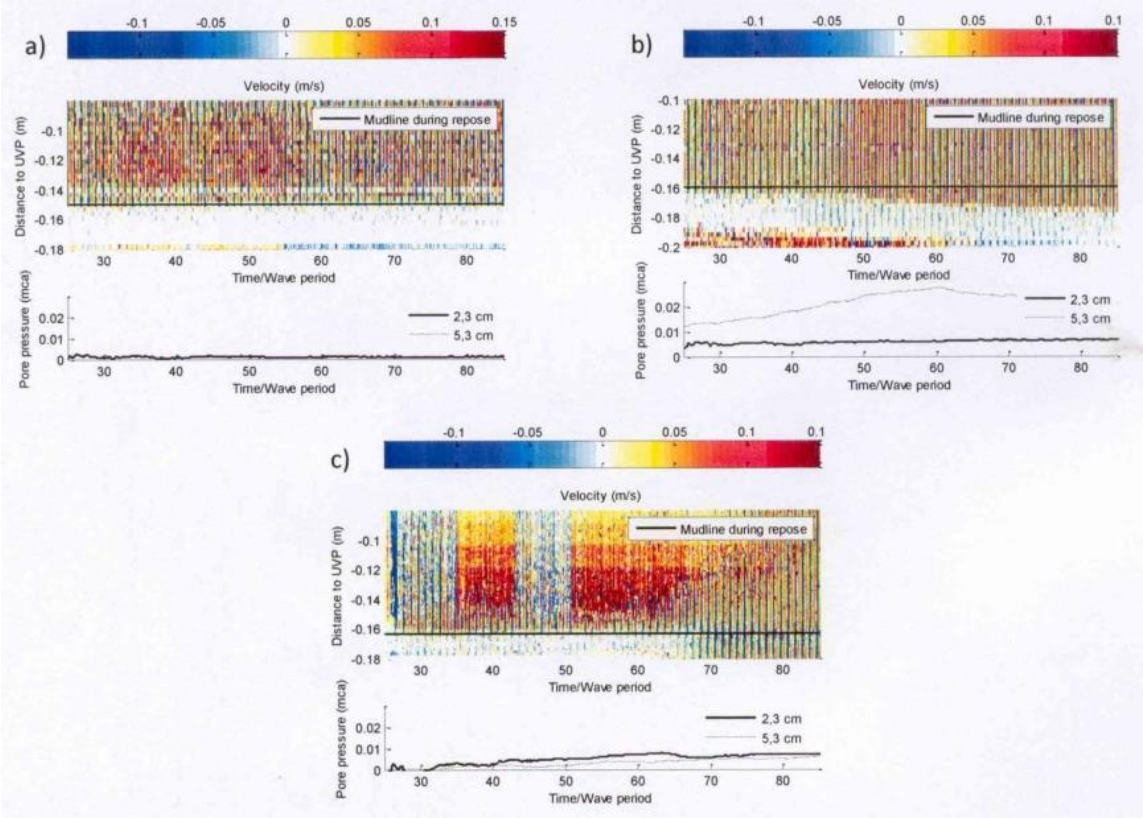

Figure 1: Velocity profiles and pressure records near the mudline for each of the three different behaviors, a) No motion, b) Erosion, and c) Liquefaction.

3. Conclusions

The experiments performed during this study fall in one of the three types presented here. During this study a clear correlation was found between the level of consolidation of the bed and its response when exposed to the same external forcing.

The pore water pressure measurements showed behaviors similar to the ones reported by de Wit and Kranenburg (1992) for kaolinite and Summer and Fredsøe (2002) for fine sands. Pore water pressure measurements are difficult to perform and on that regard we believe that the mud kinematics recorded by the UVP are a very promising alternative/complement to pore water pressure measurements in liquefaction studies.

The experiments showed that if the bed is let to consolidate after liquefaction has occurred, the same forcing that had produced liquefaction would not be able to liquefy the bed again. This suggests that liquefaction would only occur in freshly deposited muds that have not been previously exposed to significant wave forcing. This would occur just after engineering interventions have taken place, which makes the first days of the structure the most critical regarding liquefaction.

References

de Wit P.J. and Kranenburg C. (1992). Liquefaction and erosion of China Clay due to waves and current. *International Conference on Coastal Engineering: ICCE 1992* Venice, Italy, 1992.

Sumer, B.M. and Fredsøe J. (2002). *The Mechanics of Scour in the Marine Environment*. World Scientific.

Winterwerp J.C., de Graaff R.F., Groeneweg J. and Luijendijk A.P. (2007). Modelling of wave damping at Guyana mud coast. *Coastal Engineering.*

Measurements of mud rheological properties using ultrasonic waves

Jerome Peng-Yea Maa[1], Jae-Il Kwon[2], and Kwang-Soon Park[2]

[1]Virginia Institute of Marine Science, School of Marine Science, College of William and Mary, Gloucester Point, VA 23062, USA
[2]Korea Institute of Ocean Science and Technology. Ansan, Republic of Korea.

Introduction

To understand the material properties of sediment beds is a critical issue for understanding the responses of seafloor to forces applied from the water above, e.g., wave-mud interaction, erosion, consolidation, and landslide. Using the simulation of wave-mud interactions as an example, past studies on the selection of rheological properties (bulk density, ρ, dynamic viscosity, μ, and shear modulus, G) all depended on the modelers' choice without any measurement to confirm it, and thus, these simulation results could not use to help understanding the responsible processes. There are in-situ instruments for measuring the bulk density of mud, ρ, but there is no practical approach for the others. Until recently, there is a laboratory experiment to demonstrate the measurements of μ and G, using acoustic shear waves. This study reports the results of the laboratory experiment and a feasible approach for future in-situ measurements of mud rheological properties.

Muddy sediment beds can be considered as a viscous fluid with high viscosity, μ, if it is under strong agitated. It may also have shear strength if the binding forces among particles/flocs have time to be developed. After that, the mud will have some rigidity (marked by shear modulus, G). Basically, ρ, μ, and G are the three parameters required to represent the basic rheological properties if the basic viscoelastic model is selected.

Ultrasonic pressure waves have been used extensively in laboratories and fields for many applications and it has been also used for identifying the bulk density of mud (Maa et al., 1997; 2012). Although ultrasonic shear waves have also been used to measure shear wave speed for interpreting the rheological properties for foods, none of these earlier measurements is successfully, because of the misunderstanding of the signal generated.

Acoustic shear waves are required to measure μ and G. Our experience shows that the loss of shear wave transmission in mud is too high, and thus, the transmission of shear waves is not measurable. The reflection of shear waves from the contact surface, however, is measurable, and the data obtained can be used to interpret for μ and G. In this study, a practical approach that measures the μ and G for the mud is introduced. Because of resource limitation, only laboratory experiments for kaolinite slurry are reported.

Methodology

When acoustic waves travel across the interface between two media, echo waves will be produced at the interface if the acoustic impedances for these two media are different. Without considering the contact loss, the reflection coefficient is defined as $R = (Z_2 - Z_1)/ (Z_1 + Z_2)$, where Z_1 and Z_2 are the impedances for the first and second media. This principle applies for both pressure and shear waves for any wave frequency. For applying this principal, the first medium (also called delay-line material) is usually a given material with the acoustic impedance clearly known and the second medium is the target material, e.g., mud. The shear wave impedance for the target material can be expressed as

$$Z_2 = Z_{2r} + jZ_{2i} = \left(\sqrt{\rho_2 G_2} + \frac{1}{\sqrt{2}} \sqrt{\rho_2 \omega \mu_2} \right) + j \left(\frac{1}{\sqrt{2}} \rho_2 \omega \mu_2 \right) \quad (1)$$

where $j = (-1)^{1/2}$, ω is the shear wave frequency. For a fluid, i.e., G = 0, Eq. 1 indicates that $Z_{2r} = Z_{2i}$. Because of the small value of dynamic viscosity, it can be seen that the first term in Eq. 1 is the dominant term for any solid. Since the reflection coefficient, R, cannot be measured directly at the interface, our experiment is designed to measure it indirectly at a distance away, using the original source shear wave transducer. Because Z_2 is a complex number, R must be a complex number too, and thus, can be rewritten

as $R = re^{i\phi}$. By using spectrum analysis of the measured acoustic waves at the original source transducer, the results can also be expressed as $ae^{i\varphi}$. Through calibration with selected fluids that their density and viscosity are given, e.g., water, olive oil, honey, etc., a relationship between r and a, as well as ϕ and φ can be established. After doing FFT on the echo shear waves for mud, a set of a and φ can be found for correlating to r and ϕ. Thus, the R for mud can be estimated. With R estimated, the mud impedance can be calculated by using an iterative approach. Since Z_2 is a complex number, and if the test material is also a fluid, then $Z_{2r} = Z_{2i}$. Otherwise, the extra contribution must come from the shear modulus, according to Eq. 1. If knowing the density for mud, then the shear modulus of mud, G_2, can be determined.

Lab Experiments

A consolidation experiments was conducted in a consolidation chamber, Fig. 1, using a commercially-available kaolinite slurry. The slurry was well mixed in a mixing tank and carefully placed into the chamber. Right after placing, sediment samples were taken to determine the initial sediment concentration, ϕ_0, and the measurements started immediately. A shear wave transducer was used as the source and receiver, to measure the echo-waves. Continuous burst of 5-cycle sine waves were generated and fed into the transducer to produce 250 kHz ultrasonic waves: mainly shear waves, but with minor pressure waves. These waves traveled across the delay-line and came to the mud interface. Because of the difference in pressure and shear wave speeds and the properly selected length of the delay-line, pressure waves and shear waves are clearly separated and reflected separately. Pressure waves were first reflected (90 μs < time < 110 μs, after a 40 db amplifier, see Fig. 2a). Because the acoustic impedances for shear waves were very different between these two materials, a more clear echo shear waves, after a 60 dB amplified, were picked up by the source transducer which has been changed as a receiving transducer after about 60 μs. These waves were recorded using a high-speed analog to digital conversion device (CompuScope CS12100, from Gage Applied). An average of 20 measurements was saved as one data file for a better SNR.

Because of the high efficiency for pressure wave transmission, pressure wave can be detected at the other side of the test chamber (Fig. 2b). With the chamber size given, this measurement can give pressure wave speed that travel through the kaolinite. This information, worked with the acoustic pressure wave impedance, the bulk density of kaolinite can be calculated.

Results

Only one sediment, i.e., kaolinite, has been conducted for a duration of 350 hrs. Because of the high initial sediment concentration, the consolidation only proceeds a little. The bulk density only increased a little. The change of shear modulus, G, and kinematic viscosity, ν, over the 350 hrs are interesting. After about 10 hrs, the kaolinite slurry has developed a structure. More discussion will be given later.

References

Maa, J.P.-Y., K.-J. Sun and Q. He, 1997. Ultrasonic characterization of marine sediments. Marine Geology, 141:183-192.

Maa, J.P.-Y., 2012. Measurements of Mud Bulk Density, An ultrasonic approach, Report, submitted to Korea Ocean Research and Development Institute, Ansan, Republic of Korea.

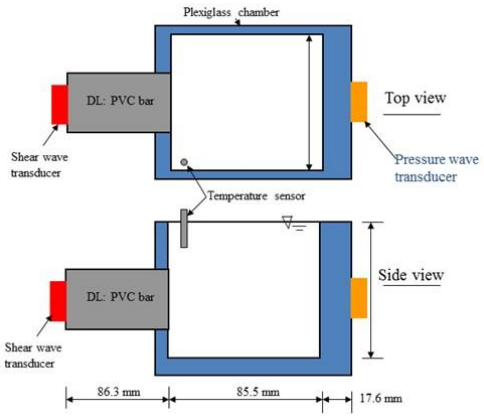

Fig.1. Experimental setup.

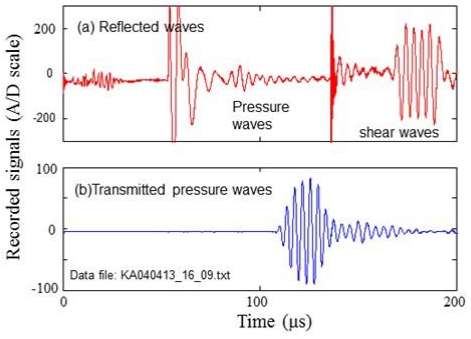

Fig. 2. An example of measured waves.

Link between surface and rheological properties of cohesive sediments

Maria Ibanez[1,2,*], Claire Chassagne[1], J.C. Winterwerp[1,2]

[1]Department of Civil Engineering, Technical University of Delft, 2628 CN Delft, The Netherlands.
[2]Marine and Coastal Systems, Deltares, Rotterdamseweg 185 Delft, The Netherlands.
[*]Corresponding author: Maria.Ibanez@deltares.nl

Introduction

The surface charge of cohesive sediment particles varies as the consequence of pH and salinity variations. The cohesion of the porous structure of the sediment is modified, through flocculation / deflocculation of the clay, swelling, etc… (Sposito 1984). This in turn will affect the rheological properties of the sediment suspensions (Mitchell 1991, Coletta et al. 1997).

In this study, we are going to investigate the change in surface charge properties of various types of sediments and link it to the change is rheological properties. Currently new models are developed in our group to evaluate the surface charge of non-spherical particles like clays (Chassagne et al. 2009). We use various electrokinetic techniques to investigate the surface charge properties in terms of so-called zeta potential and will show why these techniques are complementary. The changes in particle size of the sediments will also be linked to the rheological and surface properties.

Methodology

The zeta potential was measured with two different experimental apparatuses: electrophoresis equipment based on Doppler velocimetry (ZetaNano ZS) and a Dielectric Spectroscopy equipment, with a HP impedance meter (4194A) and home-made cells (Chassagne et al., 2009). Salts were analytical grade and the electrolytes were made from pure water with a conductivity of less than 1 microS/cm.

The particle size distribution was measured with a Malvern MasterSizer 2000 by Static Light Scattering. The viscosity of concentrated samples was measured with a rheometer Haake CV100, and in the case of diluted samples a capillary viscometer was used.

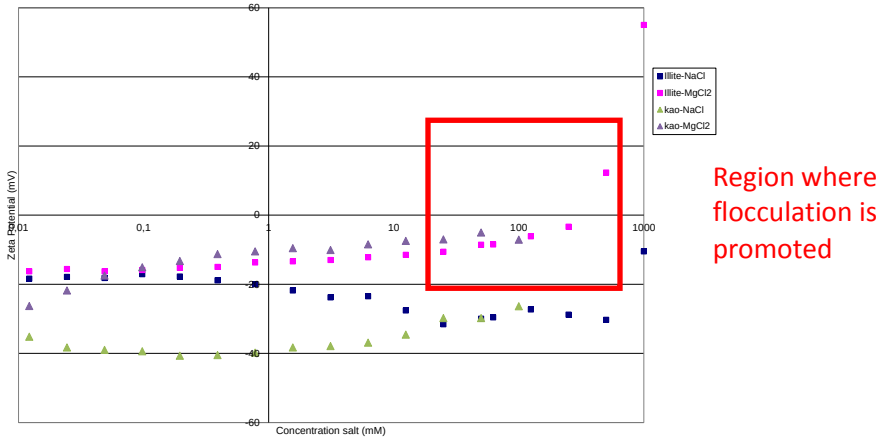

Figure 1. Zeta potential of kaolinite and illite suspensions as a function of added salt at pH = 8 for monovalent (NaCl) and divalent (MgCl2) salts: above 1 mM of added divalent salt, flocculation will be promoted as the zeta potential is small.

Results

The zeta potential (ZP) gives an indication of the surface charge of the sediment particles. It allows to estimate the point of zero charge (in the region ZP => 0), and hence the soil flocculation ability in a specific range of pH or salinity.The interactions between sediment particles depend strongly on the surface charge of the particle.

In the region where flocculation is promoted, both particle size and rheological properties will be changing in time.

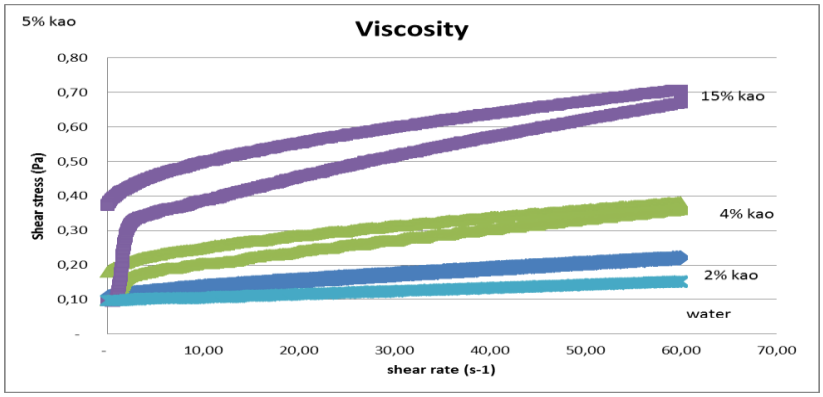

Figure 2. Shear Viscosity of kaolinite suspensions as function of volume fraction

In the non flocculating region the particle interactions are still depending on the average distance between particle, hence their volume fraction. In particular for high volume fraction the suspension display a non-Newtonian behaviour.

Conclusions

The isoelectric point (where ZP=0), where fast flocculation is promoted, is linked with the maximum shear yield stress. At pH > 7, and moderated salinity, particles are completely negatively charged and their rheological behavior is solely depending on the volume fraction. At pH < 7, a complex situation occurs, since edges and faces of the sediment have charges of different sign and face-edge flocculation is initiated.

References

Mitchell (1991) Conduction Phenomena: From theory to practice", Geotechnique, 41, 299-340

Coletta et al. (1997) Cation-enhanced removal of lead from kaolinite by electrokinetics, J. Env. Eng. Div, Am. Soc. Civ. Eng. 123 (12), 1227-1233

Chassagne et al. (2009) Electrokinetic study of kaolinite suspensions, J. Coll. Int. Sci. 336, 352-359

Scale et al. (1998) Shear Yield Stress of Partially Flocculated Colloid Suspensions. AlChE Journal, 44(3),538-544.

The laboratory experiments of wave attenuation by muddy bottom

Nourah Almashan, PhD Candidate, Johns Hopkins University, USA, nalmash1@jhu.edu
Eric Maxeiner, Senior R&D Systems Engineer, Echogen Power Systems, USA, emaxeiner@echogen.com
Robert A. Dalrymple, Professor, Johns Hopkins University, USA, rad@jhu.edu

Introduction

The interaction of waves with a muddy bottom has been the subject of a numerous studies since Gade (1958) developed the basic theory of wave attenuation in shallow water. Wave damping is potentially the result of a processes involving the mud viscosity (Dalrymple & Liu, 1978), poro-elasticity (Yamamoto et al., 1978), visco-elasticity (MacPherson, 1980), nonlinear wave-wave interactions (Hill & Foda, 1998), and non-Newtonian fluid behavior (Mei & Liu, 1987).

This study focuses on the damping of water waves propagating over a muddy bottom and the effect of the wave characteristics such as wave period, wave amplitude and history of mud on the wave attenuation. Surprisingly, in the beginning, during experiments, it was observed that surface waves lifted the mud particles from the bottom to create a lutocline. As the lutocline approached the water surface (within 3cm), interfacial waves that were nearly orthogonal to the orientation of surface waves were created on the lutocline/water interface layer. However, these interfacial waves are not a significant damping mechanism. The goal here is to understand how different test parameters affect the damping of waves as they pass over a muddy bottom.

Experimental Factors

With funding from the Office of Naval Research's Multidisciplinary University Research Initiative: Mechanisms of Fluid-Mud Interactions under Waves, we performed a series of tests in a wave tank to study the damping of waves for a series of various test parameters. The wave tank consists of a two layer fluid system with an upper layer of water with a density, viscosity and thickness of ρ_1, ν_1 and d_1, respectively, and a lower layer of mud (ρ_2, ν_2, G', G'' and d_2) where G' is the elasticity and G'' is the viscosity parameters of the mud layer. The total depth of the system is $h = d_1 + d_2$. Different parameters played a role in the experiments such as wave period, wave stroke, water depth, and mud history. The Johns Hopkins University laboratory wave tank measures 18.3 m long by 2.4 m wide with walls measuring 1.7 m high. About 6 m of each of the side walls is made of clear acrylic paneling to allow viewing of the test area. A commercial kaolinite clay was used as the bottom layer.

The tank has a piston-style wave maker with four individual paddles; flat panels that can move in unison or individually to create multi-directional waves. Sheremet and Stone's 2003 research showed that during a storm the sediments were mixed into the water column and consequently maximum wave damping occurred after the storm. To achieve the desired properties consistently, before testing, the mud was mixed manually into the water column using a rake to stir up the clay from the bottom of the tank and create a well-mixed suspension throughout the water column. All tests were conducted after a lutocline formed and were repeated a total of three times and an average of these results were taken. Four system parameters were used as independent variables: wave frequency, wave amplitude, water depth, and mud history.

Results

One surprising result revealed that interfacial waves can be created on the lutocline, when the lutocline is about 3cm from the water surface (Maxeiner & Dalrymple, 2011), see Figure 1. These waves are temporally sub-harmonic and nonlinear. This is the result of a three-wave interaction involving the surface wave and the two interfacial wave trains on the lutocline (Wen, 1995).

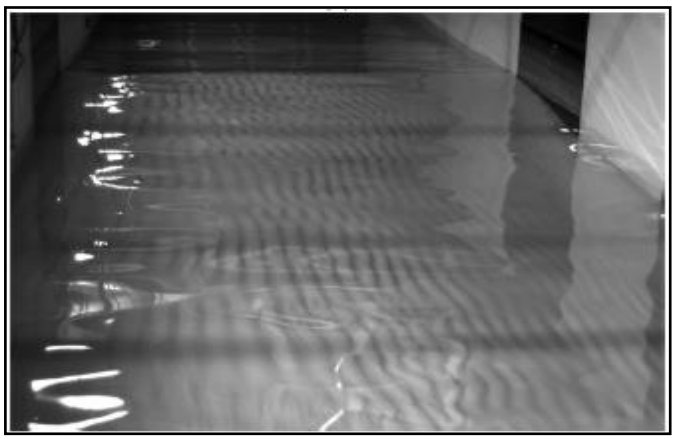

Figure 1. Image of the observed standing interfacial waves form on the lutocline that is induced by surface waves in muddy water.

Four parameters (wave amplitude, wave period, water depth, and mud history) were varied revealing contrasting results on the damping.

- Varying the wave amplitude showed that damping increased with an increase in wave amplitude for certain conditions (at water depth of 0.44 m and wave period T= 1.0s) as seen by Yamamoto & Schuckman (1984), and Soltanpour et al. (2010), yet with other tests

damping increased while wave amplitude decreased (at water depth of 0.44 m and wave period T= 0.9s) as seen by Yamamoto & Nagai (1984), and Sakakiyama & Bijker (1989). Interestingly, no study identifies both results.

- Wave period tests showed that damping increased with increasing wave period and yet damping can also decrease with increasing wave periods.
- Effects of varying the water depth showed that, in intermediate water depth, damping decreased with an increase in wave height (The damping values were relatively small). The same tests were performed in shallow water depths, revealing that the damping values increased.
- Looking at the effect of damping with different wave periods and total water depths, the results showed that the damping increased with period until it reached its peak and then it decreased. The water depths used were 21, 25, and 30cm and the total lutocline depth, at the time of measurement, was 0.12m for all experiments. These tests were also compared with MacPherson's model (1980) and showed relative agreement starting at wave period at 1.2s through 2s (Figure 2).

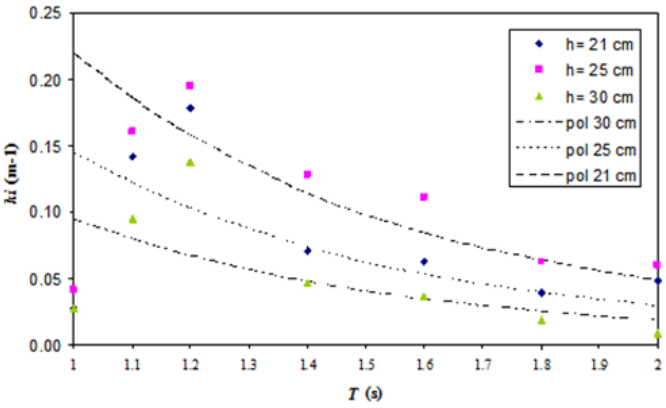

Figure 2. Attenuation coefficient versus wave period with (S= 2) and varying water depths (H = 21 cm (■); H = 25 cm (♦); H = 30 cm (▲)), the dash lines are the MacPherson model (1980).

- Effects of mud history varied the results of the tests By mixing the mud for 20 minutes and allowing it to settle, we measured the damping values at 1hr, 5hr, 25hr, 29hr, 49hr, 53hr, 125hr after initial mixing of the mud layer. We ran the wavemaker with total depth *h*= 44cm, wave period T=1s each time. Tests were repeated and averaged. Between each run, we allowed the tank to settle for 5 minutes. The results show that the damping value decreased by approximately 20% between the sets of tests. With time, the mud starts to consolidate and the lutocline decreased with time. The interesting findings are that the damping values decreased with time, but when it reached the 29hrs after setting; it begins to increase again in short time and then continued to decrease.

Conclusions

The results for the experiments were interesting for several reasons. This study showed that damping can increase and decrease with the mud properties and varying wave parameters such as wave amplitude, wave period, water depth, and mud history. The results showed that the damping increased with increased the wave period until it reached its peak and then it decreased. These results were compared with MacPherson's model (1980) and showed a good agreement. Moreover, mud history can affect the damping values.

References

Dalrymple, R. A. and P.L. Liu. (1978). Waves over Soft Mud Beds: a Two-layer Fluid Mud Model. Journal of Physical Oceanography, 8, 1121-1131.

Gade, H. G. (1958). Effects of Non-rigid, Impermeable Bottom on Plane Surface Wave in Shallow Water. Journal of Marine Res., 16(2), 61-82.

MacPherson, H. (1980). The Attenuation of Water Waves over a Non-rigid Bed. Journal of Fluid Mechanics, 97(4), 721-742.

Mei, C. C. and K. F. Liu. (1987). A Bingham Plastic Model for a Muddy Seabed under Long Waves. Journal of Geophysical Res., 94(C13), 14,581-14,594.

Yamamoto, T., H. L. Koning, H. Sellmeijer and E. Van Hijum. (1978). On the Response of a Poro-elastic Bed to Water Waves. Journal of Fluid Mechanics, 87(1), 193-206.

Sheremet, A. and G.W. Stone, (2003). Observations of nearshore wave dissipation over muddy sea beds. Journal of Geophysical Res., 108(C11).

Hill, D. F. and M. A. Foda, (1998). Subharmonic resonance of oblique interfacial waves by a progressive surface wave. Proc. R. Soc. London, Series A, 454,1129-1144.

Maxeiner, E. and R. Dalrymple, (2011). Experimental observation of standing interfacial waves induced by surface wavesin muddy water. Physics of Fluids, 23, 096603-096603-9.

Soltanpour, M., F., Samsami, and S., Sorourian, (2010). Wave-Flume experiments of dissipating waves on soft mud. Intl. Coastal Engineering Conference2010, 1-10.

Yamamoto, T., B., Schuckman, (1984). Experiments and theory of wave-soil interaction. Journal of Geophysical Mechanics, ASCE , 110, 95-112

Sakakiyama, T., and E. W., Bijker (1989). Mass transport velocity in mud layer due to progressive waves. Journal of Waterways, Port, Coastal, and Ocean Engineering, ASCE, 115(5), 614-633.

Yamamoto, T., T., Nagai, and J. L. Figueroa (1984). A laboratory experimentation on the interactions between water waves and soft clay beds. Coastal Engineering in Japan, 27, 179-291.

Wen, F., (1995). Resonsnt generation of internal waves on the soft sea bed by a surface water wave. Phys. Fluids 7, 1915.

Linking sediment transport processes and biogeochemistry with application to the Louisiana Continental Shelf

Author: Courtney K. Harris (VIMS)
Co-authors: Katja Fennel (Dalhousie), Rob Hetland (TAMU), Justin Birchler (VIMS)

Though it enhances the exchange of porewater and solids with the overlying water, the role that sediment resuspension and redeposition play in biogeochemistry of coastal systems is debated. Numerical models of geochemical processes and diagenesis have traditionally parameterized relatively long timescales, and rarely attempted to include resuspension. Meanwhile, numerical models developed to represent sediment transport have largely ignored geochemistry. This is a particularly important issue for fine grained environments, which can play a large role in geochemical cycles and may act as depositional sinks that serve as repositories of sedimentary signals. Here, we couple the Community Sediment Transport Modeling System (CSTMS) to a biogeochemical model within the Regional Ocean Modeling System (ROMS). The multi-layered sediment bed model accounts for erosion, deposition, and biodiffusion. It has recently been modified to include dissolved porewater constituents, particulate organic matter, and geochemical reactions. For this talk, we explore the role that resuspension and redeposition play in biogeochemical cycles within the seabed and in the benthic boundary layer by running one-dimensional test cases designed to represent a 20-m deep site on the Louisiana Shelf. The modeling framework is used to address two issues. First, we couple a model of short-timescale diagensis to the sediment transport model. Secondly, the behavior of short-lived radioisotopes is represented by the model to provide a quantitative means of estimating the observable products of flood deposition and storm reworking in fine grained environments.

The coupled diagenetic – sediment transport model accounts both for oxygen consumed within the sediment bed, and within the overlying water. Results from this are contrasted to calculations from an implementation similar to a standard diagenesis model. Comparing these, the results indicate that resuspension acts to enhance sediment bed oxygen demand, as well as oxygen consumption in the water column. During a cycle of erosion and deposition, oxygen from the overlying water can be added to the pore water of newly deposited sediment, while "oxygen demand units" are injected into the water column during erosion of anoxic sediment. For this reason, resuspension events impact the timing of oxygen demand, with pulses of oxygen consumption occurring during and shortly after resuspension cycles. The magnitude of sediment bed oxygen demand is especially sensitive to the model's treatment of diffusion across the sediment – water interface.

Inclusion of short lived radioisotopes ^{7}Be and ^{234}Th produce a numerical model capable of estimating the geochronological profiles created under a range of magnitudes of resuspension intensity, flood magnitude, and bioturbation. Results illustrate the relative importance of physical and biological reworking in modifying the character of flood deposits.

Comparison of Sontek ADVOcean-Hydras and Nortek ADV vectors for measuring suspended sediment concentration via acoustic backscatter

*Grace M. Cartwright (gracec@vims.edu) and Carl T. Friedrichs (cfried@vims.edu)

Virginia Institute of Marine Science, College of William & Mary, Gloucester Point, VA 23062, USA;
*Corresponding Author

This study compared acoustic backscatter (ABS) response to muddy flocs, silty clay, mixed mud plus sand, and sand in the lab and in-situ among ten relatively similar acoustic Doppler velocimeter (ADV) units: five 6-MHz Nortek Vector ADVs and five 5-MHz Sontek ADVOcean-Hydras. This approach allowed for an examination of the relative roles played by intervendor, intra-vendor, and sediment variability in determining their ABS response. As well as consistently responding more strongly to sand than to mud, ABS in counts (a logarithmic unit proportional to decibels) revealed clear offsets apparent among the various instruments within both vendors. One of the ADVs from each vendor was defined as a reference unit, and the offsets in counts of the other four ADVs from each vendor were adjusted to become consistent with the reference unit. For either vendor, precorrection ABS response was more similar if the vendor's units had been purchase together with consecutive manufacturer's serial numbers

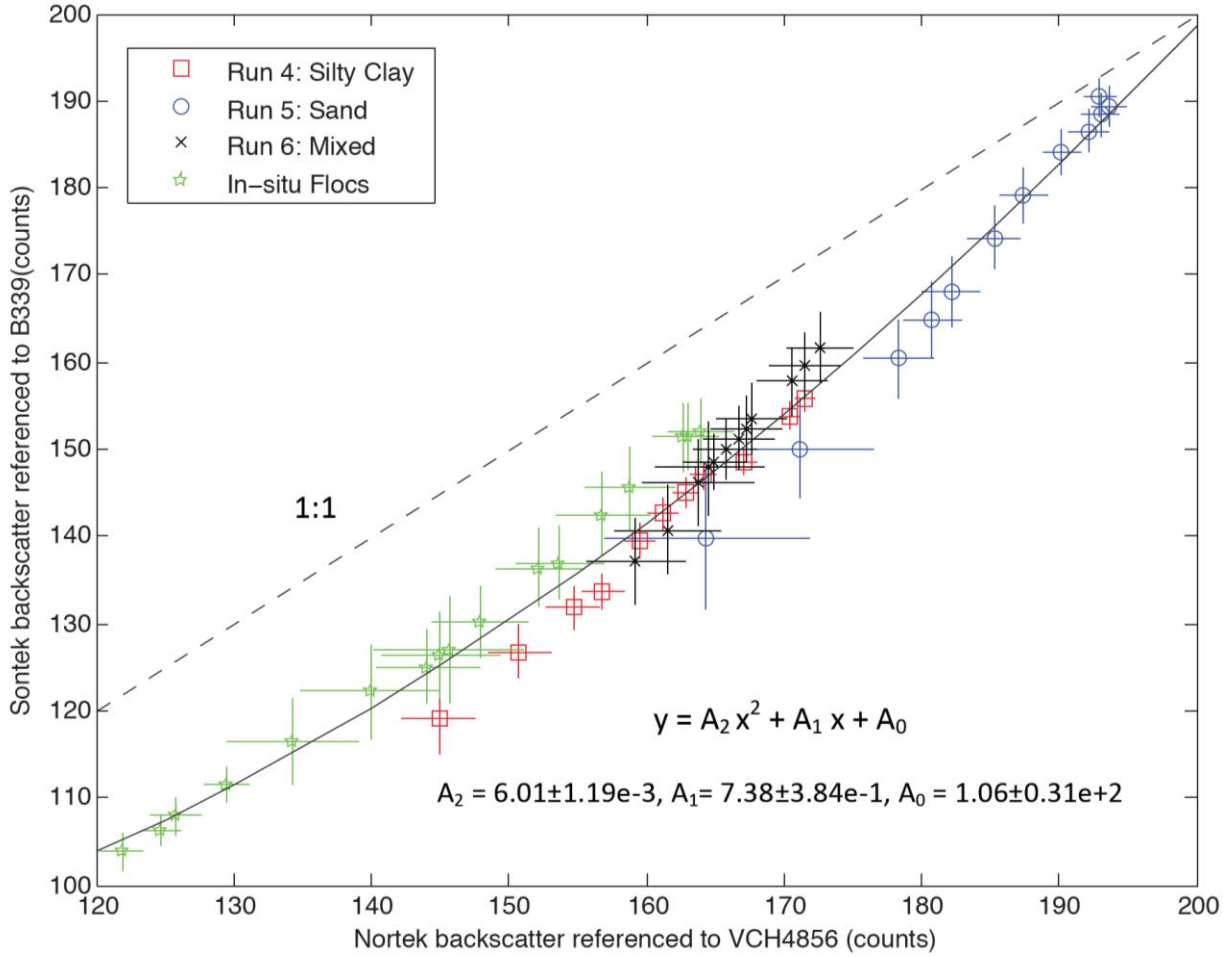

Figure 1. *Comparison of acoustic backscatter burst response adjusted to a reference sensor from Nortek Vector ADV and Sontek ADVOcean sensor pairs during lab calibrations for silty-clay (red squares), sand (blue circles), and mixed sandy mud (black x's) as well as an in-situ calibration with muddy flocs (green stars). Dotted line represents the 1:1 ratio between the two. The solid black line is the least-squares quadratic fit for all the data.*

and subsequently had not had electronic components replaced. After adjustment, ABS counts for all the Sontek vs. Nortek ADVs largely lay along a single curve. The Sontek vs. Nortek ABS curve began with a slope of ~1:1 at low backscatter; but at higher ABS, the response of the 5-MHz Sontek ADVs increased more rapidly than that of the 6-MHz Norteks, suggesting that the backscatter registered by the higher frequency Norteks was more susceptible to attenuation. Plots of the log10 of sand concentration (log10 C) vs. ABS for concentrations from ~ 10 to 600 mg/L was significantly quadratic for both the Nortek and Sontek ADV although more strongly so for the Nortek. In contrast, mud calibrations of log10 C vs. ABS (for ~20 to 700 mg/L) were not quadratic for either vendor, providing less clear evidence of ABS attenuation. For well-mixed silty mud in the lab, the slope of the calibration of log10 C vs. ABS for both vendors was close to the theoretical value expected for a single, constant grain-size suspension. In the field, however, the calibration slope of log10 C vs. ABS was significantly smaller, which suggested a change in the acoustic properties of the suspended particles with increasing C. When calculating predicted ABS in counts in response to varying proportions of different grain sizes, results showed that transforming logarithmic counts back to linear units of acoustic power before adding them added together allowed successful prediction of the expected acoustic response.

Erosion characteristics determined from microcosm experiments, San Francisco Estuary, California, USA

David H. Schoellhamer

U.S. Geological Survey, dschoell@usgs.gov

Cohesive sediment transport in the San Francisco Estuary (SFE) affects habitat for pelagic organisms, contaminant transport, marsh accretion and sustainability, and dredging. Several numerical models of sediment transport are being developed and applied to address these issues. Erosion algorithms are determined by calibrating model output to measured suspended-sediment concentration (SSC). To better inform and constrain numerical model development, an erosion microcosm is used to quantify erosion. This abstract provides initial findings of this study.

The basic procedure for this study is similar to that described by Dickhudt et al. (2011):

1) **Collect sediment cores:** Two sediment cores are collected from a study site with a gravity Gomex corer lowered to the bed from a small boat. After raising the corer back onto the boat, a 10-cm-diameter tube is immediately pushed into the top of each core to collect a sample. Samples are disturbed as little as possible.

2) **Erode the cores:** A piston inserted into the bottom of the tube is used to push the sediment surface up to 10 cm from the top of the tube. The core is eroded using a dual core University of Maryland Center for Environmental Science – Gust Erosion Microcosm System. A disk rotates at the water surface at the top of the tube and water is pumped through the water column in the tube at predetermined rates that provide nearly uniform and known shear stresses at the sediment/water interface (Gust and Mueller 1997). Turbidimeters continuously monitor the effluent. A 0.01 Pa shear stress is initially applied to flush and stabilize the system. Applied shear stress τ_b is increased stepwise to 0.05, 0.10, 0.15, 0.20, 0.30, 0.45, and 0.60 Pa over a period of about 3 hours. Water samples are collected during each step to calibrate turbidity to SSC.

3) **Analyze the SSC time series data:** The time series of erosion rate ($kg/m^2/s$) is calculated and the erosion model of Sanford and Maa (2001) is used to calculate erosion parameters. The erosion rate E for an experiment as a function of mass eroded (m) and time (t) is

$$E(m,t) = M(m)\left[\tau_b(t) - \tau_c(m)\right] \quad (1)$$

Critical shear stress τ_c is calculated at the end of each step and is assumed to increase with m which in turn increases with erosion depth. The erosion rate constant M(m) is assumed to be a constant for each step.

As of the time this abstract was written (June 2013), 21 cores collected from 6 sites throughout the SFE and during different seasons had been analyzed. A statistical summary of the initial critical shear stress for erosion at the beginning of the experiments is given in Table 1.

Table 1. Statistical Properties of Erosion Parameters

	Number of measurements	Mean	Median	Lower quartile	Upper quartile
Initial τ_c (Pa)	21	0.091	0.075	0.030	0.13
$m_{0.4}$ (kg/m^2)	18	0.051	0.035	0.020	0.062
$\bar{M}$ ($kg/m^2/Pa$)	18	0.00022	0.00012	0.000082	0.00019

The mass eroded where the bed critical shear stress equals 0.4 Pa ($m_{0.4}$) is a convenient quantity for expressing results (Dickhudt et al., 2011). $m_{0.4}$ given in Table 1 are equivalent to erosion depths of about 0.01–0.1 mm. $m_{0.4}$ was an order of magnitude less than observed in the York River in Chesapeake Bay (Dickhudt et al., 2011), indicating that SFE sediments were less erodible. In SFE, $m_{0.4}$ increased as the fraction of finer cohesive sediment increased (n = 9). York River sediment showed no such relation.

For 15 of 21 cores, M(m) generally increased with m (or depth). This indicates that, for a given excess shear stress, erodibility increases with distance below the sediment/water interface. Biostabilization at and near the sediment/water interface may be responsible. Statistical properties of the mean value of M(m) between the surface and where $\tau_c = 0.4$ Pa ($\bar{M}$) are given in Table 1.

Biota were a significant factor in these results. SFE is a more temperate estuary than the York River and biostabilization may account for smaller erosion rates. In some experiments, clams or other benthic organisms visibly bioturbated the sediment and increased calculated erosion rates.

The erosion microcosm is useful for determining erosion parameters affecting estuarine SSC at the tidal time scale for which erosion depth is on the order of millimeters or less. This scale of erosion is relevant for the issues in SFE for which numerical models are being developed. Minimal disturbance of the sediment core and rapid (perhaps less than one hour) initiation of the erosion experiment are likely requirements to obtain representative results. This erosion microcosm would not be helpful when deeper erosion is of concern, such as for riverine floods, levees, and sediment caps for contaminated sites. Additional erosion measurements in SFE will be conducted.

References

Dickhudt, P.J., Friedrichs, C.T., Sanford, L.P., 2011. Mud matrix solids fraction and bed erodibility in the York River estuary, USA, and other muddy environments: Continental Shelf Research 31:S3-S13.

Gust, G., Mueller, V., 1997. Interfacial hydrodynamics and entrainment functions of currently used erosion devices. In: Burt, N., Parker, R., Watts, J. (eds.), Cohesive sediments. Wallingford, UK. pp. 149–174.

Sanford, L.P., Maa, J.P.-Y., 2001. A unified erosion formulation for fine sediments. Marine Geology 179:9–23.

Quantifying suspended particulate matter (SPM) dynamics in estuaries: combining acoustic and optical approaches

Romaric Verney[1], George Voulgaris[2], Andy Manning[3,4,5], Julien Deloffre[6] and Philippe Bassoullet[1]

[1] Ifremer, Laboratoire DYNECO/Physed, BP 70, 29280, Plouzané, France
[2] Dept. of Earth & Ocean Sciences, University of South Carolina, Columbia, SC 29208, USA
[3] HR Wallingford, Howbery Park, Wallingford, Oxfordshire. OX10 8BA.
[4] Dept. of Geography, Environment and Earth Sciences, University of Hull, Kingston Upon Hull, Humberside, HU6 7RX, UK.
[5] School of Marine Science & Engineering, University of Plymouth, Plymouth, Devon, UK. PL4 8AA.
[6] UMR 6143 M2C, University of Rouen, 76821 Mont Saint Aignan Cedex, France

Introduction

Estuaries are coastal environments characterized by large amounts of sediment in suspension that tend to create large horizontal and vertical gradients that can vary in both space (e.g., from few mg/l/m in plumes to several g/l/m in turbidity maximum zones) and time at various scales (e.g., tidal to seasonal). Suspended particle matter (SPM) is often found in aggregate form as either microflocs, macroflocs or both. The size distribution of the aggregates also varies in both space and time leading to variations in sediment settling velocities that in turn affect sediment transport and deposition processes. Understanding of these estuarine sedimentary processes require accurate observational data using a combination of methods with optical and acoustical ones being the most prominent.

In 2011 a research project (FLUMES experiment) was carried out in the Seine Estuary, France. The experiment focus was on examining the temporal variability of SPM dynamics at different locations throughout the estuary using a variety of optical and acoustic techniques. In this contribution we present the response of the different methods used to observe and quantify SPM characteristics such as concentration, floc size distribution, density and settling velocity over the water column, at the tidal time scale. Data of SPM concentration and floc size distribution derived from both the acoustic and optical sensors are compared for the different stations that represent contrasted estuarine environments. Forward and back scattering results from the LISST and OBS sensors are combined and used to investigate changes in floc size distribution and mean size as function of the tidal cycle. These data are also compared to the imagery provided from the LabSFLOC system. The use of the ABS system in high concentrations of fine sediment and the role of flocs, and in particular the response of the acoustic system to flocculated sediment is examined.

Methods

Data from two field surveys carried out in the spring and autumn of 2011 are presented. During each survey time-series data over a period of 12 hours were collected at 4 stations in the lower part of the Seine estuary. The station locations corresponded to: (i) the plume area outside the mouth of the estuary (ii) the estuarine turbidity maximum; and (iii) the fluvial part of the estuary. The surveys were repeated during both spring and neap tidal conditions. During each tidal cycle, hydrodynamics and SPM characteristics were monitored concurrently using a suite of complementary acoustic (ADCP, 4 frequency Acoustic Backscattering Sensor (ABS)) and optical (LISST, CTD+OBS and LabSFLOC) instruments. A downward looking RDI Workhorse ADCP (1200 kHz) was installed on a floating platform, collecting current and acoustic backscatter data at a rate of 1Hz and recording an average every 2 min. The ABS, LISST and CTD+OBS sensors were fixed on a gauge that was used to profile the whole water column every 15 min. Complimentary water samples were collected hourly that were used to estimate floc size distribution and settling velocity using the LabSFLOC system and SPM composition (EPS/TEP and chl-*a*) on board the ship and for direct calibration of the optical and acoustic sensors.

Results and Discussion

Optical backscatter sensors are known to require empirical calibration with in situ sediments as to correctly account for sediment size and shapes. In general, calibrations are made for each site, seasonally, expecting that high river discharge or phytoplankton blooms can change SPM composition. Our results indicate that even for the same environment (estuary and station) OBS response (i.e., calibrations) can vary by a factor of 2 during the fortnightly cycle depending on hydrodynamics and associated sedimentary processes (Figure 1). These differences are analyzed for the different stations and further discussed in relation to floc size distribution and density properties obtained from both LISST and LabSFLOC. These results are critical as they have implication on the interpretation of medium to long term data sets obtained in similar environments using OBS data. Accurate determination of the quality and uncertainty on the observation is a prerequisite for the use of these data for the calibration of estuarine sediment transport models.

We also present the relative contribution of microflocs vs macroflocs within the Seine Estuary, both at the tidal and fortnightly scales and for different locations. SPM appears to be constituted of microflocs during the ebb tide, at all sites. During flood a more complex pattern emerges, with macroflocs being present immediately following the maximum sediment resuspension (in the estuarine turbidity maximum) but during the periods of maximum current speed and thus maximum turbulence intensity. Observations also confirm that periods of slack water provide the most favorable conditions for aggregation, whatever the amount of SPM present in the water column.

Conclusions

The FLUMES experiment provided a unique dataset dedicated to SPM observations in the Seine Estuary. It combined most of the recent acoustic and optical devices currently available. The capabilities and limitations of the different devices were analyzed, and results were combined to provide key information on SPM floc size distribution and density over the whole water column. Acoustic devices were also tested in such complex and high concentration environments. These results also provided key knowledge on sediment transport processes in a macrotidal estuary, which will be crucial for 3D sediment transport numerical modelling calibration.

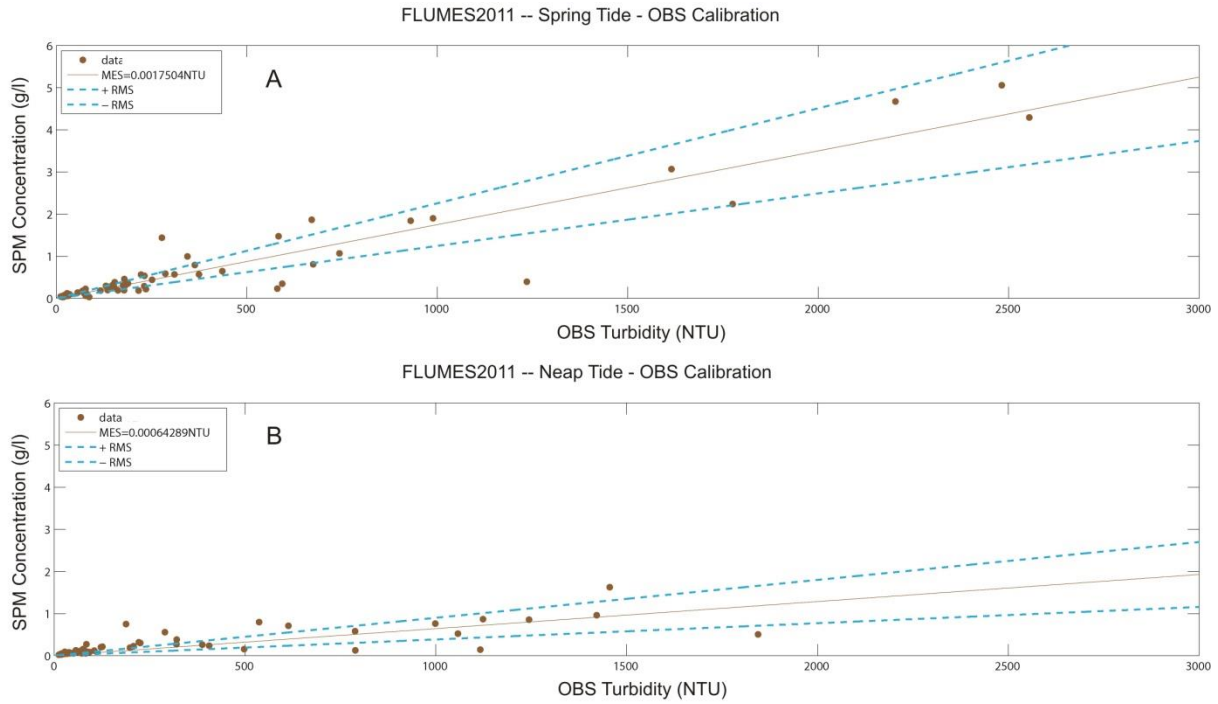

Figure 1 : OBS calibration in spring tide (a) and neap tide (b) during the FLUMES experiment in 2011 - Seine Estuary.

A numerical study on the optimal rotation ratio of an annular flume

Su-Hyun Yang[1], Ik-Tae Im[2] and Kyu-Nam Hwang[3]

[1]Dept. of Civil Eng., Jeonbuk National Univ., Republic of Korea, suhyun@jbnu.ac.kr
[2]Dept. of Mechanical Design Eng. Jeonbuk National Univ., Republic of Korea, itim@jbnu.ac.kr
[3]Dept. of Civil Eng., Jeonbuk National Univ., Republic of Korea, khwang@jbnu.ac.kr

Keywords : Annular flume, counter-rotation, optimal rotation ratio, numerical analysis

Introduction

For many years, many investigators have studied on the characteristics of movement of sediment using an annular flume. Annular flumes have the advantages of enabling flow at steady state conditions anywhere in the flume because the flow is generated by friction between the rotating top ring and the water surface in the flume. However, the bottom shear stress distribution across the flume bed is not uniform and the secondary flow is generated by the centrifugal force. In order to reduce the secondary circulation and consequently to obtain the uniform bottom shear stress in radial direction, the body of the flume is counter-rotated in the opposite direction to the top ring. When an annular flume is operated in the counter-rotation mode, a similar secondary circulation cell is generated in the opposite direction by the rotation of the flume body. The intensity of the secondary flow in decreased because two circulation cells are partially cancelled each other (Krishnappan, 1993). In order to operate efficiently an annular flume in the counter-rotation mode, the optimal rotation ratio between the top ring and the flume body defined as the rotation ratio minimizing the secondary flow and resulting in the most uniform bottom shear stress in transverse direction, must be known. In addition, the averaged bottom shear stress when the flume is operated at the optimal rotation ratios should be known since it is used frequently as one of the characteristic parameters governing the sediment transports including erosion and deposition.

In this study, the flow characteristics of the annular flume installed at Jeonbuk National University, operating in the counter-rotation mode, are analyzed using the computational fluid dynamics technique. From the analyses, we present the optimal rotation ratios for the given various top ring rotation speeds, which minimize the secondary flow and the transverse variations in the bottom shear stress. In addition, we propose the equations for both the optimal rotation ratio and the averaged bottom shear stress for a wide range of top ring rotation speeds.

Methodology

The present study uses the computational fluid dynamics method to determine the flow characteristics and the transverse distribution of the bottom shear stress in the annular flume. Assuming that water in the flume is incompressible with negligible temperature variation, velocity field is calculated using steady, incompressible Navier-Stokes equations with the k-Ω turbulent model. Details about the computation are given in Wilcox (1993) and Im et al. (2011). To verify the numerical model, the problem considered by Maa et al. (1995) is solved using the same flow conditions as they used, and then the bottom shear stress distributions are calculated from the numerical results. The numerical calculations from this study agree with the measured values by Maa et al. (1995).

Results

In order to find the optimal rotation ratio, water flow in the flume in counter-rotation mode is solved. The area-weighted average bottom shear stress is calculated when the top ring and the flume are simultaneously rotated in opposite directions. The rotation speed of top ring and the flume are varied from 0 to 10 rpm, the calculated averaged bottom shear stresses are shown in Fig. 1.

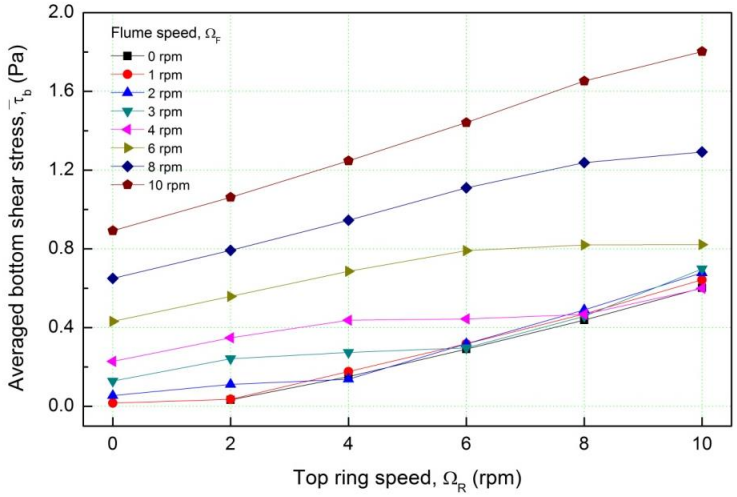

Figure 1. Variation of the averaged bottom shear stress in the counter-rotation mode.

This study uses two parameters to define the optimal rotation ratio for the annular flume in the counter-rotation mode. One is the maximum velocity ratio, the other is the difference of the stream functions between the largest and smallest values. The optimal rotation ratio is defined as the rotation ratio for which both the maximum velocity ratio and difference of the stream function are smallest. The optimal rotation ratio is calculated for all the top ring speed considered in this study and the relationship between the top ring speed and optimal rotation ratio is elicited.

The optimal rotation ratio ranges from 1.33 to 1.60 for top ring speed of 2~10rpm and the optimal rotation ratio increases as the top ring speed increases. The relationship between the optimal rotation ratio and top ring speed is found. The averaged bottom shear stress for the given optimal rotation ratio is also calculated and shows exponential increasing to the top ring speed. As a result, once the top ring speed is chosen, the optimal rotation ratio can be found using the relationship between the optimal rotation ratio and top ring speed, and then the averaged bottom shear stress can be determined from the relationship between the averaged bottom shear stress and top ring speed.

Conclusion

In this study, the optimal rotation ratio and the averaged bottom shear stress are calculated in order to apply counter-rotation of annular flume, and equations as functions of the top ring speed are estimated. The results in this study can be applied to studies of sediment erosion or deposition using the rotating annular flume.

Acknowledgments

This research was a part of the project titled ‘Development of coastal erosion control technology’, funded by the Ministry of Oceans and Fisheries, Korean.

References

I.-T. Im., S.-H. Yang, Y.-S. Cho and K.-N. Hwang (2011). Using inclined walls to control the bottom shear stress distribution in an annular flume. J. of Hydraulic Eng., 137(11), 1470-14760.

B. G. Krishnappan (1993). Rotating circular flume, J. Hydraul. Eng., 119(6), 758-767.

J. P.-Y. Maa, C.-H. Lee, and F.J. Chen (1995). Bed shear stress measurement for VIMS Sea Carousel. Mar. Geol., 129(1-2), 129-136.

Wilcox, D. C. (1993). Turbulence modeling for CFD, DCW Industries, La Canada, CA.

Laboratory measurements of cohesive sediment erosion in unidirectional flow

In Mei Sou[1] and Joseph Calantoni[2]

[1]National Research Council Postdoctoral Fellow
[2]Marine Geosciences Division, Naval Research Laboratory, Stennis Space Center, MS USA; joe.calantoni@nrlssc.navy.mil

Introduction

Cohesive sediments have significant effects on sediment transport in rivers and coastal regions. The erosion of cohesive sediment containing silt and clay can be as much as two orders of magnitude lower than non-cohesive sediment. We characterize the erosional response of cohesive sediment in unidirectional flows over intact sediment samples in a recirculating water tunnel. The erosion of a mixture of clay and sand is examined using a synchronized, high-speed, photographic imaging and stereo particle image velocimetry (PIV) measurement technique. We simultaneously observed vertical turbulent fluctuations in the flow directly responsible for the episodic initiation of sediment motion.

Methods

The experiments were conducted at the Sediment Dynamics Laboratory of the Naval Research Laboratory, Stennis Space Center, MS. The facility houses a flow tunnel to generate oscillating flows and steady flows with maximum combined velocities up to 80 cm/s. The main channel cross-section is 25 cm wide, 25 cm high, with a 2 m long test section that contains a 35 cm deep sediment well. A false floor with a stepper motor capable of vertically positioning a sediment core to 0.1 mm accuracy was inserted into the sediment well. Three high speed video cameras were used in conjunction with a high repetition dual cavity Nd:YAG laser (532 nm) to perform stereo PIV at 50 Hz sampling. Sheet optics were used to illuminate the PIV measurement window along with the sediment core. The experimental setup is shown in Figure 1. The sediment core (a mixture of clay and sand) was mounted in the false floor in the mid section of the channel. The height of the sediment, controlled by a stepping motor, was about 1 mm above the bed initially. The flow was recirculated in the channel with a 2-hp pump. The flow depth was constant at 7 cm and the Reynolds number was 14000, which is in the turbulent flow regime. Stereo PIV measurements were taken to quantify the three components of flow velocity in a vertical plane in the middle of the channel immediately upstream of the sediment core. A third camera imaged light scattered from the sediment core. All three cameras recorded synchronized image pairs at 50 Hz for 50 s generating a continuous time series of 2500 velocity fields.

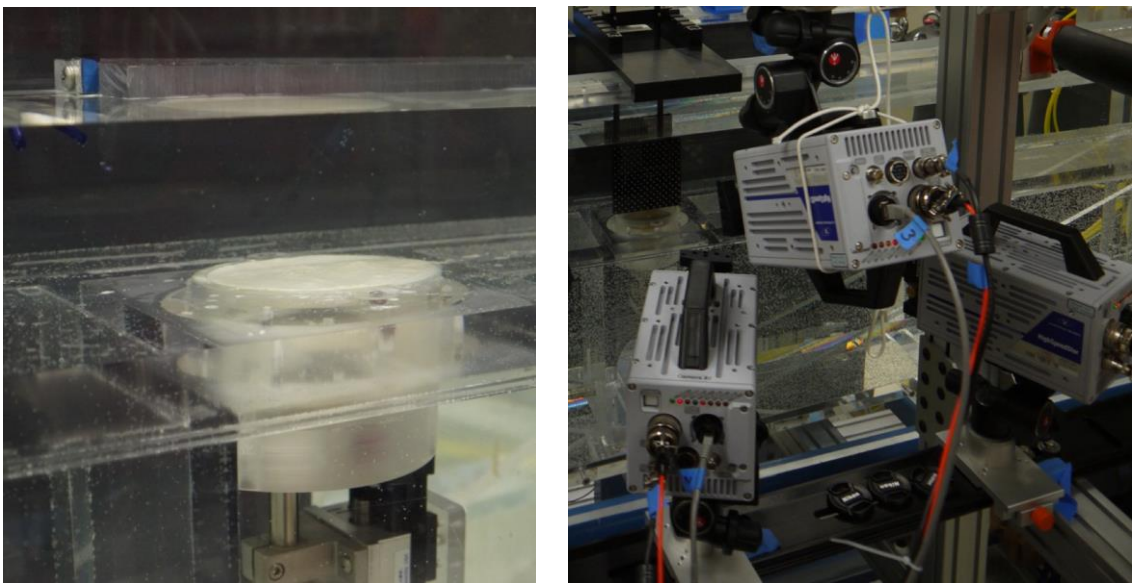

Figure 1. Sediment core above stepper motor (left) and synchronized imaging setup (right).

Results

The spatial spectra for the 2500 velocity fields were calculated along the direction flow tunnel in the middle of the PIV window. The Taylor frozen hypothesis was found valid in this case as the corresponding temporal and spatial spectra were continuous in wave number. Consequently, turbulence is expected to be advected with the mean flow.

Time snapshots of the sediment core profile, along with the horizontal and vertical turbulent fluctuations of the flow are shown in Figure 2. In this case, the mean flow is 20 cm/s (20 mm per 0.1 s). The high vertical fluctuation at x = 65 mm, y = 20 mm at t = 0 s in Figure 2a (right) is believed to be responsible for the initiation of the erosion at x = 45 mm at t = 0.1 s in Figure 2b (left). Sediment suspension was triggered by turbulent fluctuations with temporal scales less than a fraction of a second.

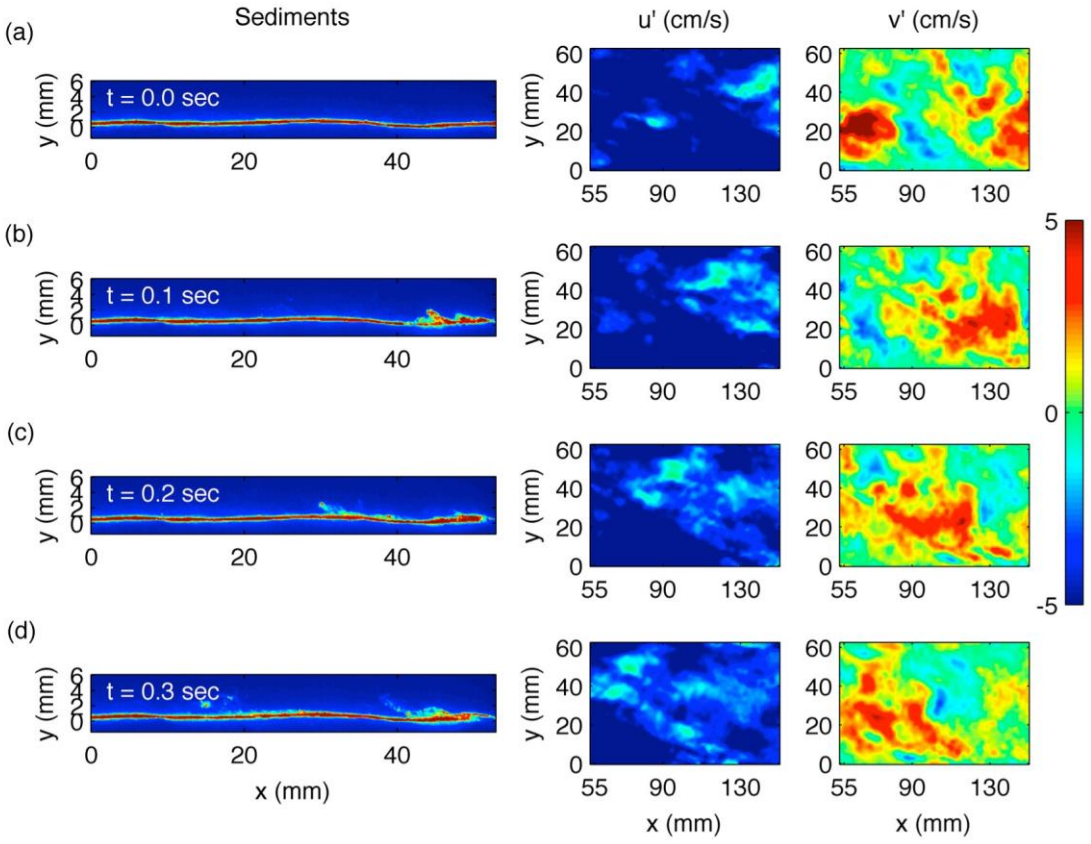

Figure 2. Time sequence of sediment erosion and turbulent fluctuations of the flow in the along channel (u), or x-direction, and the vertical direction (v). Not shown are the cross channel fluctuations. The x-coordinate runs along the center of the flow direction from the sediment core upstream through the PIV measurement window. The false color used on the sediments (left) is a visualization artifact and is not quantified by the color bar.

Conclusions

The erosion of a mixture of clay and sand in a core was examined using a synchronized stereo PIV and photographic imaging technique. Erosion was initiated by turbulent velocity fluctuations with small spatial (~2 cm) and temporal scales (<< 1 s). Making one-to-one correlations between instantaneous turbulent fluctuations and sediment erosion at these length and time scales would not be possible with lower speed imaging systems.

Acknowledgments

IMS was supported as a postdoctoral fellow through the National Research Council Research Associateship Program at the Naval Research Laboratory. JC was supported under base funding to the Naval Research Laboratory from the Office of Naval Research.

A probabilistic approach to interpret empirical erosion data for cohesive sediments using the cluster method

Faezeh Behzadnejad[a], Ali Maher[b], Ryan Miller[c]

[a]PhD candidate at Rutgers Civil and Environmental Engineering Department. E-mail address: faezeh@eden.rutgers.edu
[b]Professor of Civil and Environmental Engineering - Rutgers University
[c]Research Engineer at Weeks Soil and Sediment Management Lab., Center for Advanced Infrastructure and Transportation

1 Introduction

There exist two critical problems for the interpretation and comparison of erosion rate measurement for cohesive sediments taken by different test methods and procedures: [1] such measurements are evaluated by one of four different analysis methods [2] the nature of erosion testing is destructive, making application of multiple forcing scenarios to the same sample (as per the initial intact condition) an impossibility. Aberle et al. [2004] categorized the approaches used to interpret erosion data in the literature as such: [1] Initial peak erosion rate after application of a new bed shear stress [2] Rate of Erosion after some pre-defined initial response has passed [3] Average erosion rate over an entire test interval [4] Inclusion of a time factor in erosion rate prediction equations (commonly used power law formulation is an example of this approach). As there is no standard analytical procedure for interpreting and formulating erosion data, comparison of different studies is complicated.

In this paper a new approach is taken to convert erosion rate measurement data into information describing the erosion probability for different "material clusters" assumed to constitute the eroded portion of the surface. The advantage of such an approach over that of using discrete erosion behavior parameters for each level or interval of shear stress is that the results obtained by this method are not dependent on any particular or arbitrarily defined testing arrangement and can be used to predict erosion behavior in new flow sequences and levels to which the erodible material is exposed: facilitating a standardization of results which are obtained by different devices, test methods, and procedural sequences.

2 Background

Figure 1 illustrates the pattern typical to erosion rate measurements for Type *I* erosion, as described by Mehta and Parthenaides [1982]: "erosion rate reducing with time at constant forcing." As is standard for most test procedures successive intervals of increasing shear stress are applied to the sample over arbitrarily defined time intervals of erosion testing. The erosion rate for a given shear stress covers a range of values which are poorly defined by peak, average, or "data cropping" methods. The interval time, should it increase or decrease, will significantly affect average erosion rate values. Moreover, the length of each interval will have some effect on the erosion rate measured in the subsequent interval meaning [1] that the peak value would be affected in the subsequent interval and [2] that the selection of different shear stress level arrangements will also generate different results in continued testing scenarios (shear stress history dependence). For example if the third step of the test had a shear stress level very close to the second level (or even equal to that), the observed points would be scattered below the second step points and as a continuation of that; resulting lower erosion rates for almost similar shear stress levels.

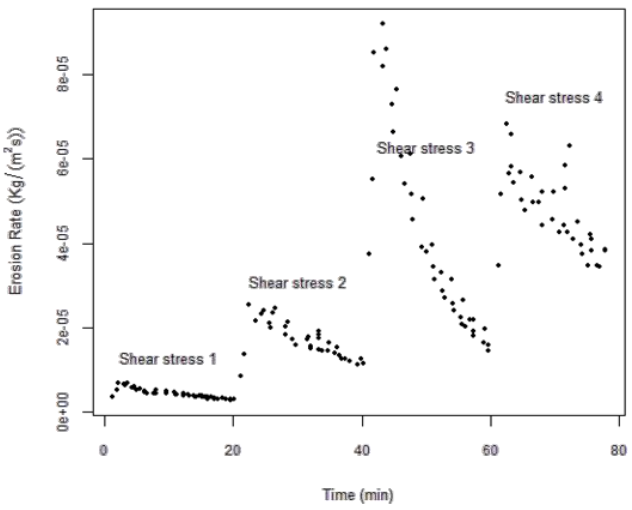

Fig. 1. Typical pattern of data observed in erosion tests.

The first three aforementioned interpretation methods are therefore more subjective measures and more sensitive to arbitrary test procedures and interpretation decisions. The fourth method (inclusion of a time factor) resolves the issue of dependence of erosion rate on time but the results still remain sensitive to shear stress history. The erosion behavior, illustrated in Figure 1, is thought to be the result of an increasing critical shear stress with depth resultant from the density gradient and strength of inter-particle bonds and has been well observed in cohesive sediments. However, a bed surface is constituted by many particles and flocculations of particles each with their own erosion behavior as a result of bedform generated turbulence and the heterogeneous nature of the sediment structure which is ill-suited for deterministic prediction in laboratory or field study.

3 Methodology

In the cluster method the sediment layer eroded during a *m* step test is treated as composed of *n* subsets or "clusters" of material categorized by their similarity in erosion properties. The following algorithm, calculates the weight of material

Algorithm 1 Eroded material calculation

Require : P,R[1,:],am_1
Fori in1 : m
  For j in1 : n
    $CE_{i+1,j} = P_{i,j} \cdot R_{i,j} \cdot AM_i$
  EndFor
  $EM_{i+1} = \Sigma CE_{i+1,j}$
  $AM_{i+1} = AM_i - EM_{i+1}$
  For j in1 : n

$$R_{i+1,j} = \frac{\left(R_{i,j} \cdot AM_i \cdot (1 - P_{k,j})\right)}{AM_{i+1}}$$

  EndFor
End For

eroded at each step as a function of the unknown variables: [1] the probability of erosion during one test step for the material belonging to each of the clusters under each of the shear stress levels to which the sediment is exposed (entities of matrix P) [2] the weight proportion of each of the clusters in the intact surface condition (entities of the first row of proportion matrix R). AM is the available material vector of length m that keeps the amount of material available for erosion at the start of each step, cluster erosion matrix CE saves the amount of material eroded from each cluster in each step, and the eroded material vector EM contains the total material eroded from all clusters during each step. Given the observed erosion rates at different shear stress levels, an optimization problem is solved to minimize $f(x)$ defined as the difference between the observed values and erosion rates predicted by the model using matlab *fmincon* function.

The constraints that the minimization is subjected to can be summarized as follows:

(1) All the variables in $x$vector should be in [0, 1] range as they are all probability or weight ratio values.

(2) $\forall i \in [1,m]$ & $\forall j \in [2, n]$ $p_{i,j} - 1 \leq p_{i,j}$

(3) If shear stress level in step i is larger than step j, $\mapsto \forall k \in [1, n]$ $p_{j,k} \leq p_{i,k}$

(4) $\sum_{i=1:n} r_{1,i} = 1$ $\quad \min_x f(x)$ *such that* $\begin{cases} Ax \leq b & \textit{Linear inequality constraints} \\ lb \leq x \leq ub & \textit{Upper and lower bound constraints} \end{cases}$

4 Results

The cluster method was applied to erosion rate and shear stress data from other researchers [Zreik, Sanford, Mehta et al.]. In Figure 2, erosion rate data from two experiments by Zriek et al. 1998 are compared to simulated values generated by the cluster method. As per the test method, erosion rate was measured for two nearly identical manufactured samples (observations 1 and 2 in Figure 2) under different test procedures. For sample 1 shear stress was incrementally increased over four intervals from 0:3 *Pa* up to 1:0 *Pa*. For sample 2, shear stress was held constant at 1:0 *Pa* in all the steps. Probability parameters obtained from the first set of data (observation 1) were used along with the total material eroded in the second set of data (observation 2) to estimate the erosion pattern for a the second test arrangement. The weight of material eroded in the first step in simulation 2 is larger than the total material eroded in 9 steps of the same shear stress level (level 4) in simulation 1. This illustrates the significance of shear stress history in affecting subsequent erosion rates.

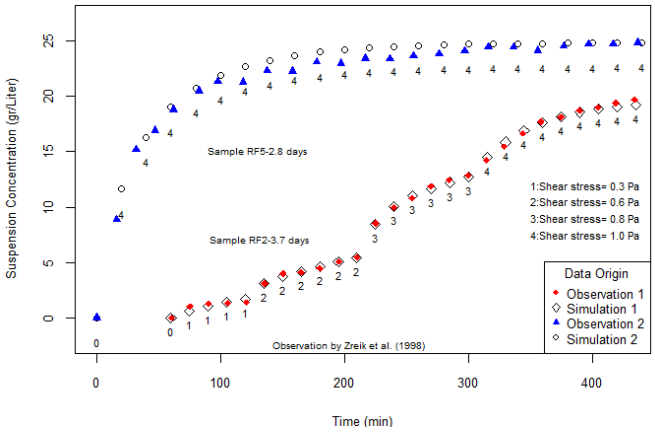

Fig. 2. Comparison of data observed by Zreik et al. with data predicted by the model.

5 Conclusion

The proposed cluster method can be used for analytical interpretation of erosion test results for different forcing sequences. This approach offers significant utility for quantifying erosion measurements in terms of less subjective or time dependent than has been previously shown. However future refinements to the method still remain: [1] The problem is ill-posed (results are sensitive to initial values) as typical for inverse problems and there is no unique optimal solution. Nevertheless it is believed that modifications in the design of experiments and the shear stress level steps therein, can make it possible to extract the most interpretable results from the set of possible solutions. [2] Further research into the application of a probabilistic model must take the magnitude of shear stress at each level into account.

References

[1] Jochen Aberle, Vladimir Nikora, and Roy Walters. Effects of bed material properties on cohesive sediment erosion. Marine Geology, 207(1):83 93, 2004.

[2] Trimbak M Parchure and Ashish J Mehta. Erosion of soft cohesive sediment deposits. Journal of Hydraulic Engineering, 111(10):13081326, 1985.

[3] Lawrence P Sanford. Uncertainties in sediment erodibility estimates due to a lack of standards for experimental protocols and data interpretation. Integrated environmental assessment and management, 2(1):2934, 2006.

[4] Lawrence P Sanford and Jerome P-Y Maa. A unified erosion formulation for ne sediments. Marine Geology, 179(1):923, 2001.

[5] Diana A Zreik, Bommanna G Krishnappan, John T Germaine, Ole S Madsen, and Charles C Ladd. Erosional and mechanical strengths of deposited cohesive sediments. Journal of Hydraulic Engineering, 124(11):10761085, 1998.

On the rehabilitation of eroding mangrove-mud coasts

J. C. Winterwerp[1)]

[1)] Deltares and Delft University of Technology, PO Box 177, 2600MH Delft, The Netherlands; han.winterwerp@deltares.nl

Mangroves belong to the most valuable wetland ecosystems in the world, supplying many so-called ecosystem services, amongst which solid coastal protection, spawning and nursery grounds for many marine species, and large carbon sequestration. Yet, mangroves are under severe pressure, and world-wide their habitat decreased from 32 million ha in 1950 to 15 million ha today.

This loss of mangrove habitat is often accompanied by severe coastal erosion, at rates of several 10s m/year, up to 100 m/yr at some locations in Indonesia. Worldwide, many 1000s km of coastline are affected, and living conditions for numerous people are endangered. The two main reasons for the loss of habitat and the subsequent severe coastal erosion are:

- subsidence – some places in Java suffer from 10 cm/yr of subsidence,
- conversion of mangroves to fish/shrimp ponds – it can be shown that the erection of bunds enveloping these ponds disturb the fine sediment balance such that an accelerating process of coastal erosion is set into motion (Winterwerp et al., 2005, 2013).

Furthermore, many of these ponds can be productive for 5 – 10 years only, owing to their poisoning by herbicides and antibiotics and/or salinization. Thus, valuable mangrove habitat and coastal area is lost, with no long-term sustainable future for the local habitants.

These problems continue already for decades, and many efforts have been undertaken to mitigate the loss of mangroves and coastal erosion through:

- large-scale plantation of mangroves – success rates are extremely low though (~10%),
- erection of solid seawalls, protecting the hinterland – also these seawalls are not very successful.

In this paper we sketch the enormity of the problem, explain the sequence of events that cause such severe erosion in response to thoughtless land-use, and reason why classical coastal protection solutions do not work.

Coastal erosion in British Guyana – collapsing hard structure which should protect the hinterland.

A drowning village on Java (Timbul Sloko) – this photo was made at low water!

References

J.C. Winterwerp, W.G. Borst, M.B. de Vries, 2005. Pilot study on the erosion and rehabilitation of a mangrove mud coast. Journal of Coastal Research, Vol. 21, No 2, pp 223-231.

J.C. Winterwerp, P.L.A. Erftemeijer, N. Suryadiputra, P. van Eijk and Liquan Zhang, 2013. Defining eco-morphodynamic requirements for rehabilitating eroding mangrove-mud coasts. Wetlands, DOI: 10.1007/s13157-013-0409-x, Volume 33, Issue 3 (2013), pp 515-526.

Characterization of sediment erodibility in an urban harbor: Newark Bay, NJ, USA

Lawrence Sanford, Jason Magalen, Edward Garland, James Wands, and Eugenia Naranjo

The talk will be on recently completed Sedflume erosion work carried out in Newark Bay by Sea Engineering Associates and analysis of that data relative to bottom sediment texture, water depth, location, bulk density, and plasticity. Additional laboratory tests were carried out to characterize the erodibility of consolidating slurries of NB muds, with similar sample characterizations. I am currently working on comparing the results to Han's general theory of erodibility.

Development of advanced instrument for measuring the erosion rate of natural sediments

Hong Ryul Ryu[1,*], Seung Oh Lee [2], Kyu-Nam Hwang [3]

[1]Department of Civil Engineering, Chonbuk national university, Dukjin-dong, Dukjin-gu, Jeonju, 561-756, Korea
[2]School of Urban and Civil Engineering, Hongik university, Sangsu-dong, Mapo-gu, Seoul, 121-791, Korea
Email: seungoh.lee@hongik.ac.kr
[3]Department of Civil Engineering, Chonbuk national university, Dukjin-dong, Dukjin-gu, jeonju, 561-756, Korea
Email: khwang@chonbuk.ac.kr
[*]Corresponding author: Email: ryu1543@chonbuk.ac.kr

Keywords: critical shear stress, erosion rate, imaging method, natural sediment.

Introduction

When the accurate estimation of geomorphologic change in coastal regions occurred by the transportation of accumulated sediments is needed, it is asked the relationship between the shear stresses and erosion rates of bed surface materials. In order to identify such erodibility of bed surface materials, various approaches like laboratory and field tests have been attempted. Field experiments are, however, hard to measure in case of climatic change such as flood or storm. Therefore, many researches have been carried out to determine the erosion parameters (critical shear stress, erosion rate, etc) in laboratory experiments. In early laboratory experiment studies, there was some drawback of visual observation by the subjective judgment of the researcher but recently the erosion rate measurement apparatus have been developed using ultra-sonic sensor, laser, optical sensor and so on. However, there were some defects in each method such as interference, opaque sight and so on despite of their expensive cost. Thus, we have designed, constructed, and examined an apparatus to measure erosion rate and critical shear stress of bed surface sediments with low expense, which is called the automated sediments erosion rate apparatus (ASERA). As the first stride of this study, the ASERA has been examined through a series of experiments to verify its efficiency with non-cohesive and cohesive sediments.

ASERA System

The ASERA is consisted of a flow circulation system, a measuring system for flowrate, pressure and water temperature, and the computer aided control system to protrude the sediment using the digital image processing as shown in Fig 1. The flume was 275 cm long, 20.32 cm wide, and 5.08 cm deep having a circular inlet and subsequent transition section and the walls of test section were made of transparent fiber glass, enabling to take images of erosion process. Electro-magnetic flowmeter (measurement range: 0-200 m^3/hr with 0.5 % uncertainty) is installed at the end of circular pipe zone with distance of 10.16 cm from the entrance of rectangular pipe zone and thermometer is installed at downstream of 90 cm of the center of hole. Two pressure transmitters (EJA 110 model in the YOKOGAWA corp. for 0~10000 Pa and EJA 120A for 0~200 Pa within an uncertainty of 1 %) were set up at a distance of ±35 cm (upstream and downstream) of the center of hole in the middle of flume. Flowrates, temperature and pressure differences were acquired through NI-DAQ USB-6008 with frequency of 10 Hz on the master computer. Automatic measurement system of sediment surface height and mechanical system to protrude sediment sample are associated with the imaging method using high quality CCD camera, thus the sediment sample can be pushed up according to the threshold condition and the difference between its height and channel bottom elevation can be maintained to be of 0.5 mm. Both sides of test section are made with an acryl acid resin to record images and measure with the eye and the top side of test section is also made with same material to mount laser pointers for measuring eroded depths.

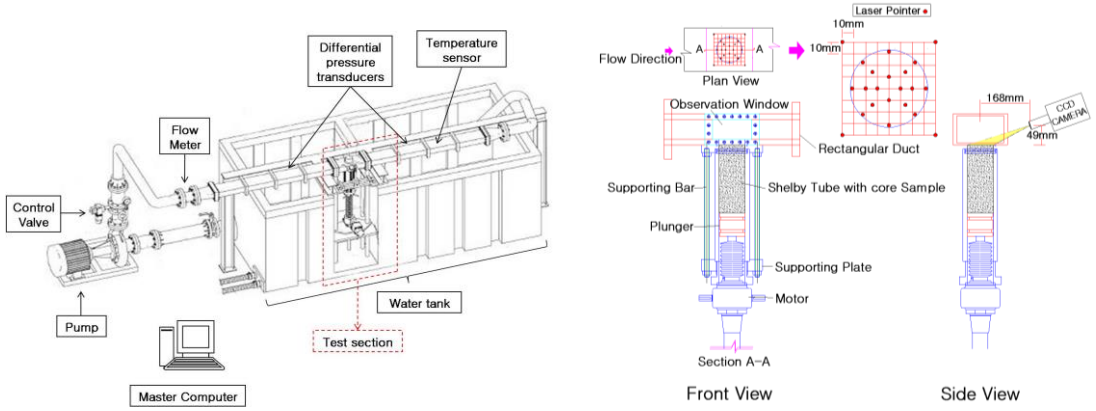

(a) Schematic of the ASERA (b) Schematic of the test section

Fig 1. Views of the ASERA

Experimental Results

Prior to the erosion experiments, tests for hydraulic characteristics of ASERA have been carried out with various flow conditions and then, a series of erosion experiments to verify its efficiency have been performed using a non-cohesive and cohesive sediments samples. 11 and 5 different uniform grained sediments of non-cohesive sediments (d_{50}=0.082~2.58 mm) were used in the verification to evaluate the critical shear stress and erosion rate, compared with the previous studies(Shields, 1936 ; Einstein, 1950 ; Einstein-Brown, 1950) as shown in Fig 2. In the case of cohesive sediment tests, 3 kinds of commercial clays(celadon porcelain clay, white porcelain clay, porterry clay) having a uniform density with depth used bed materials and before the erosion experments executed, the physico-chemical properties(particle size, mineralogical composition, % of organic material, bulk denstiy, yield stress, viscosity and CEC et al.) of bed surface samples were examined to estimate the properties of bed surface. Then, erosion experiments were executed to measure the critical shear stress and erosion rate on uniform bed condition.

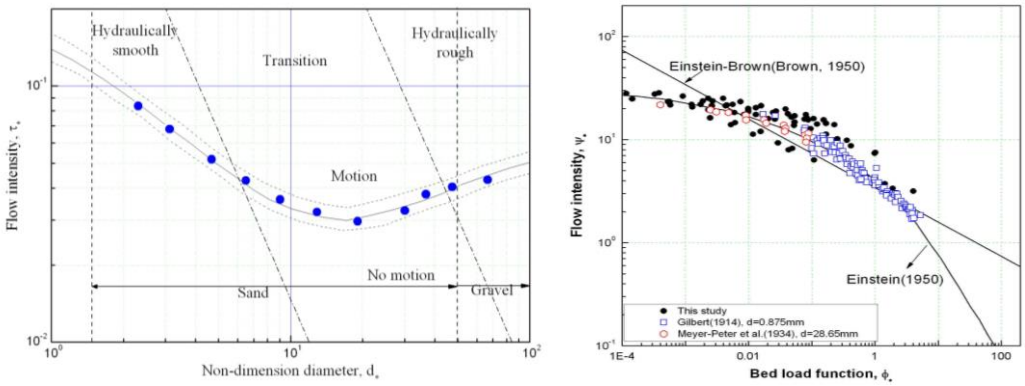

Fig 2. Comparisons of experimental results versus previous studies for noncohesive sediements

Concluding Remarks

With the ASERA, laboratory experiments were carried out to show the effieciency and practicality. According to the experimental results for the critical shear stress and erosion rate with noncohesive and cohesive sediments showed good agreement with previous studies. These result means the imaging processing method applied in the ASERA can improve the defects in the past and provide more accurate erosion rate, therefore, which would be made better use of analysis of erosion characteristics in the field.

Acknowledgments

This research was a part of the project titled 'Development of coastal erosion control technology', funded by the Ministry of Oceans and Fisheries, Korean.

Cumulative effect of erosive events increases erodibility of consolidated mud

G. Mariotti, K. Valentine, S. Fagherazzi

Boston University, Department of Earth and Environment, Boston, MA, 02215

Long term mud erosion and settling experiments were performed in two identical annular flumes, aiming to understand the behavior of a mud bed subject to periodic disturbances. A sludge of industrial montmorillonite clay with 75% water content was placed on the bottom of the flumes and salty water was gently poured on it. Each flume was subject to erosion tests, consisting of eight, ten minutes long, steps of constant velocity, resulting in bed shear stresses ranging from about 0.1 to 0.4 Pa. After each erosion test, sediments were allowed to settle in place. Erosion tests were performed every day for 80 days, except for a 24 day period after 36 days from the start of the experiment. Suspended sediment concentrations ranged from 0 to 0.6 g/l, values commonly found in mudflats under tidal currents and moderate storms. Fluid mud conditions were never experienced.

Both experiments showed similar trends, supporting the validity of the results. The mud response to the erosive tests did not reach a steady state by the end of experiments (Figure 1). Mud erodibility, computed as the amount of sediment resuspended at the end of each erosion test (at 0.4 Pa), decreased during the first 10 days, reflecting consolidation of the bed. After reaching a minimum value, erodibility showed an increasing trend with time. This trend was characterized by fluctuations, i.e. in some occasions erodibility decreased over the course of few days. The 24 four days period without erosion considerably decreased mud erodibility at low shear stress (0.1 Pa). However, this period did not change mud erodibility at high shear stress (0.4 Pa).

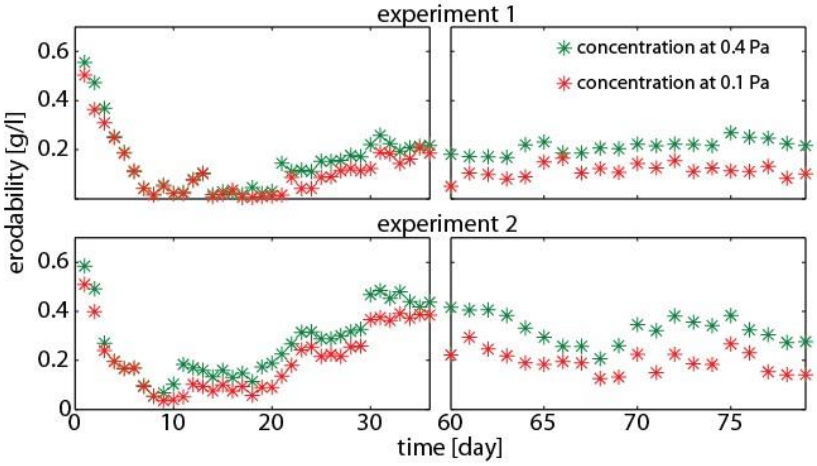

Figure 1. Erodibility (expressed as suspended sediment concentration at a fixed shear stress condition), as function of time. Each tank was eroded every day, expect for a 24 days window (day 36 to 60). At day 30, the mud in tank 2 was involuntary pocked before the erosion test, resulting in the sharp raise in erodibility.

The observed behavior cannot be explained with a deterministic approach. The erodibility of a mud bed subject to consolidation and the same erosive forcing is expect to decrease monotonically with time. We propose that the increase of erodibility with time stems from a combination of random localized erosion swipes and cumulative effects of such erosions. While the majority of the bed experienced the same maximum shear stress (0.4 Pa), small areas of the bed randomly experienced shear stress higher than the average value. Sediments eroded by the swipes settled uniformly on the bed, did not have enough time to consolidate and were resuspended during the following erosion by the average shear stress. As a result, the bulk erodibility stems from the balance between the overall consolidation trend and the cumulative effect of the swipes, explaining the fluctuations and the general increasing trend (Figure 1).

The mud response to the erosion test is expected to reach a steady state once the fluid mud regime is reached, resembling the experiments of Winterwerp et al. (1993). Since our experiments were performed on a placed rather than deposited bed, they likely reproduce the behavior of well consolidated mud beds. In conclusion, our results suggest that well consolidated beds subject to multiple erosive events might be more erodible than expected.

References

Winterwerp, J. C., et al. (1993), A laboratory study on the behavior of mud from the Western Scheldt under tidal conditions, in *Nearshore and Estuarine Cohesive Sediment Transport*, edited, pp. 295-313.

Artificial oyster reefs to mitigate erosion of tidal flats

B.C. (Bram) van Prooijen[1*], N.D. (Nicolette) Volp[1], J.T. (Jasper) Dijkstra[2], T. (Tom) Ysebaert[3,4]

[1]Department of Hydraulic Engineering, Faculty of Civil Engineering and Geosciences, Technical University of Delft, The Netherlands.
[2]Deltares, Delft, The Netherlands
[3]Netherlands Institute of Sea Research (NIOZ), Yerseke, The Netherlands
[4]Institute for Marine Resources and Ecosystem Studies (IMARES), Yerseke
[*]corresponding author: Email: B.C.vanProoijen@TUDelft.nl

Introduction

The Oosterschelde is a mesotidal basin in the southwestern part of the Netherlands. After a large flood in 1953, several dams and a storm surge barrier were built to prevent the region against future flooding from the North Sea. The constructions were completed in 1986. As a result, tidal range, tidal volume, tidal currents and sediment exchange with the ebb-tidal delta reduced significantly, leading to continuous erosion of the tidal flats.

These tidal flats are however valuable habitats as they provide essential ecosystem functions and services: recycling of organic matter and nutrients from terrestrial and marine sources, primary production, sustaining benthic organisms that are food to fish and waterbirds. Additionally, the flats form a buffer zone between deeper channels and the higher-lying vegetated habitats, protecting the latter by dissipating wave energy. Because of these services, tidal flats are worldwide protected by international conventions and legislations. The flats in the Oosterschelde are protected by the European Natura2000 legislation.

To stop the erosion of the flats in the Oosterschelde, large-scale interventions like removing the storm surge barrier and compartmentalization dams would be required. Such large-scale measures are however costly and their feasibility is uncertain. Therefore, other, smaller-scale measures to mitigate the erosion are sought for. Artificial oyster reefs are an example of such mitigation measures. Such reefs dissipate wave energy and should therefore reduce erosion rates at the lee side of the reef. Additional to the reduction in erosion, these reefs are meant to enhance the local habitat around the reef and it is expected that the reefs grow by natural recruitment of young oysters.

Three pilot reefs were built in the Oosterschelde in 2010 with the following dimensions: length × width × height = 200m × 10m × 0.20 m, see Figure a. Measurements have been carried out to determine the effect on hydrodynamics (waves and tides), suspended sediment concentration and morphology. Biological measurements, like the recruitment on the reef, are carried out as well but not considered here.

The aim of this study is to understand the effects of the reef on hydrodynamics and wave characteristics, subsequently on sediment transport and finally on tidal flat morphology. The ultimate goal is to develop guidelines for the design of oyster reefs that result in a reduction in erosion and enhance the ecological value of the surroundings.

Measurements and Interpretation

Water level and wave measurements were carried out at locations in front of and behind the reef. These measurements show that, as expected, the waves are only impacted by the reef for a specific range of water levels. Figure b shows the wave and water level measurements at locations in front of and behind the reef. We can identify three regions:

A waves are fully blocked by the reef;
B waves are dissipated by the reef;
C the reef has no influence on waves.

The separation line between area B and C starts at the top of the reef and has a slope of 0.2. This slope is too small to be interpreted as a breaker criterion only. It contains dissipation processes by partly blocking of the wave in front of the reef; bed friction on the reef and turbulence generation behind the reef. Waves at the front of the reef that are in region A and B, dissipate to the red line.

Sediment transport was not directly measured. However, the effect of the reef on sediment transport can be estimated by considering the Shields parameter. We consider this dimensionless bed shear stress to be fully dominated by waves. Effects of tidal flow will be discussed later. As the Shields parameter depends on the water depth and wave height, conditions for a certain bed shear stress form a line in the diagram of Figure b. The line for the critical Shields parameter (θ = 0.04) is plotted in Figure b. On the left side of this line, no sediment transport takes place; on the right side there is sediment transport. Lines for higher bed shear stresses are plotted as well. Although the reef does not affect the waves for all conditions, we see that the reef is effectively dissipating the waves for conditions where sediment transport takes place.

The area of influence of the reef for initial erosion/sedimentation depends on the height of the reef, the slope of the tidal flat, water level and wave height. It can be shown that the area of influence can be approximated by the area behind the reef where the bed level is lower than the level of the top of the reef. This is verified with measurements of bathymetry development. Figure c shows the bathymetric changes of the area around the reef for the period June 2010 till October 2012. In general, the region around the reef is eroding. In the lee side of the dominant southwestern wave direction, erosion stopped and even some sedimentation takes place. It is noteworthy to consider the natural sand ridge as well. The ridge is moving in northeastern direction. Erosion is limited in the lee side of the ridge for the region where the bed level is lower than the top of the ridge. Furthermore, the subchannel is silting up.

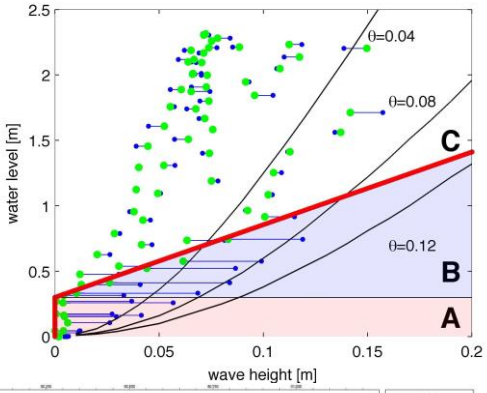

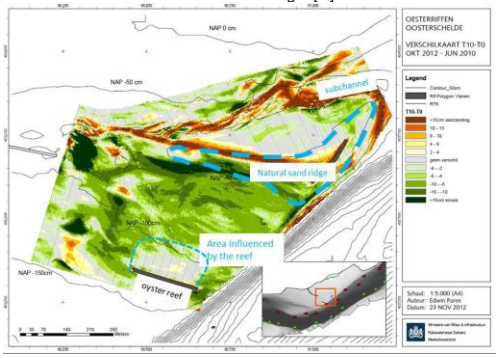

***(a)**: Bird's eye view of the oyster reef.*
***(b)**: Water level versus wave height. The blue dots represent the locations in front of the reef; the green dots the ones at the lee side. The patches indicate the three regions (A, B and C) as described in the text. The curved black lines represent the combinations of water levels and wave heights with equal Shields parameter θ.*
***(c)**: Bathymetric change over the period June 2010 till October 2012. The artificial reef is indicated as well as the natural sand ridge. Green is erosion and red accretion.*

Conclusions

Oyster reefs are relatively low epibenthic structures. The reefs dissipate waves therefore only during a relatively short period of the tide: the period with local low water depths. This is however the period where waves result in the largest bed shear stresses. A reduction of erosion (even some accretion) is therefore found at the lee side of the reef. The effect is limited to approximately the region where the bed level is lower than the level of the top of the reef. This implies that the region of influence is large for flats with small bed slopes and small at steep slopes. The measurement period was too short to measure long-term effects of the reefs on tidal flat morphology. A feedback between the morphology on hydrodynamics is therefore to be considered. This will be further investigated by measurements around long living (> 20 years) natural reefs and by numerical modeling.

Río de la Plata fine sediment transport main patterns

M. Fossati[a], F. Pedocchi[a], F. Cayocca[b] and I. Piedra-Cueva[a]

[a]Instituto de Mecánica de los Fluidos e Ingeniería Ambiental, Facultad de Ingeniería, Universidad de la República, Montevideo, Uruguay.
[b]Institut Français de Recherche pour l'Exploitation de la Mer (IFREMER), Francia
mfossati@fing.edu.uy, kiko@fing.edu.uy, Florence.Cayocca@ifremer.fr, ismaelp@fing.edu.uy

1. Introduction

The Río de la Plata (RP) (Figure 1) is a large water body that borders with Argentina on the South and with Uruguay on the North. 97% of its continental water inputs come from the Paraná and Uruguay rivers with an annual mean discharge of 22,000 m^3/s. The RP has complex river-estuarine-oceanic dynamics and it is classically divided into two regions separated by a bathymetric feature known as Barra del Indio. This transverse feature crosses the RP width from Montevideo on the North to Punta Piedras on the South shore. Barra del Indio marks the limit beyond which both the river section and the bathymetry suddenly increase (Figure 1), and it is also the location of the salinity front (Sepúlveda, et al., 2004). The RP water circulation is dominated by a fluvial regime in the inner zone, while micro-tidal estuarine dynamics dominate the outer zone (mixing zone). The suspended sediment load arrives to the RP mainly from the Paraná river, supplying and average of 160 million tons/year of fine sand, silt, and clay. The fine sands mostly settle in the innermost part of the RP and are responsible for the progradation of the Paraná Delta Front (Menéndez and Sarubbi, 2009). The fluvial fine cohesive sediments are further advected into the inner region of the RP. Using satellite data, Framiñan and Brown (1996) concluded that the turbidity front location is related to the RP bathymetry, and it coincides with the 5 m isobath at the southern coast following the Barra del Indio geometry across the river. Other than this observation, the limited amount of in situ data and scarce use of regional scale sediment dynamics models have seriously limited the understanding of the processes dominating the fine sediment dynamics and its main patterns.

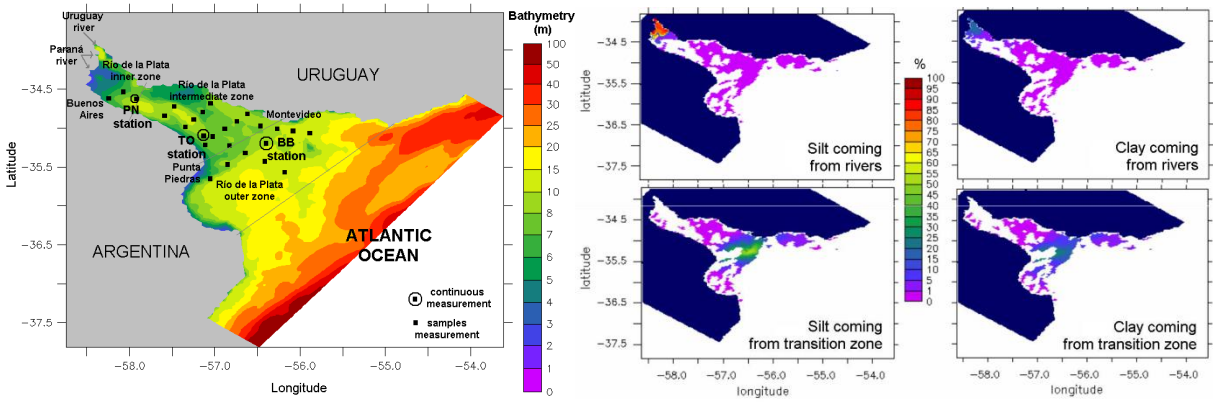

Figure 1: *Left panel: Bathymetry, location, measurements stations, and zones of the Río de la Plata. Right panel: Bottom sediment percentages of the silt and clay fractions coming from rivers and the transition zone after a one year simulation.*

This paper investigates the main fine sediments transport patterns in the intermediate, transition (frontal) and outer zones of the RP. The methodology combines the analysis of new field measurements together with new simulation results from numerical modeling. The new data include hydrodynamic (temperature, salinity, currents) and turbidity time series over several months in 3 stations (PN, TO, BB, Figure 1), vertical CTD and turbidity profiles acquired during 6 campaigns spanning 13 months, and bottom samples from 26 stations. The MARS3D hydrodynamic (Lazure and Dumas, 2008) and sediment dynamics (Le Hir et al., 2011) model was implemented with a 3 km spatial resolution configuration and 10 vertical sigma levels over the entire RP, down to 200 m waterdepth offshore. This configuration takes its boundary conditions from a 2D 10 km resolution configuration spanning over the entire continental shelf, from 55°S (Malvinas) up to 26°S (southern Brazil), in order to account for the regional circulation. The model computes erosion, advection and deposition of several sediment classes (clay and silt were simulated in this case). Erosion due to wave action is taken into account using the SWAN model (Booij et al, 1999). The hydrodynamic and wave models were first calibrated using several measurements of water elevation, ADCP currents profiles, salinity and significant wave height in different areas

of the RP. Several sensitivity analyses (erosion rate, bottom friction, settling velocity) were performed in order to adjust an optimal set of calibration parameters. Turbidity data were then used in order to calibrate the sediment dynamics model. The clay and silt sediment fractions were simulated considering different settling velocities.

2. Methodology

The information collected by water samples, bottom sediment samples, as well as the CTD profiles (all collected during fair weather conditions) were analyzed to investigate the sediment parameters variability between campaigns and the spatial variability over the RP. The turbidity time series were analyzed and correlated with the bottom shear stress (tidal currents and waves) obtained from the numerical models. The correlation between the turbidity and salinity profiles collected in the transition and outer RP zones were computed in order to investigate the influence of stratification on turbidity. Following the ternary diagram proposed by Flemming (2000), a new textural classification was obtained from the newly assessed bottom sediment size distribution.

A two-year period was simulated with the model using silt and clay sediment fractions. The initial bottom sediment fractions and river inputs were marked according to their area of origin and tracked throughout the run. The results allowed to describe the role of the different sediment sources and the relative contributions of river inputs and local erosion on the overall suspended material dynamics of the RP.

3. Results and Conclusions

The analysis of the numerical model results together with the collected data allowed to define several zones exhibiting different types of sediment dynamics in the RP. In the inner zone, the sediment dynamics are mainly influenced by the fluvial discharges. In the intermediate and outer zones, bottom erosion and deposition processes determine the suspended sediment characteristics. The southernmost part of the intermediate zone close to the Argentinean coast is dominated by the astronomical and meteorological tides, while the zone close to the Uruguayan coast is dominated by wave action. In addition, the northern coast exhibits an accretion trend, while the southern coast exhibits an erosive trend. The outer zone dynamics are governed by wave action, with the vertical salinity stratification determines the vertical structure of the suspended sediment profiles. Sediment deposition dominates the front area and the outer zone of the RP with the exception of limited areas close to the Argentinean coast and the shallow zones in the northern RP, where erosion dominates.

The sediment tracking procedures showed that most of the rivers sediments are deposited in the inner RP (Figure 1). The suspended sediment transport in the intermediate RP is regulated by a continuous cycle of advection, sedimentation, deposition, and erosion processes dominated by tides (with intensification during storms). These reworking processes explain how bottom sediments from the inner zone progressively move towards the landward part of the intermediate zone. Bottom sediments from the intermediate zone are transported through two different pathways depending on their origin: sediments originated on the northern side are strictly transported along this side while sediments originated on the southern side are transported through the entire cross-section. Within the transition zone deposition dominates and a sediment accumulation area exists. In the outer zone the sediment dynamics are mainly dominated by the erosion of the bed during storms. During storms large amounts of sediments are picked up, inducing high turbidity levels. When the storm ends, these sediments are redistributed by the three- dimensional estuarine currents and ending mainly in the coastal areas of the RP. The typical time scale of this redistribution process is of approximately one week.

References

Booij, N., Ris, R. C., Holthuijsen, L. H., 1999. A third-generation wave model for coastal regions, 1. Model description and validation. *Journal of Geophysical Research*, vol 104, N°. C4, April 15, 1999.

Flemming, B. W. (2000). A revised textural classification of gravel-free muddy sediments on the basis of ternary diagrams. *Continental Shelf Research* 20:1125–1137.

Framiñan M., Brown O., (1996). Study of the Río de la Plata turbidity front, Part I: spatial and temporal distribution. *Cont. Shelf Research*. 16:727-742.

Lazure, P., Dumas, F. (2008). An external–internal mode coupling for a 3D hydrodynamical model for applications at regional scale (MARS). *Adv Water Resources*, Volume 31, Issue 2, Feb 2008, 233–250.

Le Hir P., Cayocca F., Waeles B. (2011). Dynamics of sand and mud mixtures: a multiprocess-based modelling strategy. *Cont. Shelf Research.* 31:135-149.

Menéndez, A & Sarubbi, A. (2009) A Model to Predict the Paraná Delta Front Advancement, in: *RCEM 2009 Proceedings of the River, Coastal and Estuarine Morphodynamics*, Argentina, September 2009.

Sepúlveda H., Valle-Levinson A., Framiñan M., (2003). Observations of subtidal and tidal flow in the Río de la Plata Estuary. *Cont Shelf Research*. 24:509 –525.

Experiments and numerical modelling of mixed-sediment consolidation

Florent Grasso, Philippe Bassoullet, Pierre Le Hir and Philippe Cann

IFREMER – DYNECO/PHYSED, Centre de Bretagne, BP 70, 29280 Plouzané, France (florent.grasso@ifremer.fr).

Introduction

The simulation of cohesive sediments requires that a time variation of erodibility due to consolidation be taken into account. Several techniques for simulating consolidation have been proposed in the literature; the simplest methods consist in: (i) splitting the sediment into layers characterized by their density and/or shear strength, and (ii) translating the consolidation into a residence time concept [e.g., Teisson, 1991] or into a regular mass transfer with the underlying layer that is more consolidated [e.g., Le Hir and Karlilow, 1992]. Another empirical technique is based upon an increase of sediment density (or shear strength) at each time step for each layer, according to a relaxation law towards an equilibrium vertical density profile [e.g., Sanford, 2008]. Another family of consolidation closure comes from the Kynch theory, considering sedimentation as a vertical mass advection. In this case, a constitutive relationship relates the sedimentation rate to the sediment concentration and composition [e.g., Le Hir *et al.*, 2001].

The most comprehensive approach, at least for primary consolidation, comes from soil mechanics [Gibson *et al.*, 1967]. The density increase results from a vertical exchange of pore water; in this case, the forcing is the pressure gradient associated with the vertical increase of total weight after deduction of effective stress and water weight. Although numerous studies are based on Gibson's theory [e.g. De Boer *et al.*, 2007], they rarely apply to mixed sediments [e.g., Toorman, 1999; Merckelbach and Kranenburg, 2004]. Settling and consolidation processes of mud, however, are strongly influenced by sand [Torfs *et al.*, 1996]. Based on new consolidation experiments, this study aims at analysing and modelling sedimentation processes for different mud/sand mixtures.

Data and Methods

Consolidation tests were based on 55 settling column experiments carried out between 2001 and 2009 with sediment samples collected in five French bays and estuaries. Consolidation tests lasting from 20 days to 20 months were carried out in order to analyze: (i) the influence of the initial sediment sample height (from 0.1 to 1 m), (ii) the initial mass concentration Ci (from 25 to 600 kg/m^3) and (iii) the sand content (from 20 to 80%), on consolidation processes. Consolidation experiments were quantified with the temporal consolidation height and mass concentration (Ct), and the final vertical profiles of mass concentration, grain size, cohesion and water content.

Here, numerical modelling of mixed-sediment consolidation [Le Hir *et al.*, 2011] is based on Gibson *et al.*'s [1967] theory and Merckelbach and Kranenburg's [2004] work. This model simulated a natural mud consolidation experiment (sand content of 16%) with a good agreement, but it still has to be confronted to the extensive mixed-sediment consolidation dataset presented in this study.

Results and Discussion

The results for long-term (around a year) consolidation experiments were consistent between the different site locations. For a given initial mass concentration and sand content, the settling phase was delayed for initial taller samples, but the final consolidation rate was almost independent from the initial sediment sample height. As an example, the final consolidation rate in Mont Saint Michel Bay (MSMB) for muddy silts with a small sand content (<15%) was approximately 68±1% for an initial mass concentration of 219 kg/m^3 and different sample heights from 0.1 to 1 m. For a given initial sample height (1 m), consolidation rates were larger and the settling phase started earlier for low concentrated mixtures. The consolidation rates from MSMB samples varied from 90 to 45% for initial mass concentrations ranging from 66 to 392 kg/m^3. Intriguingly, consolidation tests with lower initial mass concentrations can lead to larger final mass concentrations, as illustrated on Figure 1 (compare Ci =54 kg/m^3 and Ci =405 kg/m^3). The vertical analysis at the end of the high-concentrated test revealed that the mass concentration increased on the first 30 cm, but remained almost constant downward. Hence, during the consolidation of

high-concentrated sediments, water may be "trapped" in depth by a faster surface consolidation; this process would explain the settling process limitation in the entire sediment sample.

We also analyzed the influence of sand on mixed-sediment consolidation by investigating a range of sand content varying between 20 and 80% for initial mass concentrations ranging from 200 to 600 kg/m^3. Consolidation was faster and greater for low concentrations and high sand content; it was associated with sediment coarsening at the bottom, as observed by Torfs *et al.* [1996].

These new experiments represent a rich dataset to improve our understanding of mud/sand mixture consolidation and to validate numerical modelling. The consolidation model proposed by Le Hir *et al.* [2011] is able to simulate realistic consolidation rates, vertical concentration profiles and settling acceleration due to sand. Future work will extensively compare its results to the consolidation experiments presented in this study.

References

De Boer, G. J., L. M. Merckelbach, and J. C. Winterwerp, 2007. A parameterised consolidation model for cohesive sediments. In *Estuarine and Coastal Fine Sediment Dynamics,* Maa, J. P.-Y., L. P. Sanford, and D. H. Schoellhamer (Eds.), *Proceedings in Marine Science*, 8, 243-262.

Gibson, R. E., G. L. England, and M. J. L. Hussey, 1967. The theory of one dimensional consolidation of saturated clays. *Géotechnique*, 17, 261-273.

Le Hir, P., and N. Karlilow, 1992. Sediment transport modelling in a macrotidal estuary: do we need to account for consolidation processes? In *Proceedings of the 23rd International Conference on Coastal Engineering: ICCE 1992*,pp. 3121–3134.

Le Hir, P., A. Ficht, R. Silva Jacinto, P. Lesueur, J.-P. Dupont, R. Lafite, I. Brenon, B. Thouvenin, and P. Cugier, 2001. Fine sediment transport and accumulations at the mouth of the Seine estuary (France). *Estuaries*, 24(6B), 950-963.

Le Hir, P., F. Cayocca, and B. Waeles, 2011. Dynamics of sand and mud mixtures: A multiprocess-based modeling strategy. *Continental Shelf Research*, 31, S135-S149.

Merckelbach, L., and C. Kranenburg, 2004. Equations for effective stress and permeability of soft mud–sand mixtures. *Géotechnique*, 54(4), 235-243.

Sanford, L., 2008. Modeling a dynamically varying mixed sediment bed with erosion, deposition, bioturbation, consolidation and armouring. *Computers & Geosciences*, 34, 1263-1283.

Teisson, C., 1991. Cohesive suspended sediment transport: feasibility and limitations of numerical modelling. *Journal of Hydraulic Research*, 29(6), 755-769.

Toorman, E. A., 1999. Sedimentation and self-weight consolidation: constitutive equations and numerical modelling. *Géotechnique*, 49(6), 709-726.

Torfs, H., H. Mitchener, H. Huysentruyt, and E. Toorman, 1996. Settling and consolidation of mud/sand mixtures. *Coastal Engineering*, 29, 27-45.

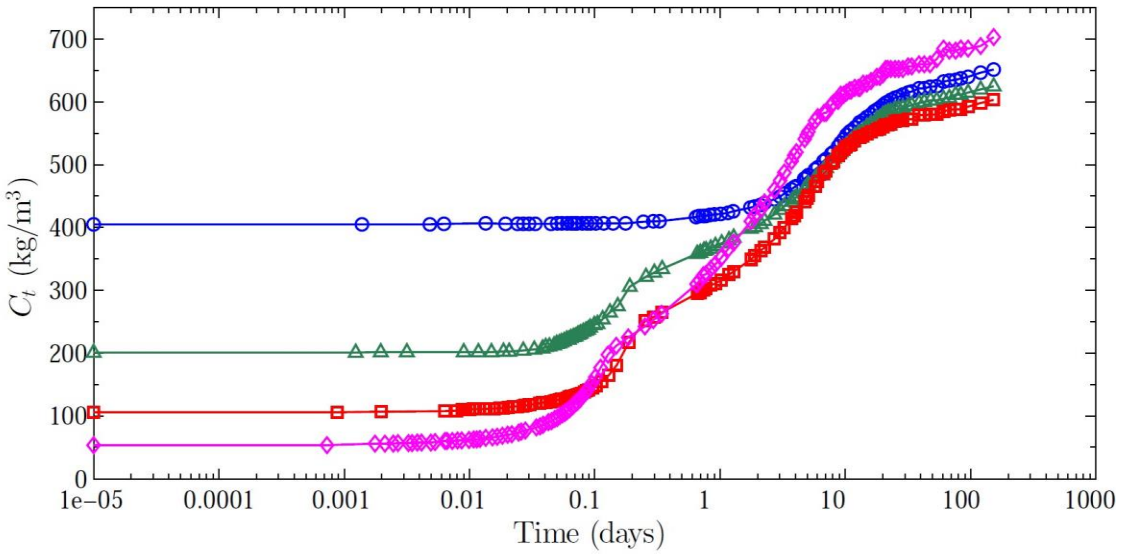

Figure 1. Time evolution of mass concentration (C_t) for four consolidation tests with the same initial sample height (1 m) and different initial mass concentrations: C_i = 54 kg/m^3 (diamonds), C_i = 106 kg/m^3 (squares), C_i = 201 kg/m^3 (triangles) and C_i = 405 kg/m^3 (circles). Sediment mixtures were collected at the Mont Saint Michel Bay in 2007, composed of muddy silts with a small sand content (around 15%).

Modeling mixed sediment transport in the bay of Brest

Alexis Beudin, Georges Chapalain and Nicolas Guillou

Laboratoire de Génie Côtier et Environnement Centre d'Études Techniques Maritimes Et Fluviales Technopôle Brest Iroise – BP5 – 29280 Plouzané, France

Introduction

Subject to river inputs, the 180 km^2 bay of Brest connected to the Atlantic Ocean through a 2 km narrow strait exhibits a two-dimensional sedimentary continuum from mud and fine sands in estuaries, sub-bays and coves to coarse sands, pebbles and boulders at the sea entrance (Fig. 1). For few decades, this sedimentary environment of the bay of Brest has been impacted by the invasive gastropod *Crepidula fornicata.* Near-bed processes induced by this benthic species were investigated experimentally in laboratory by Moulin et al. (2007) and in the field by Chapalain and Thouzeau (2007). The present modeling study deals with the dynamics of mixed sediment mediated by biotic factors with emphasis on the fate of fine fractions.

Materials and Methods

A two-dimensional horizontal (2DH) numerical model based on the hydrodynamic module TELEMAC-2D (Hervouet, 2007) and the sediment transport module SISYPHE (Villaret *et al.*, 2011) is used. The sedimentary assemblage is treated as a number of components of different grain sizes and erosive properties, i.e., non-cohesive and cohesive. Parameterizations of major effects produced by *C.fornicata*, namely macro-roughness, bed shear stress partition, water-sediment filtration and production of biodeposit are implemented. Model predictions are compared with available field point measurements collected by Chapalain and Thouzeau (2007) in the south-eastern part of the bay. A tracking technique consisting in marking bed sediment of different geographical areas is used to discriminate the various origins of a local suspension.

Results and Discussion

Flood-dominance together with a specific multi-gyre flood current pattern induce a paradoxical further seaward extension of suspended sediment during flood than during ebb (Fig. 2), and trapping of fine sediment in the coves. In relation to sediment availability on the seabed, a net efflux of suspended sediment out of the bay is predicted. At measurement points above *C. fornicata* canopy, suspended sediment is predicted during ebb to be made of mud, mostly advected from remote estuarine area, and during flood to be composed half of mud and half of very fine sand resuspended locally. Significant spring-neap tidal variations of suspended sediment concentration are predicted. Fine sediment deposition rates and accretion patterns in relation to *C. fornicata* influences are evaluated.

References

Chapalain, G. and Thouzeau, G., 2007. *Rôle des structures biogènes sur l'hydrodynamisme et les flux sédimentaires dans la couche limite de fond*, PNEC, 24 p.

Guérin, L., 2004. *La crépidule en rade de Brest: un modèle biologique d'espèce introduite proliférante en réponse aux fluctuations de l'environnement*, PhD thesis, Université de Bretagne Occidentale, 426 p.

Hervouet, J.M., 2007. *Hydrodynamics of free surface flows : modelling with the finite element method*, Wiley, 340 p. Le Berre, I., 1999. *Mise au point de méthodes d'analyse et de représentation des interactions complexes en milieu littoral*, PhD thesis, Université de Bretagne Occidentale, 236 p.

Moulin, F., Guizien, K., Thouzeau, G., Chapalain, G., Mülleners, K. and Bourg, C., 2007. Impact of the invasive species, *Crepidula fornicata*, on the hydrodynamic and transport properties of the benthic boundary layer, *Aquatic Living Resources*, 15: 15-31.

Villaret, C., Hervouet, J.M., Kopmann, R., Merkel, U. and Davies, A.G., 2011. Morphodynamic modelling using the Telemac finite-element system, *Computers and Geosciences*, 53: 105-113.

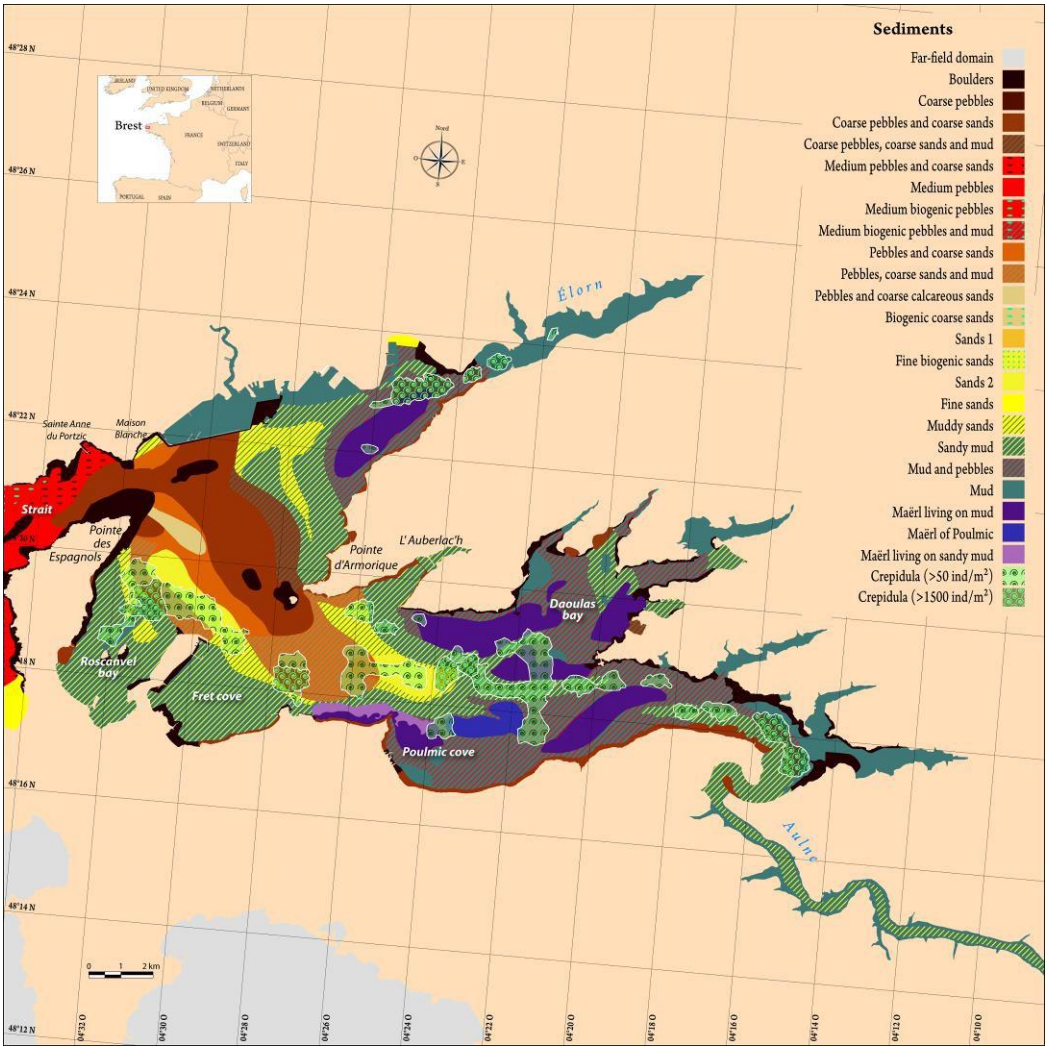

Fig 1. Superimposed maps of bed sediment (Le Berre, 1999) and <u>C. fornicata</u> covering (Guérin, 2004).

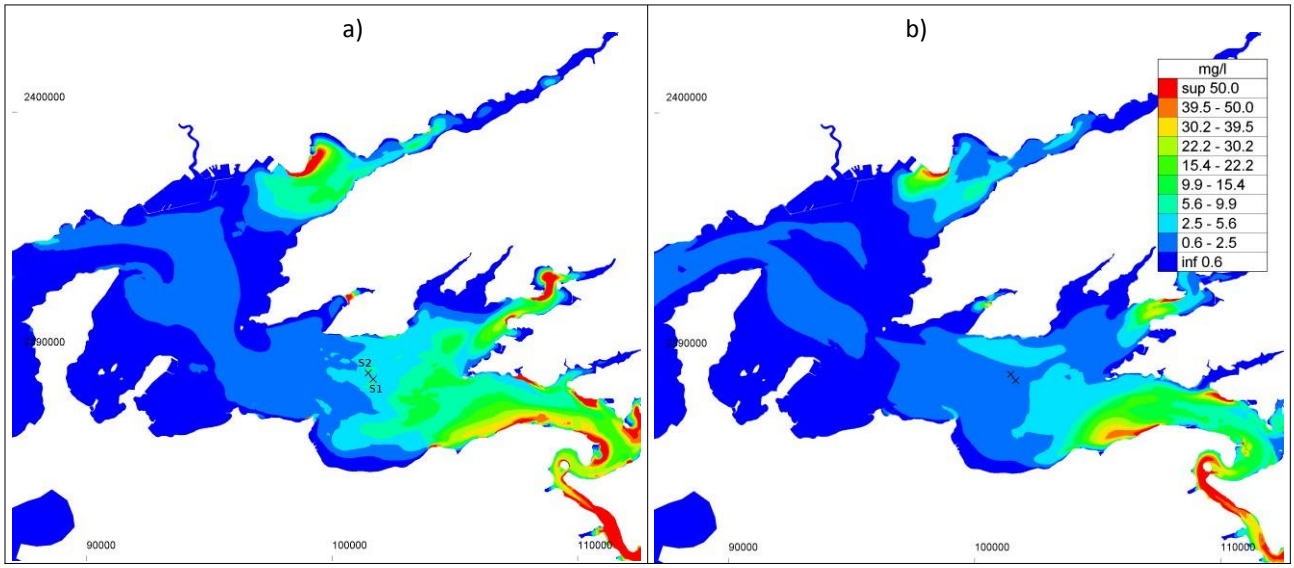

Fig 2. Depth-averaged total suspended sediment concentration (mg/l) predicted at flood (a) and ebb (b) of an average tide.

Effect of sand-mud interactions on SPM levels in and the fine sediment balance of the Dutch Wadden Sea

T. van Kessel[1], K. Cronin

Deltares, P.O. Box 177, 2600 MH Delft, The Netherlands;
[1]corresponding author, e-mail: thijs.vankessel@deltares.nl

Introduction

The Wadden Sea is an internationally renowned intertidal system providing valuable habitats for fish, birds and tourists. It stretches along the northern part of the Dutch and German coastline and the western part of the Danish coastline.

Every tide, a large water volume is exchanged between the North Sea and the Wadden Sea. Also every time, a small part of the fine sediments entering the Wadden Sea deposit on tidal flats. During periods with strong tides or storms, part of these fines resuspend and contribute to elevated SPM levels in the Wadden Sea. Also other mechanisms contribute to higher SPM levels in the Wadden Sea. On average, SPM levels in the Dutch part are about 50 mg/l, whereas SPM levels in the North Sea just outside the Wadden Sea are about 5 to 10 mg/l only.

Notwithstanding the protected status of the Wadden Sea (it is a UNESCO world heritage site and is protected under the EU water framework directive), a lot of human activities take place, such as dredging, spreading of dredged material, fishing. Also, the effect of soil subsidence and sea level rise requires the input of additional sediment to maintain average water depth and inundation times. Changes in the frequency and pathways of storms may affect wave action and the external supply and internal redistribution of sediments. Salinity levels may also change by altered freshwater inputs and changing residual current patterns, affecting residence time.

Methodology

The effect of these natural changes and human interventions on SPM levels in and the fine sediment balance of the Wadden Sea is very relevant for the management of this area. Changes in SPM concentration, bed level and bed composition have potentially a large effect on primary production and habitat suitability. To quantify these changes, a fine sediment dynamics model of the Dutch Wadden Sea is being developed. One of the important features of this model is the application of a bed module on sand-mud mixtures that has been developed in the framework of the Building with Nature research programme.

The bed module describes the influence of in interaction between sand and mud on the erosion of such mixtures. Sand-dominated and mud-dominated regimes are discerned. Vertical stratification in the bed is taken into account (Figure 1) with a hybrid Eulerian–Lagrangian framework to reduce artificial mixing. Vertical mixing (e.g. by bioturbation of the propagation of unresolved bed forms) can be added.

Results

The INTERCOH presentation (or poster) and accompanying paper will describe results from the fine sediment model. First, it will be demonstrated how well the model is able to reproduce observed SPM levels, bed composition (Figure 2) and mud deposition (validation). Subsequently, result on several scenario's are presented, amongst which the influence of changing SPM levels in the North Sea on the sediment dynamics in the Wadden Sea, the influence of bioturbation and biostabilisation and the impact of dredging works. Finally, the main factors influencing the mud balance of the Wadden Sea will be determined.

This research has been funded jointly by Deltares and the Dutch Ministry of Public Works and is carried partly out in the framework of a Dutch-German-Danish collaborative scientific project ('PACE') on the SPM dynamics of the entire Wadden Sea including several partners in each country.

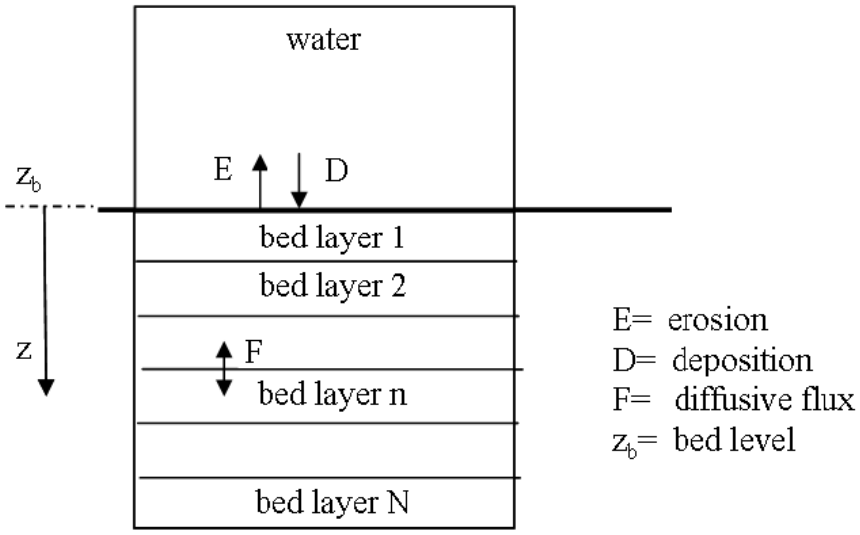

Figure 1: Schematic representation of sand-mud bed module.

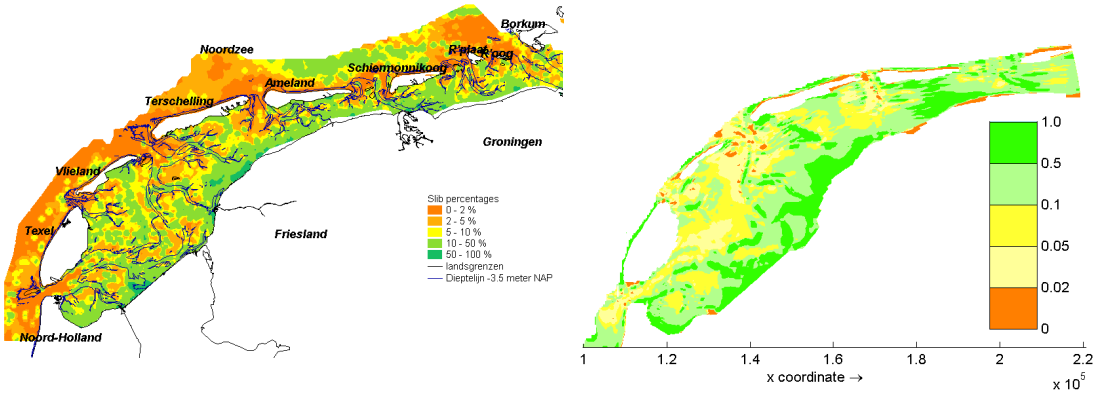

Figure 2: Observed (left) and computed (right) mud fraction in the seabed in the Western Wadden Sea.

The influence of cohesive sediments on dune development

R.J. Schindler[1,2], D.R. Parsons[2], L. Ye[2] & A.J. Manning[1,3]

[1]School of Marine Science & Engineering, University of Plymouth, Plymouth, UK. robert.schindler@plymouth.ac.uk
[2]Department of Geography, Environment and Earth Science, University of Hull, Hull, UK.
[3]Coasts & Estuaries Group, HR Wallingford, UK.

1. Introduction

The experiments presented here assess the effects of different sand:clay ratios on dune bedform development in controlled laboratory environments as part of the UK NERC-funded COHBED project.

Existing flow and sediment transport predictions for bedforms are seriously impeded by an almost complete lack of process-based knowledge of bedform behaviour in natural sediments that consist of complex mixtures of cohesionless sand and cohesive muds. Indeed, existing predictive models are entirely based on cohesionless sands, despite the fact that mud, in pure form or mixed with sand is the most common sediment on Earth (Healy *et al.*, 2002).

These relationships have been captured in bedform phase diagrams (e.g. Southard & Boguchwal, 1990; van den Berg & van Gelder, 1993; van Rijn, 1993) and parameterised in bedform predictors, which are empirical equations that relate mean flow forcing and bed sediment size to equilibrium bedform height and length (van Rijn 2007). Yet, despite decades of research, these tools are still based on highly simplified physical parameters, with simplistic assumptions that clastic sediment consists of a biologically inactive single grain size with bedforms that react instantly to changes in flow energy.

We show, *for the first time*, the profound influence of clay on the height, length, development rate and equilibrium morphology of dune bedforms.

2. Methods

Experimental Design

Experiments were undertaken at the *Total Environment Simulator* flume/wave tank facility at the University of Hull, UK. The active channel was sectioned into a 10 × 2 m area within the tank. A flat sediment bed, with varying proportions of sand:clay, was laid within the channel to 0.15 m depth. A unidirectional flow of 0.25 m depth was passed over the sediment for 10 h. A depth-mean velocity of 0.8 m s^{-1} was used throughout, corresponding to the centre of the dune regime for non-cohesive sands (*ibid*).

Run 1 used sediment with an 82:18 ratio of sand:clay. Previous experiments in the ripple bedform regime have showed that a higher clay content prevents bedform formation (Baas et al., 2013). A further seven experiments with stepwise reductions in clay content were undertaken, where the final experiment exhibited a sand:clay ratio of 4.5% (see Figure 1).

Measurement

Bedform development was monitored through ultrasonic ranging transducers spanning a 4.5 × 0.5 m swath. Flow and turbulence structure were sampled at-a-point through 5 × ADVs at 100 Hz, including a profiling system continuously adjusted to bedform height.

Suspended sediments were observed through (1) ABS profiles at 1, 2 and 4 MHz, (2) vertically spaced OBS sensors, (3) a LISST-100X and (4) physical water samples used for both gravimetrically derived suspended sediment concentrations and grain size distributions. In addition, water samples were analyzed using *LabSFLOC* (e.g. Manning et al., 2002), facilitating the measurement of the size, settling velocities and thus densities of suspended particulates, thereby allowing flocculation to be monitored throughout.

Sediment cores were taken every 0.5 h to examine evolving stratigraphy, and the spatially-varying structures of final bedform suites were assessed using multiple core samples. Grain size analyses were undertaken on sub-sections of each core.

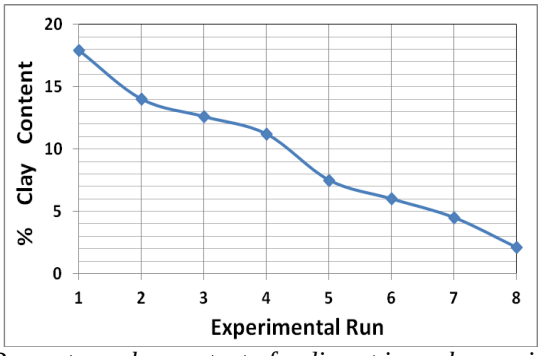

Figure 1. Percentage clay content of sediment in each experimental run.

3. Results

Experiments were completed in May 2013. Initial qualitative analyses show substantial differences in bedform type: The height and wavelength of bedforms is inversely related to percent clay content. For instance, Run 1 generated 2D ripples; Run 8 generated 3D dunes closely corresponding to non-cohesive bedforms, with other bedform types spanning the ripple-dune transition evident between each. For example, Figure 2 compares final bedforms suites after Run 4 (11.2% clay) and Run 7 (4.5%). Detailed quantitative analyses are forthcoming.

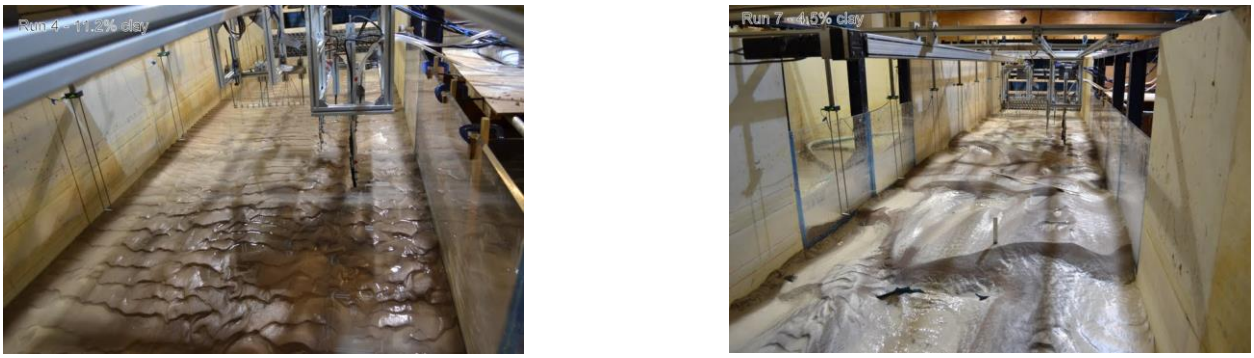

Figure 2. Final bedform suites after (left) Run 4 (11.3% clay) and (right) Run 7 (4.5% clay).

4. Conclusions

Initial results indicate that the ripple-dune transition, and all low-regime bedforms, can occur under constant flow conditions and that the proportion of clay within a non-cohesive matrix, rather than flow forcing, dictates the type of bedform generated. The experiments presented herein therefore offer a step-change in our understanding of the movement, formation and geometry of bedforms synonymous with coastal and estuarine waters globally.

Quantifying and modelling bedform dynamics, including the complexities of sediment mixtures, is key to parameterising physical processes at the flow-bed interface and ultimately to predicting natural sediment transport at local and regional scales (French, 2010). Such predictions rely strongly on accurate knowledge of relationships between the form and size of bedforms, hydrodynamic forcings, and bed material properties.
We can conclude that, if the effects of cohesive sediments are not included when they are present, predictive models will be inaccurate and in many cases misleading.

Acknowledgments

This work was funded by the UK Natural Environment Research Council (NERC) under the 'COHBED' project (NE/1027223/1).

References

Baas *et al.* (2013) *Geomorphology*, 182, 19-32.
French (2010) *Earth Surf. Proc. Landforms*, 35, 174-189.
Healy *et al.*, (2002) *Proceed. Marine Sci*, 4.
Manning *et al.*, (2002) *Cont. Shelf Res*., 27, 1080-1095.
Southard and Boguchwal (1990) *J. Sed. Petrol*., 60, 658-679.
van den Berg and van Gelder (1993) *IAS Spec. Publ.*, 17, 11-21.
van Rijn (1993) Principles of Sediment Transport in Rivers, Estuaries and Coastal Seas. Aqua Publ., A'dam.
van Rijn (2007) *J. Hydr. Engng*, 133**,** 649-667

Time scale effects that influence the behavior of silty sediments

S. te Slaa[1,2], D.S. van Maren[1,3], Q. He[2] and J.C. Winterwerp[1,3]

[1] Hydraulic Engineering Department, Faculty of Civil Engineering and Geosciences, Delft University of Technology, The Netherlands
[2] State Key Laboratory of Estuarine and Coastal Science, East China Normal University, Shanghai, China
[3] Deltares, Delft, The Netherlands

Introduction

Silt is defined as sediment in the size class between 2 and 64 μm which has a non-cohesive base mineral. Previous work (Roberts et al., 1998) suggests that the erosion behavior of silt is strongly determined by consolidation timescales, which in turn is influenced by the shear rate history. Unfortunately, this behavior is only qualitatively addressed, and terms like "pseudo-cohesive behavior" or "apparent cohesion" are used to describe erosion and consolidation processes of silt-sized material. This pseudo-cohesive behavior probably results from the low permeability of silty sediments. In low permeable sediment, over- or underpressures build up in the soil when subjected to shear. Underpressures are generated by bed shear stress over a consolidated bed, whereas overpressures exist in a consolidating bed. When over- or underpressures are dissipated within the timescale of shearing, the response of the soil is drained its behavior is non-cohesive. When the dissipation time exceeds the shearing time, the response is undrained and erosion and consolidation depict (pseudo) cohesive behavior. This study elaborates on the physical background for the timescale and shear rate dependent behavior of silt.

Methodology

The relative importance of cohesive and non-cohesive processes is investigated with consolidation experiments using silt-sized sediment. Soil properties indicate that silt is a non-cohesive material (e.g. friction angle). However, the properties of the soil dynamics can be non-cohesive or cohesive. The generation and dissipation time of excess pore water pressures defines the type of behavior. Therefore, the term pseudo-cohesion is a property of the soil dynamics whereas cohesion is a soil property.

Results of Consolidation Experiment

The dissipation of excess pore water pressures in a freshly deposited silt bed is accompanied by a small density increase (Figure 1). However, the vertical excess pore water profiles imply an upward decreasing permeability in the silt bed caused by segregation during the settling phase of the sediment. As a result of segregation, the finest particles are found in the upper layers of the deposited bed. These particles form the least permeable layer of the sediment and hence a permeability threshold "impermeable crust" is formed. The formation of such a crust is dependent on the initial concentration and grain size distribution. At high sediment concentrations, segregation is limited and the permeability of the bed is more vertically uniform.

Conclusions

Since excess pore water pressures dissipation is accompanied by a density increase, a cohesive approach in quantifying the behavior of the used silt (D_{50} = 36 μm) is justified. The ratio between the dissipation time of the excess pore water pressure and the densification of the bed cause the behavior to be cohesive. This study will further quantify the boundary conditions which determine the change in consolidation, but also in erosion, of silt from cohesive to non-cohesive and vice versa.

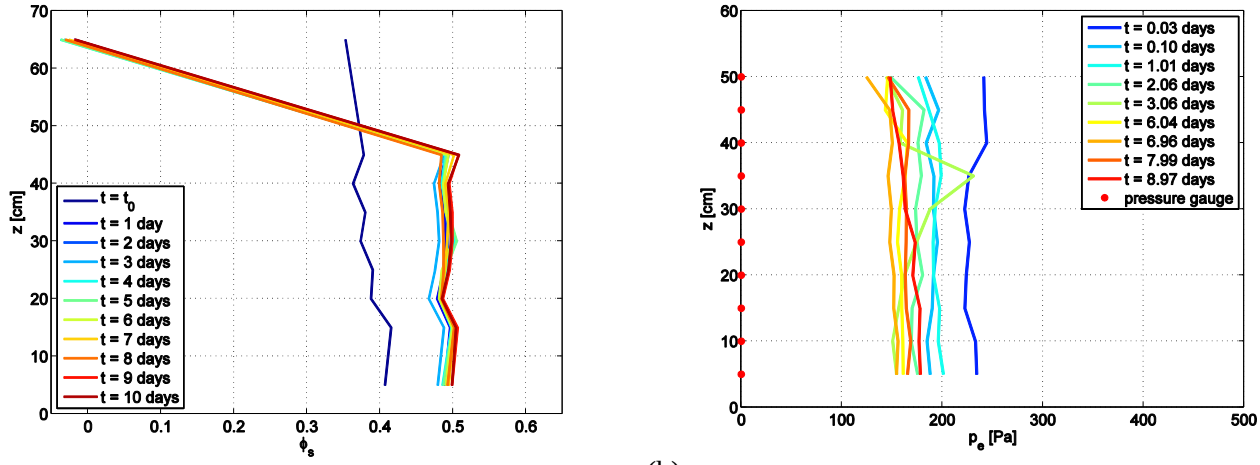

(a) (b)

Figure 1 Evolution of excess pore water profiles (a) and density (b) in time, measured in a freshly deposited silt bed with a D50 of 36 µm. The surface of the silt bed is found at a level of 52 cm.

References

Roberts, J., Jepsen, R. and Gotthard, D., 1998. Effects of particle size and bulk density on erosion of quartz particles. *Journal of Hydraulic Engineering*, 124: 1261.

Exploring electrical impedance techniques to study sedimentation and bed deposits of sand-mud mixtures

O.S. Ibikunle, A.J.S Cuthbertson, H. Haynes & W.J. McCarter

Institute for Infrastructure and Environment, Heriot Watt University (E-mail: A.Cuthbertson@hw.ac.uk)
Keywords: electrical resistivity/impedance, sand-mud mixture, formation factor, bed deposit, density

Accurate prediction of formation processes of mixed (sand-mud) sediment bed deposits, which is a common occurrence in many estuarine and near- shore coastal marine environments (Williamson, 1991), is essential in determining their transport, interactions and fate. This is of major importance for the maintenance and management of navigation channels, ports and harbours, as well as in assessing the effects of increased turbidity on water quality and aquatic habitats within these marine environments (Torfs, et al., 1996; Cuthbertson et al., 2008). One of the major obstacles to improved understanding of mixed (sand-mud) sediment bed formation under different natural flow conditions has been the availability of reliable, non-invasive, experimental measurement techniques to characterize these sediment bed deposits. Traditionally, density profiles and porosities of the resulting sediment beds from experimental sedimentation processes have been obtained by passing high energy X-rays or attenuated gamma rays through the sediment bed (e.g. Been and Sills, 1981; Ellis, 1987; Torfs, et al., 1996; Pane and Schiffman, 1997; Manning, et al., 2010; etc.). However, such X-Ray/gamma ray techniques are relatively inflexible, expensive and have potential health and safety implications. The work presented herein details a proposed experimental procedure for exploring non-invasive, electrical impedance measurement techniques to characterize the spatial and temporal variation in sediment bed structure and composition resulting from differential settling of mixtures consisting of cohesive kaolin clay and non-cohesive sand. The hypothesis for this study is that when an electric current passes through water-saturated marine sediments, the electrical resistivity of the sediments will depend on the conductivity of the pore water and the microstructure of the sediment (e.g. porosity, pore geometry, etc.), because sediment grains themselves are poor conductors. The relationship between bulk resistivity (R_S) of a saturated sediment sample, the interstitial pore fluid (Rf) and the fractional porosity (φ) is given by the Archie (1942) equation, which is expressed as a Formation Factor (FF), such that:

$$FF = \frac{R_s}{R_f} = a\varphi^{-m} \tag{1}$$

where a and m are empirically-derived factors.

The settling and depositional processes for various sand(S):clay(C) mixture compositions [% by dry weight: (i) 100S:0C; (ii)75S:25C; (iii) 50S:50C; (iv) 25S:75C; and (v) 0S:100C], mixed into slurry with 0.5M brine solution, were monitored in a 50 × 50 × 600 mm acrylic sedimentation column (see Fig. 1). Preferential settling during mixture placement was prevented by upturning the settling column prior to the settlement process being initiated. The 4-point electrode configuration (shown at five elevations E1 – E5 in the setting column, Fig. 1) consisted of two 2mm pin electrodes implanted in the settling column, in-between the square plate electrodes. This configuration allowed a profile of 4-point electrical impedance measurements to be taken at hourly intervals over a 3-day period, employing a Hewlett Packard HP4263B LCR meter with a sample frequency of 10 kHz and signal amplitude of 1000mV. Mixture temperatures were also monitored with a bead thermistor mounted on the side of the column, allowing the electrical resistivity measurements to be expressed at a standardized temperature of 20°C. To facilitate better understanding of the settling and depositional processes for different sediment mixtures, time-lapsed photographs were also taken at variable time intervals during each test (see Fig. 2).

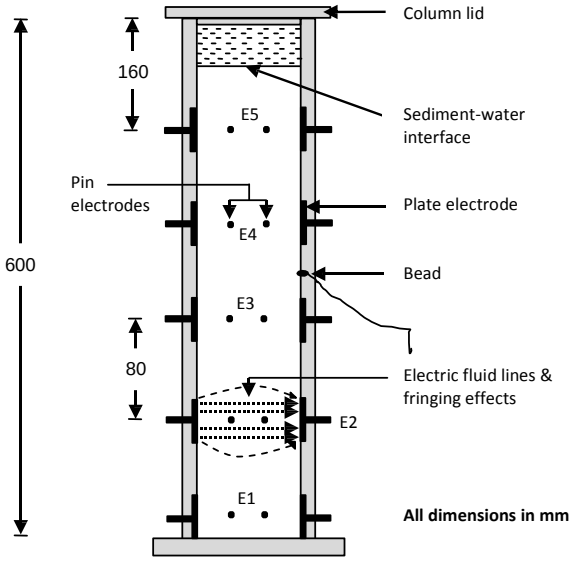

Figure 1. Sedimentation column showing electrode pairs (E1-E5) (Adapted from Blewett, et al., 2001).

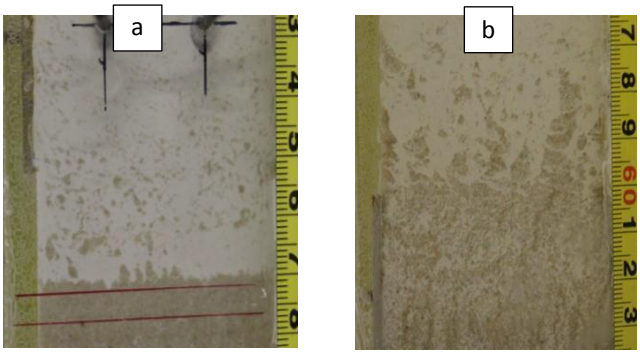

Figure 2. Images of mixed sediment deposits for (a) 25C:75S and (b) 50C:50S (at 72 hours).

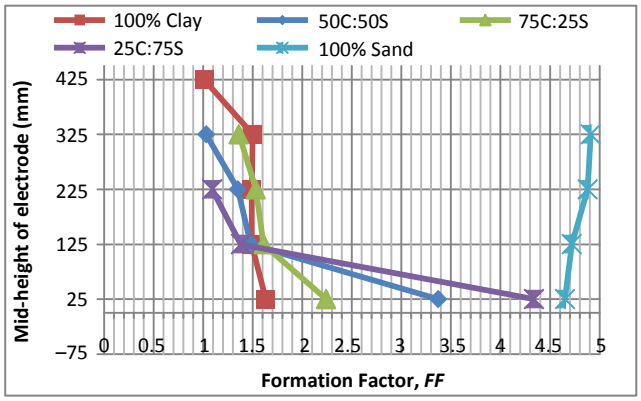

Figure 3. Density Profiles obtained by plotting FF against Electrode Elevation at 48th hour interval.

The density profiles for the deposited mixtures can be inferred through the normalized resistivity measurements obtained at electrode locations E1– E5 (see Fig. 3). In this regard, the impedance techniques employed in the current experiments agreed to a lesser or greater extent with previous observations on the effects of sand content on settling, deposition and consolidation of muds (e.g. Williamson and Ockenden, 1992; Toorman and Berlamont, 1993; Torfs, et al. 1996; Manning, et al., 2010; and Xu, et al., 2012). Therefore, despite some technical issues that must addressed when using electrical impedance techniques for characterizing mixed sediment beds, such as electrode polarization and temperature effects, the results from the current work establish that the electrical impedance technique may provide an extremely useful, non-invasive, characterization technique to study the sedimentation processes of sand-mud mixtures.

The current work to-date has concentrated on illustrating the applicability of impedance technique for characterization of mixed sediment deposits. On-going experimental studies will, however, concentrate on the quantitative interpretation of the resistivity data to better illustrate the sedimentation behavior of sand-mud mixtures. For example, the relatively coarse spatial resolution of the electrode arrangement in the existing settling column meant that detailed vertical characterization of the settling process characteristics was not possible. Thus, in order to gain higher resolution impedance measurements (and hence better characterization of the mixed sediment deposits), a larger, demountable settling column has been constructed with closely-spaced 4-point pin electrodes (with vertical spacing varying from 5mm). In addition, a novel oedometer test set-up is under development to study how consolidation process affects the bulk resistivity of mixed sediment deposits. The possibility of extrapolating the oedometer test results to obtain fractional porosity (and, by extension, density) of the mixed bed deposits would thus provide a more complete experimental study.

References

Archie, G. E., (1942). The Electrical Resistivity Log as an Aid in Determining some Reservoir Characteristics. Transaction of the American Institute of Mining and Metallurgical Engineers, Volume 147: 54-62.

Been, K., Sills, G. C., (1981). Self-weight Consolidation of Soft Soils: An Experimental and Theoretical Study. Geotechnique, 31(4): 519-535.

Blewett, J., McCarter, W.J., Chrisp, T.M., Starrs, G., (2001). Monitoring Sedimentation of a Clay Slurry. Geotechnique, 51(8):723-728.

Cuthbertson A., Dong, P., King, S., Davies P. , (2008). Hindered Settling Velocity of Cohesive/non-cohesive Sediment Mixtures. Journal of Coastal Engineering, Volume 55:1197-1208.

Ellis, D. V., (1987). Well Logging for Earth Scientists. pp 532 ed. Amsterdam: Elsevier.

Manning, A.J., Baugh, J.V., Spearman, J.R., Whitehouse, R.J.S., (2010). Flocculation Settling Characteristics of Mud:Sand Mixtures. Ocean Dynamics, 60:237-253.

Pane, V., Schiffman, R.L., (1997). The Permeability of Clay Suspensions. Geotechnique, 47(2): 273-288.

Toorman, E. A., Berlamont, J. E., (1993). Settling and Consolidation of Mixtures of Cohesive and Non-cohesive Sediments. Adv. Hydro-Sci. Eng., 1:606-613.

Torfs, H., Mitchener, H., Huysentruyt, H., Toorman, E., (1996). Settling and Consolidation of Mud/Sand Mixtures. Coastal Engineering, 29:27-45.

Williamson, H. J., Ockenden, M. C., (1992). Tidal Transport of Mud/Sand Mixtures, Laboratory Tests, s.l.: Wallingford, Report SR 257.

Williamson, H. J., (1991). Tidal Transport of Mud/Sand Mixtures. Sediment Distributions- A Literature Review. HR Wallingford, Report, Volume SR 286.

Xu, G., Gao, Y., Hong, Z., Ding, J., (2012). Sedimentation Behaviour of Four Dredged Slurries in China. Marine Georesources & Geotechnology, 30:143-156.

Sediment disposal and long term morphological impact

H. Jacob Vested[1], Morten Pejrup[2] and Rolf Deigaard[1]

[1] DHI, Agern Allé 5, DK 2970 Hoersholm, hjv@dhigroup.com, Denmark
[2] Copenhagen University, Denmark

Abstract
Graadyb tidal area is located in the northern Wadden Sea on the west coast of Denmark. Sediments are characterized as both fine and sandy. The tide is semi-diurnal with an average tide of about 1.5 m and the area is strongly influenced by wind induced water fluctuations and surface waves. The Port of Esbjerg is located within Graadyb and is subject to siltation of fine sediments within the harbour basins. The material dredged in the basins is disposed within the Wadden Sea for practical reasons and in order to avoid long term morphological impact on the tidal flats and marshlands. The objective of this paper is to present a methodology to investigate the impact of sediment disposal practices on long term morphology of an estuarine environment. The methodology is based on a combination of measured marsh land accretion data (sediment cores), numerical modelling of fine-grained sediments and the establishment of a sediment budget for the tidal area.

Introduction
Graadybs tidal area is the most northern part of the Wadden Sea. It has a surface area of about 135 km^2 and the average tidal prism (difference in water volume between low and high water) is in the order of 160 mio. m^3. The major source of input of fine sediments is the North Sea (about 60%). The remaining sources of fine sediments are local streams, primary production (organic material) and internal coastal erosion. It is estimated that the annual deposition of fine sediments is about 88,000 tonnes of dry matter, Pedersen and Bartholdy (2006).

The concentration of suspended matter in the area varies between 20-100 mg/l and is rarely below 10 mg/l. During storms it can reach up to 500 mg/l. The median grain size of the primary sediment particles is between 20-30 µm and the organic content is 10%. The deposition of fine sediments is distributed with 1/3 on the tidal flats and 2/3 on the marshland (Bartholdy and Pheiffer-Madsen;1985). The marshland accretion occurs mainly during more extreme high waters.

The harbour basins of the Port of Esbjerg make up an area of about 900,000 m^2. The basins act as sediment traps and the yearly average amount of sediment dredged amounts to 80,000 to 100,000 tonnes dry matter of fine sediments. The dredged material apart from a minor part, which is polluted, is disposed at two locations near the port area and within the tidal area. Disposal practice has been to avoid backfilling to the harbour basins and keep the sediment within the tidal area. Disposal sites are referred to as E for Ebb and F for Flood flow, respectively. I.e. during falling tide, material is disposed at E and during rising tide at F. The material disposed at E may leave the tidal area with the ebb currents and a part may return with the rising tide. The material disposed at F flows to the southern part of the tidal area where it is likely to settle.

Methodology
By means of analysis and subsequent dating of sediment cores within the tidal area it is possible to estimate the average annual accretion over periods of many years (decades). The annual accretion within the tidal area is measured in very small numbers (order of millimeters) and the variation from year to year is significant.

By analysis of sediment cores from a site within Graadyb tidal area it was found that the accretion rate in the period 1963-1986 was reduced compared to the period 1986-2003, (Andersen et al. 2011). This was a surprise in view of results elsewhere that show that tidal flats and marshlands are able to follow the sea level rise. One explanation could be that the sediment concentration in the tidal area had been reduced from the earlier period to the later.

A reduction in the average sediment concentration could be due to changes in climate especially wind climate. However, the period 1986-2003 was windier, which indicates the opposite trend. Although sediment starvation might be due to several other phenomena, one hypothesis could be that it is the maintenance dredging and disposal of the sediment, which impacts the long term morphology of the tidal flat and marsh land.

In order to examine this hypothesis the amount of sediment M, which is available in the tidal area must be evaluated. The mass M is interpreted as the amount of sediment, which is available for the vertical accretion of the tidal flats and marshlands within the tidal area. The mass M consists of the sediment in suspension plus the amount of sediment that potentially can be resuspended during a storm event.

$$\frac{dM}{dt} = (S_{IN} + S_{II} + S_{ID}) - (S_{EN} + S_{ED} + S_{EH} + \gamma S_{ID}$$

where S_{IN} is the import of fine sediment from the North Sea, S_{II} is the contribution from internal sources, S_{ID} is the sediment disposed within the tidal area, S_{EN} is the export of fine sediment to the North Sea, S_{ED} is the deposition within the area and S_{EH} is the amount of siltation in the harbour basins. γ is the fraction of the disposed material that exits the tidal area to the North Sea. By assuming that the accretion rate is proportional to the amount of sediment in the system M, the impact of different disposal conditions can be determined.

By simulation with a numerical 2D horizontal fine sediment transport model, the pathways and budgets of deposed sediment can be determined. A real year with a representative combination of weather conditions and with a full disposal practice was simulated and the fraction γ was determined. The other terms in the equation have been determined on the basis of observation of accretion rates in sediment cores. Hereby the differential equation for M can be solved and the impact of different disposal practices on the accretion rate can be assessed.

Results

The equation for the mobile sediment stock M has been solved for different disposal practices. It is shown that the decline in accretion rate can be explained by an increase in the amount of sediment dredged and thereby a relatively larger loss of sediment from the system. The equation has also been applied to assess the impact on the system from a larger demand for sediment disposal due to construction of a new harbour basin and a new sediment disposal strategy.

Conclusions

Assessment of the long term impact on morphology in estuaries due to anthropogenic pressure requires a thorough understanding of how the sediment system works. This is extremely difficult due to interaction between sediment processes working at all length- and time scales, the slow changes overlaid with inter annual and climate variability and lack of historical data and measurements.

The investigations show that there is a link between the size of the mobile sediment stock M, the accretion rate and disposal practice. The integrated assessment of the impact does not allow for a spatial variation; but the trends are identified.

Acknowledgment

The authors acknowledge the assistance from our colleagues Klavs Bundgaard and Ulrik Lumborg who made the numerical model simulations for this work as well as the Danish Coastal Directorate and Port of Esbjerg.

References

[1] Pedersen J.B.T. and J. Bartholdy (2006). Budgets for fine-grained sediment in the Danish Wadden Sea. Marine Geology 235 (2006) 101–117

[2] Andersen, Thorbjørn Joest; Svinth, Steffen; Pejrup, Morten. (2011). Temporal variation of accumulation rates on a natural salt marsh in the 20th century determined by 137Cs chronologies – the impact of sea level rise and increased inundation frequency. Marine Geology, 178-187, volume: 279

[3] Bartholdy, J. and Pheiffer-Madsen, P., 1985. Accumulation of fine-grained material in a Danish tidal area. Marine Geology 67, pp. 121–137.

Spatial and temporal variations in erodibility in a meso-tidal, muddy channel-flat complex

P. L. Wiberg and B.A. Law

Department of Environmental Sciences, University of Virginia, Charlottesville, VA 22904

Field measurements of sediment size, porosity and erodibility were collected 3 times over the course of a year in a muddy, mesotidal flat-channel complex in Willapa Bay to examine seasonal and spatial variations in sediment properties and transport potential. Grain size measurements of the sediment surface and eroded sediment and measurements of sediment strength were carried out in conjunction with erosion tests made using Gust erosion chamber; porosity was measured for a subset of the samples. Laboratory erosion measurements of deposits made from slurries of flat and channel sediment were used to quantify consolidation time scales ranging from 6 hrs to 4 days. Erodibility of the tidal flats was consistently low, with spatial variability comparable to seasonal variability despite seasonal changes in biological activity. In contrast, channel-bed erodibility underwent large seasonal variations, with mobile sediment present in the channel thalweg during winter that was absent in the spring and summer, when channel-bed erodibility was low and comparable to that of the tidal flats. Sediment on the northern (left) channel flank was mobile in summer and winter, whereas sediment on the southern flank was not. Seasonal changes in channel-bed erodibility are sufficient to produce order-of-magnitude changes in suspended sediment concentrations during peak tidal flows.

Mitigating high turbidity in a shallow lake: Findings of an extensive field experiment with sheltering structure

T. Vijverberg[1], P.Boderie[2], J. Postema[3]

[1]Royal HaskoningDHV, PO Box 151, 6500 AD Nijmegen, The Netherlands (thomas.vijverberg@rhdhv.com / +31 243284040)
[2]Deltares, PO Box 177, 2600 MH Delft, The Netherlands (Pascal.Boderie@deltares.nl)
[3]Rijkswaterstaat IJsselmeergebied - Centrale Informatievoorziening, dir. Informatievoorziening Services, PO Box 600, 8200 AP, Lelystad, The Netherlands (jeroen.postema@rws.nl)

Introduction

Lake Markermeer is a large, enclosed shallow lake in the centre of the Netherlands. One of the major problems in the lake is its decreasing ecological value which is, among other reasons, caused by a gradual increase of suspended sediment concentration and associated increase of light attenuation in the water column (Vijverberg et al, 2010 – INTERCOH '09). Rijkswaterstaat - part of the Dutch Ministry of Infrastructure and the Environment - set up a six-year research project by the acronym "NMIJ" (aiming at a resilient and Natural lake Markermeer-IJmeer) to investigate possibility of several mitigation measures to the problem, such as sheltering structures, silt traps, shallow swamps and shores. Royal HaskoningDHV and Deltares are commissioned to carry out the program and are asked to give advice on a final spatial development of Lake Markermeer. Within the program, several research tools are available: desk studies, numerical modelling studies and field experiments. This paper describes the setup, measurement strategy, results and conclusions of an extensive field experiment with an 1800 m long sheltering structure in Lake Markermeer (Fig.1).

Figure 1: Pictures of the 1800 m long sheltering structure (left) and one of the four measurement poles (right).

Field Experiment Sheltering Structure Lake Markermeer (2011-2012)

The aim of the field experiment sheltering structure was to improve the knowledge about the physical effect of such a measure on the flow, waves and fine sediment dynamics. Furthermore the data from the field experiment was used to validate the Delft3D fine sediment model of Lake Markermeer, which was developed and calibrated by Deltares in 2008. This model is also used in the NMIJ project. The field experiment consisted of an 1800 m sheet pile structure, which was located at the western side of the lake. Half of the structure was constructed above the water level to completely block the wave energy. The other half was constructed below still water level. The total duration of the experiment was one year, from September 2011 to September 2012. Within that period an extensive measurement campaign was carried out, using two types of measurements:

1. Fixed and continuous measurements at 4 poles (Fig. 1 right), 2 located north of the structure, and 2 south. At all poles water levels and waves where measured with a ranging pole, flow velocity with a ADCP, SPM time series at 3 heights in the water column with OBS/YSI sensors and sedimentation rates with traps. At one pole a local wind station was installed.
2. Mobile measurements were carried out from a vessel in an area around the structure. Bed samples at 6 locations were taken monthly, water samples (used for calibration) two weekly and sediment mud thickness was measured 4 times within the year. Besides SPM measurements (Fig. 2b) were carried out after a storm event to determine the affected area of the structure.

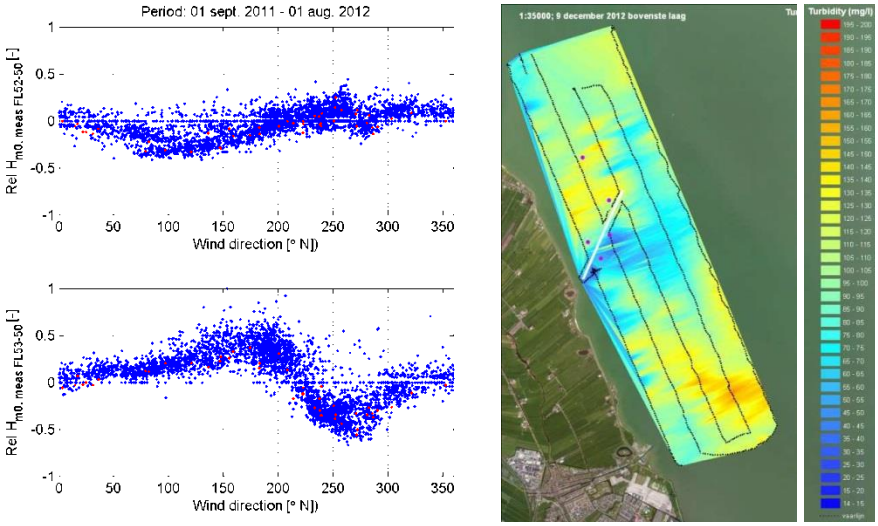

Figure 2: Left panel (a): difference in wave height at two poles, with respect to the undisturbed situation. Right panel (b): results of the SPM concentration measurements after a storm period.

Conclusions from the Field Data

As an effect of the sheltering structure there is a complex interaction between waves and flow in the area. The structure reduces wave heights with maximum 60 to 70 cm (Fig. 2a). The area of wave sheltering and the absolute reduction is dependent on the wind direction. For westerly winds, wave sheltering is at the east side of the structure, for easterly winds at the other side.

For flow sheltering the situation is different. The large scale flow is always deflected at the south side of the structure, causing flow sheltering at the north. The flow velocity at the south side increases with a factor 2, to 0.3-0.4 m/s. This effect is only observed during stormy periods, as the large scale circulation in the lake can only occur when wind speed is high during a certain period. For this reason it is possible that wave and flow sheltering is found at alternating sides of the structure.

This complex interaction of flow and waves has influence on the reduction of SPM concentration. In general, due to the increase of waves and flow at the south side of the structure, the SPM concentration increases at that side with maximum 50 mg/l. At the north side of the structure there is a difference between the top layer of the water column and bottom layer. The effect at the top layer is dependent on the wind. At the bottom a reduction of 30 to 50 mg/l is found.

SPM concentration measurements after a storm show that the sheltering effect is found in an area which has the same order of the length as that of the structure (Fig. 2b). Measurements after an ice period show that the minimum SPM concentration is 30 mg/l. It is expected that this is a lower limit of the SPM concentration in the lake. For an optimal reduction of SPM, future sheltering structures should be built above the still water level. At the north side of the structure where the structure is below still water level, fines can be transported over the structure with the flow. This results in a higher SPM concentration on that side, especially in the top of the water column.

The structure has a limited effect on the sediment composition and grain size distribution in the water column and at the bed. However, the sediment trap data shows differences between the seasons: in summer the organic content of the fines is higher (30%) than in winter (10%).

Sedimentation of fine sediment occurs in the total area around the structure. North of the structure the sedimentation rate is higher than at the south side, which can be explained by the sheltering effect. However, the sedimentation rate is limited to several cm per year.

Fine sediment dynamics in a shallow lake: Model setup and application to a sheltering structure field experiment

P. Boderie, T. van Kessel, A.Smale, C. Thiange and M. Genseberger[1]

[1]Deltares, PO Box 177, 2600 MH Delft, The Netherlands (pascal.boderie@deltares.nl)

Introduction

Lake Markermeer is a large (720 km^2) enclosed shallow lake (less than 4m) in the centre of the Netherlands. Since its creation in 1972 Markermeer is characterised by high turbidity (average concentration 50 mg/l and values reach 200 mg/l during storms l). This is explained by a large pool of fine-grained marine sediment deposits available at the lake bed, which originates from the period that the Markermeer was a saline, tidal environment. Sediment dynamics are dominated by wind as wind- induced waves stir up sediment from the lake bottom and subsequently wind-induced currents transport the mobilized sediments.

The interest in Markermeer is increasing since it has been registered as a Natura 2000 area and since it shows a degrading natural environment with declining numbers of birds, fish, mussels, etc. As high turbidity in the lake is one of the supposed causes of the degradation, The Dutch Directorate Public Works and Water Management plans a series of measures to mitigate high suspended sediment concentrations. Measures include construction of sediment traps and sheltering structures. Within a five-year research project, a process-based numerical model on hydrodynamics and sediment dynamics was developed to evaluate the effectiveness of such measures in terms of turbidity reduction. This paper describes the model and its application to an extensive field experiment around an 1800 m long sheltering structure in Lake Marken (described by Vijverberg et al.; submitted to INTERCOH 2013).

Materials and Method

A 3D a process-based numerical model (Delft3D-flow, Stelling & van Kester (1994) and Lesser *et al.*, 2004) adopting a curvi-linear grid with 7 sigma layers with a high spatial resolution was used. The hydrodynamics and sediment dynamics model was setup and calibrated using available field observations as model input (bathymetry, bed composition) and long-term high frequency data for model forcing (mainly wind and water levels). Although modelling wind-induced fine sediment dynamics in a shallow lake is an established activity, the present application introduces several features that are interesting and non-standard:

- Quality of the observations: both long-term high-frequency observations of suspended matter to assess temporal variability and remote-sensing images to assess spatial variability are available
- An objective, analytical calibration procedure for the sediment model is discussed, going beyond standard curve-fitting of parameters; As an example, spatial variable bottom roughness values are derived from bed composition maps including mussel beds
- The (dynamic) equilibrium sediment distribution on bed is computed by the model instead of prescribed by the user. Starting with a uniform distribution, the simulation period is chosen sufficiently long (typically two decades for Markermeer) in order to reach a dynamic equilibrium.
- A unique opportunity to validate the full-scale model on a local-scale field experiment. The field experiment consists of an 1800 m dam-like structure surrounded by among others 5 measurement poles and was constructed in 2011 for the purpose of collecting field observations
- Two alternative methods for simulating waves are evaluated in this study. In the full scale model the wave modelling is based on a fetch-approach (Groen and Dorrestein, 1976) whereas the local- scale model uses an advanced spectral wave model (SWAN, Booij et al., 1999) to account for wave reflection and absorption locally around the structure.
- Usually scarce measurements of wave induced currents (ADCP measurements) are available and show classical phenomena like shearing, underpinning the need for a 3D modelling approach.

Results and Conclusions

It is demonstrated that the observed fine sediment dynamics, although showing apparently complicated behavior and highly variable in spate and time, can be explained reasonably well with relatively simple process formulations for resuspension, transport and deposition (Figure 1A and 2B). The satisfactory agreement between modeled and observed bed composition can only be obtained by applying a spatially varying bed roughness based on actual shell and mussel density maps. Wave predictions based on the spectral wave model (Figure 2A) are superior to those based on the simpler fetch approach. The model is capable of predicting relevant wave characteristics around the silt screen including reflection and partial absorption phenomena. Prediction of low velocity currents in a weak dynamic system such as Markermeer is no sinecure. This study confirms the need to include wave- driven currents in the simulation (Figure 1A) after which a significant improvement in the resemblance with the measurements emerged. The calibrated model is in use to evaluate the relative impact of measures for reducing the suspended sediment concentrations in Markermeer.

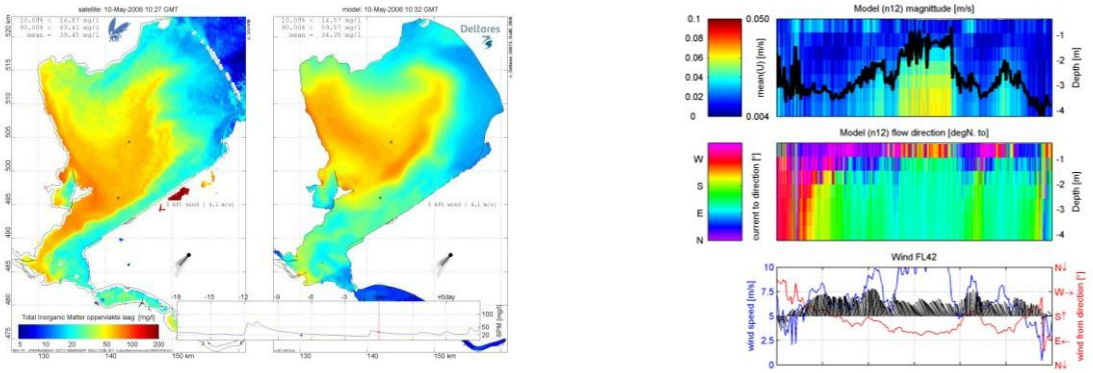

Fig. 1: Model performance at the full scale of the lake: ***1A****: TSM model vs remote sensing (left) and* ***1B****: flow magnitude (right upper) and flow direction (right middle) simulated for the middle of the lake for October 2011 with a dominant ESE wind (right lower).*

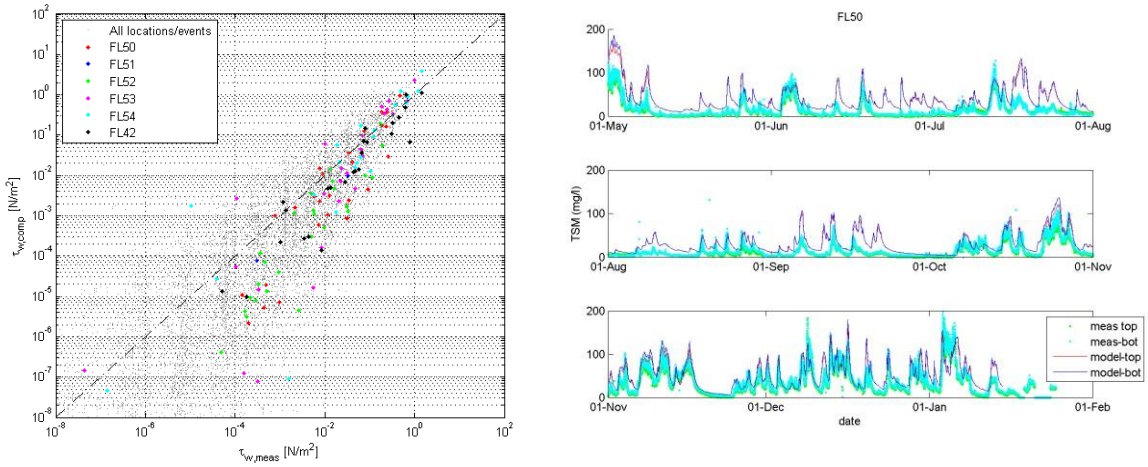

Fig. 2: Model performance at local scale. ***2A:*** *wave induced bed shear stress based on measurements (horizontal axis) versus prediction (vertical axis) for various measurement poles around the sheltering structure. Gray points: all simultaneous records, coloured points maximum during turbidity event.* ***2B****: resemblance between modelled and measured total suspended matter near the sheltering structure (left).*

Consequences of climate change on estuarine ecogeomorphology (C3E2)

Pierre Le Hir[1], Florence Cayocca[1], Régis Walther[2], Philippe Bassoullet[1], Hervé Jestin[1], Romaric Verney[1]

[1] Ifremer, Laboratoire DYNECO/Physed, BP 70, 29280, Plouzané, France
[2] ARTELIA, 6 rue de Lorraine, BP 218, 38432 Echirolles cedex, France

Introduction

Besides temperature increase, main impacts of climate change in estuarine environments are sea level rise and possible change in storm regimes downstream, variations of river flow and solid fluxes upstream. For instance, in northern Europe, a lengthening of low river discharge is often predicted, leading to salinity intrusion and upwards shift of turbidity maximum in estuaries, with possible effects on water quality.
A previous numerical study on the Loire and the Seine estuaries (France) demonstrated that sea level rise only induces moderate upwards shifts of saline waters and turbidity maximum, much less than the qualitatively similar effect of river flow reduction. However these computations were run assuming no morphological change, and the question arises to evaluate climate change consequences when erosion/deposition are likely to modify the morphology and then tide propagation and asymmetries along the estuary. These morphological processes are long term processes, in the same range as climate (or global) changes, so that we can wonder that consequences are likely to differ depending on the actual rate of climate change. Supported by the French Ministry of Environment, the present study is devoted to these questions. A focus is related to the impact on the salted marshes frequently located on estuarine banks. In fact, these areas are vertically located at a level similar to high water elevation on spring tide. For these reasons, a slight mean water level increase is likely to alter the frequency of lateral marshes recovering dramatically. A main question is to know whether the marsh elevation is likely to increase at the same rate as sea level, or inundation is becoming more frequent.

Methodology

Two models have been developed to address these questions. A first one accounts for morphological coupling and deals with schematized and simplified morphologies. The study aims at classifying the estuarine systems response to climate change according to the various types of forcing (mainly tidal amplitude, river run off), bed sediment nature and sediment inputs, and morphological configurations in (quasi-)equilibrium with these respective forcings. In particular, the cross-section shape is discussed, together with the intertidal and subtidal widths. The model is fully process-based, with a sediment module that accounts for sand and mud mixtures.

A second model is a similar process-based model with muddy mobile sediment, applied to the macrotidal Loire estuary configuration. Its finite element coding allows a very refined computation grid in intertidal areas, and simulation of specific hydrodynamics in a realistic and complex network of creeks and vegetated areas. This model is used for predicting sediment deposition on the marshes, and its variation according to tide elevation and turbidity maximum location in relation with river flow.

In order to validate the realistic model of the Loire estuary, a set of field measurements has been deployed on the northern Loire marshes, including pressure gauges to measure the tidal dynamics, turbidimeters and current meters to measure flow and suspended sediment concentration both within and between the creeks. Different techniques have been attempted to approach the very slow rate of deposition, which occurs during small episodes on spring tide and/or meteorological surges.

Results

First the Loire model results could be validated in terms of tide propagation on extended upper areas of lateral marshes, thanks to the high resolution of the model (down to few meters) and nearly without calibration of bottom friction. It is noticeable that uncovering process may last the whole low tide period,

some areas remaining inundated although their altitude is more than 1 m above mean sea level. Predicted suspended sediment concentrations in the range 100 to 300 mg/l could be validated by field measurements (Fig.1), so that model results in terms of sediment fluxes and deposition rate can be reasonably interpreted. However, the validity of residual particulate exchanges and sediment trapping remains uncertain. The relationship between residual deposition / submersion height and location of the turbidity maximum is discussed. Finally, the effect of sea level rise is simulated and changes in sediment trapping are evaluated (Fig. 2).

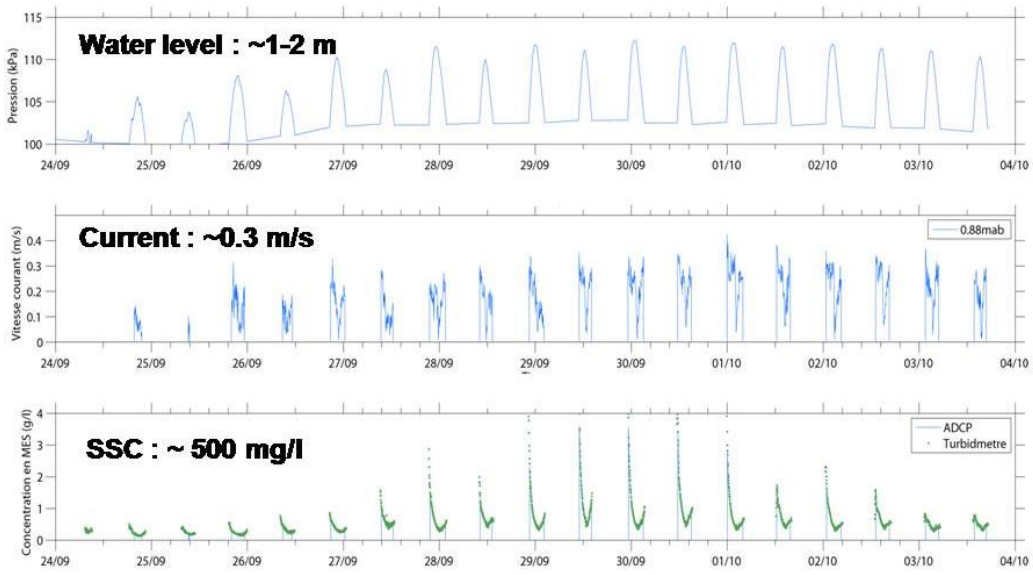

Figure1 Field measurements in a creek of the Loire estuary marshes

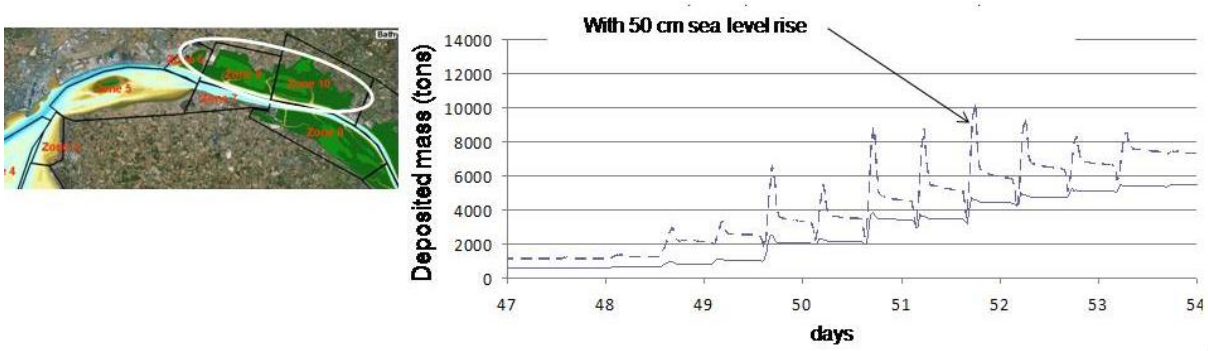

Figure 2 Simulation of deposited sediment, integrated over marshes in the Loire estuary (white limited area on the map) on spring tide. Deposition but also erosion events clearly appear.

On the other hand, the schematic morphological model appears to be able to reconstitute the formation of lateral banks around mean tide level, and simulates their progressive elevation with the mean sea level rise.

Conclusion

Not all consequences of river input variations and sea level rise have been considered at the moment, and attention has been focused on the specific question of sediment trapping processes on lateral marshes. It seems that sedimentation and then marshes rise is likely to occur at a similar rate as sea level rise.

Simulating the turbidity increase in the lower Ems River

D.S. van Maren[a,b], J. Vroom[a], M. Schoemans[a,c]

[a] Deltares, Delft, the Netherlands
[b] Faculty of civil engineering and geosciences, Delft University, Delft, the Netherlands
[c] Faculty of Geosciences, Utrecht University, Utrecht, the Netherlands

Introduction

Many estuaries worldwide suffer from increasing suspended sediment concentrations (SSC) as a result of anthropogenic impact (mainly channel deepening combined with associated maintenance dredging). Such an increase is often gradual until a critical thresh point is exceeded after which the sediment concentration sharply rises. This transition may be irreversible, and therefore a better understanding and quantification of such transitions is of paramount importance. An example of an estuary in which the turbidity dramatically increased is the lower Ems River (Germany). Before the 1980's this estuary was characterised by concentrations of several 100 mg/l, with a turbidity maximum situated at the tip of the salt wedge. In order to facilitate navigation, the channel was continuously deepened and straightened, leading to a gradually increasing tidal range. The sediment concentration probably initially increased gradually as well, until a tipping point was exceeded where the sediment concentration sharply increased leading to extensive fluid mud formation and associated ecological deterioration.

Methods

In order to better understand the role of deepening on changes in tidal and sediment dynamics, a numerical process-based model was setup, in which various stages of the estuary were reproduced. The model was first calibrated against present-day conditions. Subsequently, various bathymetric changes were implemented. For each historic scenario, the model was re-calibrated against available water level information by varying the hydraulic roughness. The required roughness changes correspond well with physically based expectations on sediment-induced changes in the hydraulic roughness. Finally, a sediment transport model was setup and run for the various historic scenarios, with sediment parameter settings for the different historic scenarios.

Results

From 1945 to 1985 the computed suspended sediment concentration peaked at several 100 mg/l (see left panel in Fig. 1), only slightly increasing in time. This increase in suspended sediment concentration from 1945 to 1985 is related to a more pronounced tidal asymmetry; the contribution of estuarine circulation was probably low. The most dramatic deepening occurred in the late 1980's, after which also the suspended sediment concentrations sharply increased (with several orders of magnitude, see Fig. 1). The simulated suspended sediment concentration for present-day conditions exceeds 10 g/l, in line with observations. This increase is only limitedly related to increasing asymmetry, but probably more to a reduction of flow velocity, leading to a lower sediment transport capacity. Although fluid mud is not explicitly modelled, the model results contribute to our understanding of the mechanisms that have led to fluid mud formation within the Ems River.

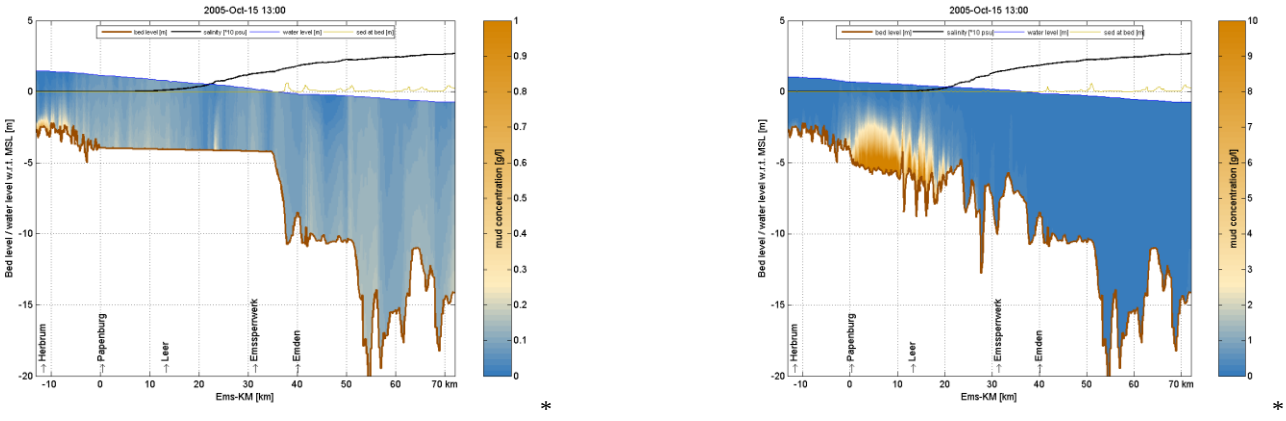

Figure 1. Computed suspended sediment concentration in the lower Ems River for conditions in 1985 (left) and in 2005 (right).

Fine-grained sediment transport in the Belgian coastal zone: Data analysis and modeling

Joris Vanlede (corresponding author)
Flanders Hydraulics Research, Antwerp, Belgium
Delft University of Technology, Faculty of Civil Eng. and Geosciences, The Netherlands
email: joris.vanlede@mow.vlaanderen.be
tel: +32 3 224 61 76

Bart De Maerschalck
Flanders Hydraulics Research, Antwerp, Belgium
Joon Lee
IMDC, Antwerp, Belgium

Introduction

The suspended sediment processes and the mud fields in the Belgian-Dutch coastal area are studied by means of an integrated approach of data analysis of existing field data and modeling using a 3D hydrodynamic and sediment transport model.

The numerical model covers the Belgian coastal zone and part of the Western Scheldt and reaches up to thirty kilometers offshore. The model has to be able to reproduce the high turbidity zone along the Belgian-Dutch coast.

Figure 2: Model grid. Measurement station MOW1 is indicated with the red dot.

Methodology

Model calibration is still in progress as of writing this abstract. The model is calibrated against various types of datasets. The spatial patterns are verified against (surface) SPM data derived from satellite data. The mud content in the bottom is verified against grab samples.

For the verification of the temporal patterns (tidal, spring-neap and seasonal timescales) tripod measurements have been used from the last 10 years. These measurements have first been analysed statistically in order to extract temporal patterns in SPM and velocity.

All available time series have been assembled on a timescale relative to HW, and assigned to the spring, neap or average tidal class according to tidal amplitude (results not shown here). Assembling the data allows to visualize temporal patterns in the SPM and velocity data. Figure 2 shows that the highest SPM concentrations at station MOW1 occur during the ebb tidal phase. Figure 3 shows that the moments with the highest mean concentrations also correspond to the moments of greatest variability in the SPM signal. During slack periods, the natural variability collapses to a background concentration between 50 and 100mg/l.

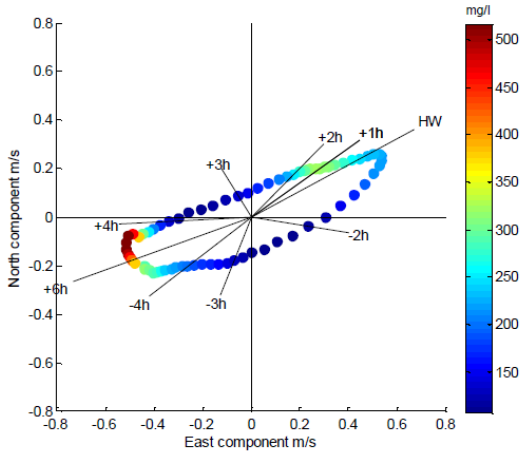

Figure 3: Tidal ellipse with SPM color scale [mg/l], relative to HW. Average SPM at 2,2mab, average velocity at 1,2 mab for station MOW1.

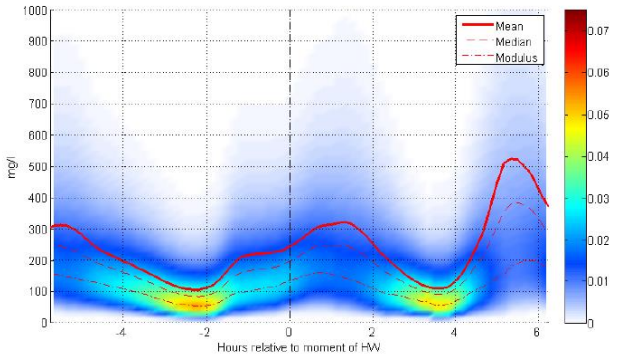

Figure 4: Time dependent probability density relative to HW at 2,2mab for station MOW1

The mud transport in the Belgian Coastal Zone has been studied with numerical models before. An important feature of the model presented here is that it has sufficient resolution around the port of Zeebrugge to accurately capture the exchange of water and sediment between the open sea and the harbor, which is necessary to have a good representation of the siltation of the harbor basin. This is considered important, as the annual dredging effort (~10 MT/yr) in the port of Zeebrugge and its access channels is important in relation to the estimated residual suspended sediment flux from the Dover channel along the Belgian coastal zone (~22 MT/yr).

Applications

After model calibration, the model will be applied to investigate the return flow from the disposal location of dredged sediment back to the harbor and access channels. This scenario analysis fits in the ongoing research into the optimization of the sediment disposal locations.

Study on mud sedimentation and the spreading of *v*egetation on the riverbank in a tidal river

Hiroyuki Yamanishi

Institute of Lowland and Marine Research, Saga University, JAPAN

Keywords: the Ushizu river, field survey, fluid mud, sediment trap, Phragmites australis

1. Introduction

The Ushizu river is located in the Ariake bay in Japan and high suspended sediment concentrations can be often realized under normal conditions because of a strong tidal difference. Futawatari and Kusuda (1993) performed long term field observations in the Rokkaku river which has the Ushizu river as a tributary. The results revealed the existence and migration in the river of maximum concentrations of suspended solids in a fortnightly cycle. Such a high concentration sediment transport causes a large mud accumulation in the river bottom and banks. As a result, it will make a big problem of a river cross-section closure and prevention of river flowing. Also, the mud sedimentation may be accelerating the wide spreading of *Phragmites australis* in the river bank. River problems in question will take place as a result of two phenomena - sedimentation and a spreading vegetation. Thus, Flood protection and drainage works are very important for lowland development and river management. The purpose of this study is to survey suspended sediment transport, the behaviours of fluid mud, sediment flux and try to control the siltation and the growth of *Phragmites australis* in the Ushizu river.

2. Methodology

2.1. Monitoring of sedimentation on the inclined bed

A long term survey was carried out with regard to the monitoring of sedimentation on the river banks. Sedimentation data were collected by measuring the mud surface level of several staffs set on the inclined beds once in about two weeks. Also, in order to understand the behaviour of suspended matters on an inclined bed, some velocity meters, turbidity meters and a water gauge were set up in the same slope. The interval of measure of velocity and turbidity was in two minutes, and that of the water level was in a minute. In addition, to estimate the sediment flux on the mud bottom, some sediment traps with the diameter of 6.9 cm were set. The opening level of sediment trap located on the mud bottom was changed to investigate the difference of fluid mud and the settling matters through the upper water. The mooring survey was carried out in two tides.

2.2. Linkage between mud accumulation and the growth of vegetation

Recently, Japanese rivers have been managed by the view point of river ecological aspect as well as the flood control and water resource management. The Ushizu river is a well mixed type and the upper tidal distance is approximately 12km from the river mouth. Mud sedimentation and the spread of *Phragmites australis* in the river bank form original scenery. However, they cause a river cross-section closure and the capacity degradation of river flowing. This survey is to clarify the relation between mud sedimentation and the growth of *Phragmites australis* as a part of river environments. Specifically, the intrusion distance of *Phragmites australis* to the river and the habitat density of *Phragmites australis* along the river bank was measured as well as the topographical change in the cross-section. The measurement of habitat density used a quadrat with 0.5m.

3. Results

3.1. Characteristics of sedimentation and suspended solids transport on the inclined bed

Figure 1 shows time series of sediment height on the inclined bed measured from August, 2010 to January, 2013. **Figure 2** also indicates the location of measurement staffs and the mud surface elevation in May, 2010 and May, 2012. From **Fig. 1**, it was shown that mud sedimentation was accelerated over the mean water level and mud sedimentation rate was about 0.8 to 1mm/day during non-flooding term. On

the other hand, the maximum rate of scoured mud was about -0.6mm/day in flooding term and the sediment was eroded about 30 to 40 cm depth. However, when the non-flooding season comes again, the mud accumulation arises in the upper mean water level. The result brings the net increase of the sedimentation on the waterline area. Furthermore, according to the time variations of water depth, suspended solids concentration and flow velocity on the inclined bed, high concentration of suspended solids inflows near the bank in flood tide and the large amount of suspended solids settled to the bottom rapidly during the decelerating flow and the slack water. As a result, fluid mud is formed near the bed and moves along the bottom easily. This argument was also defended by the results of sediment flux that changed the opening height of sediment trap. **Figure 3** demonstrates the schematic mechanism of sedimentation close to the waterline on the river bank.

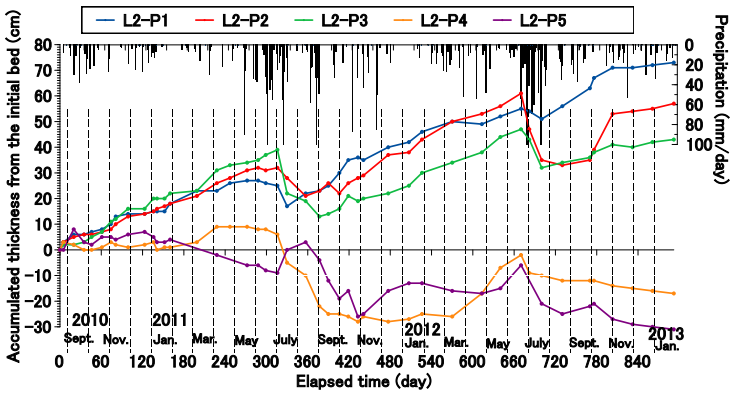

Fig. 1 *Time series of sediment height on the inclined bed.*

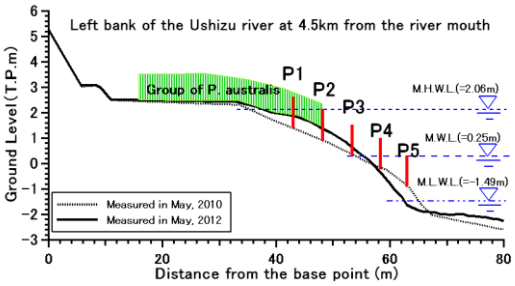

Fig. 2 *Measuring point in the cross section.*

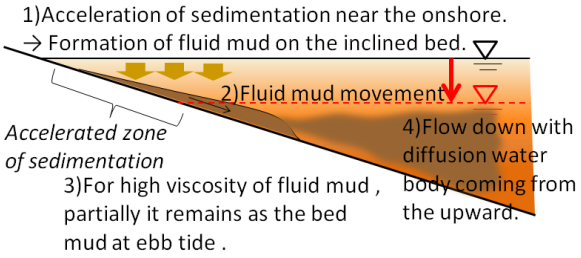

Fig. 3 *Schematic mechanism of sedimentation on the bank.*

3.2. Interaction of mud sedimentation and the growth of *Phragmites australis* near the waterline

Sedimentation near the waterline is strongly related to acceleration to waterside intrusion of *Phragmites australis* and the average rate of intrusion progress was about 2.6cm/day though it depends on the step of the growth of *Phragmites australis*. Also, the network structures of the underground stem were measured. In addition, according to some results of the survey data on the habitat of *Phragmites australis*, it was shown that the distribution of population density changes in response to the change of waterline as the habitat boundary. Further, a mathematical model for the spreading of *Phragmites australis* was introduced, and the results of simulation showed the possibility of control of mud sedimentation and *Phragmites australis*.

4. Conclusions

This can be summarized in the followings: 1) Mud sedimentation in the river bank was accelerated over the average water level, the rate of sedimentation is about 1mm/day; 2) The growth rate of *P. australis* and the network structures of the underground stem were measured; 3) The interaction between siltation and vegetation close to the edge of water in the river bank is highlighted, and an idea of sedimentation and vegetation control is suggested.

Acknowledgment

This study was a joint work with the Takeo office of the Ministry of Land, Infrastructure, Transport and Tourism (the MLIT), and was supported in part by a Grant of River Improvement and Protecting from Floods Research of the MLIT.

References

T. Futawatari and T. Kusuda (1993) Modeling of suspended sediment transport in a tidal river, *Nearshore and Estuarine Cohesive Sediment Transport* (ed. A.J.Mehta), pp.504-519.

Floc discharge and sediment accumulation at altered macro-tidal Yeongsan estuary of Korea

Guan-hong Lee[1)], Hyun-Jung Shin[1)], Josh Williams[2)], Timothy M. Dellapenna[2)], Seok Yun Kim[3)], Jin-Ho Chang[4)]

[1)]Department of Oceanography, Inha University, Incheon, 402-751, Korea
[2)]Department of Marine Science, Texas A&M University, Galveston, Texas, 77554, USA
[3)]Department of Oceanography, Bukyong National University, Busan, 608-737, Korea
[4)]Department of Marine Resources, Mokpo National University, Muan, 534-729, Korea

Estuaries provide habitats for living organisms and support high productivity. However, many estuaries over the world have been degraded due to alteration caused by various human activities. Efforts have been made in recent decades to understand the nature of altered estuaries and the natural response to these modifications with the intension of restoration and/or improved management practices of estuaries. Macro-tidal Yeongsan estuary of Korea has been altered due mainly to the construction of an estuarine dam in 1981 as well as the reclamation of extensive tidal flats along the Yeongsan estuary. As a part of four-year (2010-2013) research program, 'Development of Integrated Estuarine Management System of Korea', a series of field experiments have been conducted to understand sedimentation process, especially the governing processes of source, transport and sink of fine sediments, in the altered Yeongsan estuary. The field campaign includes grain size analysis of surficial sediment, bathymetric survey, coring of bed sediment and subsequent dating analysis. In addition, transport mechanism was investigated by measuring of vertical profiles of flow, suspended sediment concentration and floc size using CTD, ADCPs, LISST and floc camera during wet and dry seasons. The construction of the dam caused significant impact to the Yeongsan estuary by blocking estuarine circulation and reducing tidal current velocity. Moreover, the dam operation became the main controlling factor for the discharge and transport of freshwater and sediment. Most of the discharged sediments from the river were fine sediments in the form of flocs. The discharged fine sediments were transported in the surface freshwater layer above the stratification. The flocs settled down further offshore where stratification weakened, and returned landward by tidal currents, causing sediment accumulation near the estuarine dam. Consequently, the Yeongsan estuary underwent high rates of sediment accumulation up to 10 cm per year.

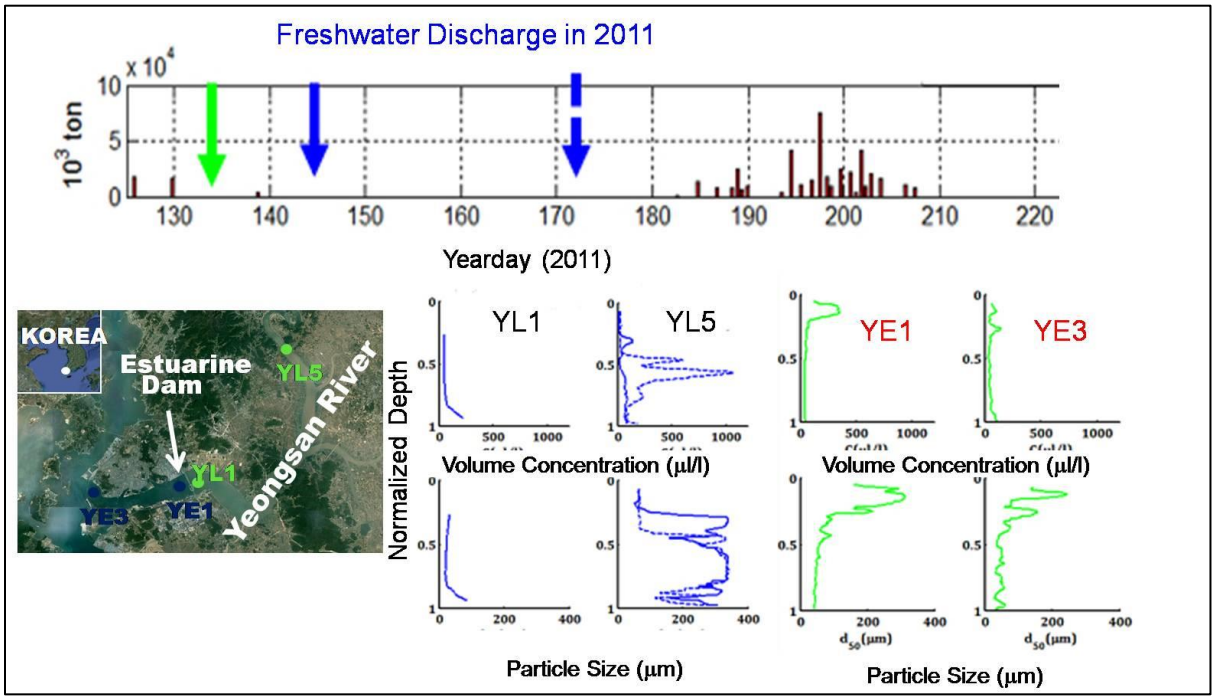

Figure 1. Volume concentration and particle size in the water column of Yeongsan estuary.

Hindered settling: A discussion

J R Spearman[1] and A J Manning [1,2,3]

[1)] HR Wallingford, Howbery Park, Wallingford, Oxfordshire. OX10 8BA; Contact email: j.spearman@hrwallingford.com
[2)] School of Marine Science & Engineering, University of Plymouth, Plymouth, Devon, UK. PL4 8AA.
[3)] Department of Geography, Environment and Earth Sciences, University of Hull, Kingston Upon Hull, Humberside, HU6 7RX, UK.

Hindered settling – the process by which the settling of sediment particles becomes impeded due to the proximity of other sediment particles - can be an important process for the coastal modeller, especially in muddy environments. It is also a significant process in other disciplines such as chemical engineering, the modelling of debris flow, the study of turbidites, piping of slurries, and the understanding of dredger hopper processes.

The prime texts regarding hindered settling for coastal modellers (e.g. Richardson and Zaki, 1954; Whitehouse et al, 2000; Winterwerp, 1999) were written on the basis of work on mono-disperse solutions. These formulae are not directly applicable to the possibly more widely encountered poly-disperse solutions. Some authors (e.g. Davis and Gecol, 1994; Wang et al, 1995; Winterwerp and van Kesteren, 2004; Cuthbertson, 2008, Dorell et al, 2011) have adapted these equations, to make them more attributable to bi-disperse or poly-disperse settling. The applications to poly-disperse non-cohesive sediments have been relatively successful (e.g. Davis and Gecol, 1994; Dorell et al, 2011). However, the results of including cohesive and non-cohesive sediments have been mixed – due to uncertainty in the laboratory results (Dankers, 2007), lack of experimental data (Cuthbertson et al, 2008) or a reliance on empiricism (Wang et al, 1995).

Amongst the uncertainties encountered by the researchers of hindered settling is the increase in viscosity with increasing cohesive and non-cohesive sediment concentration. Many of the hindered settling approaches listed above are based on the assumption that the viscosity of the suspension fluid varies with solid concentration in similar fashion to a dilute suspension of spheres. For concentrated or cohesive (floc) suspensions this is not the case (e.g. Lewis and Nielsen, 1968; Mueller et al, 2010) and the effect of solids concentration on viscosity becomes more complex.

As the concentration of cohesive sediment in a suspension rises above the gelling point, the rheological changes, including the establishment of yield stress, further serve to impede the settling of coarser grains through the suspension. By substituting the non-Newtonian apparent viscosity for the Newtonian viscosity normally associated with settling velocity formulae, the settling behaviour of coarser grains in non-Newtonian mixtures can be estimated in the normal way (He et al, 2001). Such non-Newtonian processes have been demonstrated to prevent particle segregation stop the settling of sand grains entirely for clay suspensions of more than 13% by volume (Amy et al, 2006; Manica, 2012; Pierson, 2005).

For mixed cohesive and non-cohesive suspensions the poly-disperse approaches available require testing against a wider range of validation test data sets and further development. Unfortunately the small amount of experimental data is rather limiting but more recent measurements by teSlaa et al (2013) offer the potential for researchers in this field to further develop these theories.

This paper will discuss the status of the current state of hindered settling knowledge, using a generalised framework (Cuthbertson et al, 2008) as a basis for discussion, identifying knowledge gaps and lessons to be learned from other research areas.

References

Amy L A, Talling P J, Edmons V O, Sumner E J and Lesueur A (2006) An experimental investigation of sand-mud suspension settling behaviour: implications for bimodal mud contents of submarine flow deposits, Sedimentology, 53:1411-1434.

Cuthbertson, A., Dong, P. and Davies, P., (2008). Hindered settling velocity of cohesive/non-cohesive sediment mixtures. Coastal Engineering, doi:10.1016/j.coastaleng.2008.05.001.

Dankers PJ T (2007) On the hindered settling of suspensions of mud and mud-sand mixtures, PhD Thesis for the Technical University of Delft.

Davis R H and Gecol H (1994) Hindered settling function with no empirical parameters for polydisperse suspensions, AlChE Journal, 40: 570-575.

Dorrell, R M, Hogg, A J, Sumner E J and Talling P J (2011) The structure of the deposit produced by sedimentation of polydisperse suspensions, Journal of Geophysical Research, Volume 116, F01024.

He Y B, Laskowski J S and Klein B (2001) Particle movement in non-Newtonian slurries: the effect of yield stress on dense medium separation, Chemical Engineering Science, 56: 2991-2998.

Lewis T B and Nielsen L E (1968) Viscoisty of dispersed and aggregated suspensions of spheres, Transactions of the Society of Rheology, 12:3, 421-443.

Manica R (2012) Sediment Gravity Flows: Study based on experimental simulations, In: *Hydrodynamics - Natural Water bodies*, Harry Schulz (Ed), InTech. Available from http://www.intechopen.com/books/hydrodynamics-natural-water-bodies/sediment-gravity-flows-study-based-on-experimental-simulations .

Masliyah J H (1979) Hindered settling in a multi-species particle system, Chem. Eng. Sci, 34(9), 1166-1168.

Mueller D, Llewellin E W and Mader H M (2010) The rheology of suspensions of solid particles, Proc. R. Soc. A, 466:1201-1228.

Pierson T C (2005) Hyper-concentrated flow – transitional process between water flow and debris flow, In: Debris-flow Hazards and Related Phenomena, Dr Matthias Jakob, Professor OldrichHungr (Eds), Springer Praxis Books 2005, pp 159-202.

Richardson J F and ZakiW N(1954) The sedimentation of a suspension of uniform spheres under conditions of viscous flow, Chem. Eng. Science, 3: 65-73.

teSlaa S, He Q, van Maren D S and Winterwerp J C (2013) Sedimentation processes in silt-rich sediment systems, Ocean Dynamics, 63: 399-421.

Wang Z, Nestmann F and Dittrich A (1995) Fall velocity of sediment in clay suspensions, Sixth International Symposium on River Sedimentation, New Delhi, Indi, 314-322.

Whitehouse R, Soulsby R, Roberts W and Mitchener H (2000) Dynamics of estuarine muds, Thomas Telford Publications, London.

Winterwerp J C (1999) On the dynamics of highly-concentrated mud suspensions, PhD Thesis Delft University of Technology.

Winterwerp J C and van Kesteren W G M (2004) Introduction to the physics of cohesive sediment in the marine environment. Developments in Sedimentology, 56, van Loon, T. (Ed.), Amsterdam: Elsevier, 466p.

Spatial distributions of floc properties within the Sacramento–San Joaquin River delta, northern California, USA

Andrew J. Manning[1,2,3] and David H. Schoellhamer [4,5]

[1)] HR Wallingford, Howbery Park, Wallingford, Oxfordshire, OX10 8BA, UK
[2)] Department of Geography, Environment and Earth Sciences, University of Hull, Kingston Upon Hull, Humberside, HU6 7RX, UK
[3)] School of Marine Science and Engineering, Plymouth University, Drake Circus, Plymouth, Devon, PL4 8AA, UK
[4)] U.S. Geological Survey, Placer Hall, 6000 J Street, Sacramento, CA 95819, USA
[5)] Department of Civil & Environmental Engineering, University of California, Davis, USA
Contact emails: andymanning@yahoo.com; amanning@hrwallingford.com; dschoell@usgs.gov

The Sacramento–San Joaquin River Delta (Delta) is where the rivers of the Central Valley of California merge to become the San Francisco Estuary. The rivers deliver sediment from the Central Valley watershed (approximately 96,000 km^2) to the Delta. One of the major drivers of sediment transport and turbidity in the Delta is the supply of fine sediment from the watersheds, particularly the Sacramento River.

Deposited sediment creates and sustains the Delta landscape, including habitats such as tidal marsh, floodplain, open channels, and flooded islands. Massive sediment supply during the period of hydraulic mining in the late 1800s caused deposition in Sacramento Valley rivers, the Delta, and San Francisco Bay (Gilbert 1917). Today, a key management question is whether the existing Delta landscape can be sustained as sea level rises. Sea-level rise and floodplain, marshplain, and channel-form changes are habitat stressors, which can be counteracted by artificial and natural movement of sediment. Sediment also deposits in ports, marinas, and shipping channels, which sometimes require dredging to maintain navigation (Schoellhamer et al., 2012). Local erosion and deposition rates are also important drivers because these processes control how the sediment supplied from the rivers gets distributed throughout the Delta. The erosion and deposition processes are strongly dependent on the local sediment properties, particularly when cohesion and flocculation are important (as they are in the Delta). Thus, it is important to make local, in situ measurements of erosion rates and settling velocities in order to guide parameterization of a numerical model.

The U.S. Geological Survey is collecting data that will support the development, calibration, and validation of numerical models of sediment transport and turbidity in the Sacramento-San Joaquin Delta. The following research questions were posed: How much flocculation of sediment particles occurs in the Delta, and what are the settling velocities of the flocs? How do settling properties vary spatially and temporally in the Delta? What are the particle size distributions of the bed sediment in the Delta? What are the spatial patterns in size distributions and how do these patterns change temporally? Are there "hotspots" of deposition within the Delta? To address a number of these research questions, a Co-operative Agreement was established between research scientists at the USGS and HR Wallingford (UK). This paper presents the preliminary findings from a spatial study of turbidity mobility and floc depositional properties throughout the Delta. A selection of floc properties, both individual and parameterised, will be presented and discussed. It is anticipated that the floc information will provide some insight into the mobility of the suspended sediment within the Delta and assist the calibration of Delta-specific numerical models. A conceptual model for sediment transport in the Delta has been proposed by Schoellhamer et al. (2012).

The Delta data to be presented in this paper were primarily collected during June 16-22, 2011, with additional samples collected during March 26, 2010. During the 2011 surveys, instrumentation was deployed from the USGS houseboat *RV Humphrey*. Instrumentation was deployed from land-base platforms in 2010. The floc data were acquired using the INSSEV-LF: IN-Situ Settling Velocity

instrument. The LF (LabSFLOC) version of INSSEV is a hybrid system which combines two key components: i) the low intrusive LabSFLOC (version 1) system (a high resolution video-based device to measure the individual floc properties; ii) an in-situ estuarine floc sampling acquisition unit (to initially obtain the suspension sample). For the latter, a 2.2L Van Dorn horizontal sampling tube with a 14 kg torpedo-shaped weight suspended from the underside of the tube was used to collect a water sample nominally 0.7 m above the estuary bed. Manning et al. (2010) provide further details of these floc acquisition procedures.The LabSFLOC– Laboratory Spectral Flocculation Characteristics – instrument (Manning, 2006) was set-up in the vessel. It utilises a low-intrusive high magnification analogue video camera (Manning and Dyer, 2002) to observe flocs as they settle in a 190mm high by 100mm square Perspex settling column. The LabSFLOC camera resolution could practically view flocs down to 20 μm in size and as large as 4 mm. Settling velocities generally ranging from 0.01 $mm.s^{-1}$ to 35 $mm.s^{-1}$ can be measured by LabSFLOC. Similarly, INSSEV can operate within SSCs of just a few $mg.l^{-1}$, with a practical upper operating limit of ~8.5 $g.l^{-1}$.A small sub-sample containing a floc population was carefully extracted from the horizontal Van Dorn using a modified pipette. This sample was immediately transferred to the LabSFLOC settling chamber, whereby the flocs passed from the vertically held pipette to the chamber and settled solely under gravity. The floc collection and sub-sampling protocol are both proven floc sampling techniques (see Manning, 2006), which permit minimal floc interference and flocs which are representative of the ambient population – especially in terms of floc size and settling velocity distributions. The floc sampling techniques also provide control volumes, which permit settling flux estimations. These floc sampling techniques have been used during recent San Francisco Bay surveys since 2008 (Manning and Schoellhamer, in press).

A total of 31 floc population samples were obtained from 21 individual sites within the Delta. Ambient Delta SSCs in the nearbed region ranged from 4-52 $mg.l^{-1}$ during the surveys. A combined total of more than 2200 individual flocs were measured during the March 2010 and June 2011 Delta survey. Floc sizes (D) ranged from 27μm microflocs to macroflocs of nearly 500 μm in diameter. Macrofloc settling velocities (Ws) ranged between 0.7-5 $mm{\cdot}s^{-1}$, with the macroflocs representing 10-60% of the SSC throughout the entire Delta survey. This paper will indicate how floc populations vary throughout the Delta, and identify characteristic floc dynamical properties and structural composition, at key locations within the Delta. The depositional mass settling flux distribution will also be assessed and linked to a Delta conceptual model for sediment transport.

References

Gilbert GK. 1917. Hydraulic-mining debris in the Sierra Nevada. Washington, DC: U.S. Geological Survey Professional Paper 105. 154 p. Available from: http://pubs.er.usgs.gov/publication/pp105.

Manning, A.J. (2006). LabSFLOC – A laboratory system to determine the spectral characteristics of flocculating cohesive sediments. HR Wallingford Technical Report, TR 156.

Manning, A.J., and Schoellhamer, D.H. (in press). Factors controlling floc settling velocity along a longitudinal estuarine transect. Marine Geology.

Manning, A.J., Schoellhamer, D.H., Mehta, A.J., Nover, D. and Schladow, S.G. (2010). Video measurements of flocculated sediment in lakes and estuaries in the USA. Proceedings of the Joint Federal Interagency Conference on Sedimentation and Hydrologic Modeling, Riviera Hotel, Las Vegas, Nevada, USA, 27th June – 1st July 2010.

Schoellhamer D.H., Wright, S.A. and Drexler, J.Z. (2012). Conceptual Model of Sedimentation in the Sacramento– San Joaquin River Delta. San Francisco Estuary & Watershed Science, October 2012.

Variation of flocs flux at Xuliujing, Changjiang River

Guo Chao, He Qing

State Key Laboratory of Estuarine and Coastal Research, East China Normal University, Shanghai, 200062, P. R. China

This work was mainly based on a series field observations in the neap tide nearly each month in the past few years at Xuliujing, Changjiang Estuary, China. The in situ flocs were observed by LISST with the information of hydrodynamics and sediment characteristics.

A lot of attention had been paid on sediment flux from river into the estuary, however, few works focused on the flocs flux, but we knew that more than 80% of the total volume of sediments in suspension were flocculated particles[1], i.e. flocs flux might be a more accurate way to demonstrate the transport of sediment in nature, including not only the amount of sediment, but also the form of it.

We were interested in the variation and tendency of flocs flux among different months and years. It was found that flocs flux varied much between flood season and dry season. Flocs flux was larger in flood season, which had a tight relationship with the condition of normal sediment flux but not the same. Hydrodynamics and sediment characteristics like flow velocity, suspended sediment concentration (SSC) and composition of suspended particles were considered to be the major factors affected the changing of flux.

References

[1] Droppo and Ongley, 1994, Flocculation of suspended sediment in rivers of Southeastern Canada. Water Res 28(8):1799-1809

Long-term variability of SPM concentration and floc-size associated with residual flows in the Belgian coastal zone

Michael Fettweis[1], Matthias Baeye[1], Dries Van den Eynde[1], Nirnimesh Kumar[2]

[1] Royal Belgian Institute of Natural Sciences – Dir. Natural Environment, Brussels, Belgium
[2] University of South Carolina · Earth and Ocean Sciences, Columbia, USA

Various processes may induce variations of suspended particulate matter (SPM) concentration on temporal and spatial scales. On short time scales, the predominant forcing is related to tides, waves and atmospheric circulation. These variations are caused by resuspension, mixing, settling and deposition of fine-grained sediments, as well as by advection due to subtidal flows. On longer time scales neap–spring cycles and meteorological, seasonal and climatological variations become significant. Meteorological patterns, acting on regional and global scales, are responsible for wave induced resuspension and determine the advection of water masses. Annual variations are caused by seasonal changes in wind pattern and biological activity and are obvious from obvious from satellite images, where we clearly see the lower/higher surface SPM concentration and higher/lower surface Chl-a concentration during summer/winter.

The geographical variability of the SPM concentration in the North Sea and specifically the Belgian coastal zone has been linked to wind, weather and climate (Baeye et al. 2011, Fettweis et al. 2012). Based on the alongshore flow direction, two flow regimes in the Belgian coastal zone were characterized in terms of sediment flux and vertical mixing. The southwestward directed flow regime corresponds to decreasing salinity and increasing SPM concentration. The higher waves result in the largest extent of the coastal turbidity maximum and enhance the erosion of the seabed and the mixing capacity. The northeastward directed flow readily shows increasing salinity, but decreasing SPM concentration. Turbulent shear and SPM concentration, which vary according to hydrodynamics, control the flocculation. Flocculation combines biomass and minerals particles together into a larger aggregate with often different floc strength. The seasonality of biological activity significantly influences flocculation and thus controls deposition/erosion and sediment dynamics. How can the changes in SPM concentration, floc size and floc strength that have been observed be correlated with the seasonality of the biological (spring and summer algae bloom) and hydro-meteorological conditions?

Despite the improved understanding of flocculation dynamics, our knowledge is still insufficient to describe the impact of the organic matter and residual flow regimes. More specifically the impact of high primary production in spring and summer on flocculation, settling, formation of high concentrated mud suspensions and the resuspension of fine-grained sediments during different wind regimes is not yet fully unravelled. The Belgian near-shore area, located in the southern North Sea, is a relevant site to investigate links between biomass, SPM concentration and hydro-meteorological forcing. The aim of this work is to link the flocculation dynamics to the seasonality of hydro-meteo and biological processes using long term in situ data of SPM concentration, turbulence, and floc size. Wind- and seasonal driven SPM and floc dynamics have been studied using a combination of in-situ bottom-mounted sensors (ADCP, ADP, OBS, LISST) that gives data over the entire water column. Flow profiles, SPM concentration and near-bed sediment dynamics are discussed, and a vertical mixing parameter is introduced in order to evaluate the vertical mixing of the SPM in the water column. The results allowed us to separate and recognize processes that control the variability of SPM concentration and floc size and that can be used as an attempt for understanding the long-term evolution of the system.

Baeye M, Fettweis M, Voulgaris G, Van Lancker V. 2011. Sediment mobility in response to tidal and wind-driven flows along the Belgian inner shelf, southern North Sea. Ocean Dynamics 61, 611–622. doi:10.1007/s10236-010-0370-7

Fettweis M, Monbaliu J, Nechad B, Baeye M, Van den Eynde D. 2012. Weather and climate related spatial variability of high turbidity areas in the North Sea and the English Channel. Methods in Oceanography 3-4, 25-29. doi:10.1016/j.mio.2012.11.001

Modeling floc size distribution of suspended kaolinite using two quadrature methods of moment

Xiaoteng Shen* and Jerome P.-Y. Maa

Department of Physical Sciences, Virginia Institute of Marine Science, College of William and Mary, Gloucester Point, VA 23062
*Corresponding author: xiaoteng@vims.edu

Introduction

In estuaries or adjacent coastal regions, the properties of cohesive sediment are responsible for engineering issues such as siltation and dredging in navigation channels and harbors, as well as environmental issues such as pollutants transport and ecosystem responses. The complexity of the cohesive sediment is mainly due to flocculation, which is the result of simultaneously occurring aggregation and breakup processes. Nevertheless, a widely-acceptable numerical model that can be applied to a relatively large study domain has not been established yet. In this study, the population balance model has been applied to describe the floc size evolution of kaolinite suspension. The unfixed and fixed pivot quadrature methods of moment (QMOM) are employed to solve the population balance equation respectively with flocculation source and sink term. Rather than only focus on the moments and the mean size of the particles (Prat and Ducoste, 2006), however, the quadrature nodes and weights in the QMOM are used to monitor the floc size distribution (FSD), via properly adjustable factors for the standard moments. Model results were demonstrated by comparison with experiment data from published papers (e.g., Mietta et al., 2005) for different mass concentration and/or shear rate. This study suggests that the quadrature points and weights could appropriately predict the FSD under selected conditions.

Methodology

Model Setup

The population balance equation is employed to simulate the floc size evolution by tracking the number concentration of flocs. To make it possible to calibrate and verify our model using published data, the box formulation is selected for test (Marchisio et al., 2003), neglecting the advection term, diffusion term, etc. The aggregation and breakage source and sink terms includes: (Ⅰ) birth of flocs due to aggregation of smaller particles, (Ⅱ) death of flocs due to aggregation with other particles, (Ⅲ) birth of flocs due to fragmentation of bigger particles, and (Ⅳ) death of flocs due to breakup into smaller particles.

Applying moment transformation and N-node quadrature approximation with adjustable factor p (Su et al., 2007), the population balance equation is transferred into a series of differential equations for the moments, with the source and sink term only a function of quadrature abscissas (nodes) L_i (i=1,2,…,N) and their corresponding weights ω_i (i=1,2,…,N). For unfixed pivot QMOM, the N unknown abscissas L_i and N unknown weights ω_i are extracted from the first $2N$ adjustable moments m_k (k=0,1,…, $2N$-1) using Wheeler's algorithm; for fixed pivot QMOM, the N abscissas are specified first, and N unknown weights are obtained from the first N adjustable moments by solving a system of linear equations. By choosing proper adjustable factor, moments can be tracked with lower order but more quadrature nodes, which make it possible to re-generate the FSD using QMOM approach.

Numerical Experiment

This flocculation model is firstly checked by pure aggregation, pure breakup, and ideal aggregation-breakage cases, comparing with the numerical data given by Marchisio et al. (2003) and Su et al. (2007). After that, attention is paid to suspended kaolinite. Mietta et al. (2005) performs the class method to simulate the floc size variation in a settling column lab experiment under the effect of turbulent shear, using measured data with suspended sediment concentration (SSC) 0.5g/L and shear rate $5s^{-1}$, $10s^{-1}$, $20s^{-1}$, and $40s^{-1}$, respectively. The experimental data as well as their numerical results are extracted from the figures in their paper to verify our QMOM-flocculation model.

Results and Conclusions

The population balance model is utilized to explore the flocculation processes of cohesive sediment, solving by fixed and unfixed pivot QMOM approach with an adjustable factor. The FSD is tracked through the quadrature nodes and corresponding weights. Model results are verified by published experiment data. This suggests that the use of abscissas and weights of quadrature approximation in QMOM could contribute to reasonable predictions of the FSD for selected flow conditions. Further study still needs to extend this approach in natural environment, such as estuaries and coastal areas, in particular when local flocculation properties are focused on and with advection and diffusion terms added.

References

Marchisio, D.L., Vigil, R.D., and Fox, R.O., 2003. Quadrature method of moments for aggregation-breakage processes. Journal of Colloid and Interface Science 258, 322-334.

Mietta, F., Maggi, F., Winterwerp, J.C., 2005. Sensitivity to breakup function in a population balance equation for cohesive sediments. In: Proceeding of the 8th Intercoh Conference, Saga, Japan.

Prat, O.P., Ducoste, J.J., 2006. Modeling spatial distribution of floc size in turbulent processes using the quadrature method of moment and computational fluid dynamics. Chemical Engineering Science 61, 75-86.

Su, J.W., Gu, Z.L., Li, Y., Feng, S.Y., Xu, X.Y., 2007. Solution of population balance equation using quadrature method of moments with an adjustable factor. Chemical Engineering Science 62, 5897-5911.

A rapid method for settling velocity and flocculation measurement within high suspended sediment concentration rivers

V. Wendling[1,*], N. Gratiot[1], C. Legout[1], I.G. Droppo[2], A.J. Manning[3], G. Antoine1,[4], H. Michallet[5], M. Jodeau[4]

[1]LTHE (UJF, IRD, CNRS),Grenoble, France
[2]Environment Canada, Burlington, Ontario, Canada
[3]HR Wallingford, United Kingdom
[4]LNHE, EDF Chatou, France
[5]LEGI (UJF, INPG, CNRS), Grenoble, France.
[*]corresponding author: valentin.wendling@ujf-grenoble.fr

Introduction

In headwater catchments, fine sediment transport is a main issue with regard to monitoring erosion, pollutant fluxes, and reservoir siltation. In these environments, suspended sediment concentrations exhibit high temporal variations during runoff events and commonly exceed 10 g/l. The settling velocity of suspended sediment is a key variable to understand and model sediment transport. For such concentrated events, hindered settling and flocculation processes increase the difficulty to model sediment transport. Currently, no automated method for the measurement of settling velocity and propensity to flocculate within high concentration sediment environments exists. Methods used to measure individual particle settling velocity (e.g., LISST, video) are limited to low concentrations (<1g.l). They can be adapted to higher concentration after dilution in particle-free water, however, measured settling velocities may not be representative of the initial sample as hindered and flocculation effects are eliminated or reduced.
In order to measure quasi in situ sediments settling velocity spectrum and propensity to flocculate in high concentrated environment, we assessed a processing method based on light transmission measurement within a quiescent settling column condition.

Methods

Tests were conducted in a 20 cm high settling column, equipped with 16 regularly spaced transmission sensors along the vertical. Settling measurements were done immediately after sampling, in order to prevent any evolution of the sediment structure. In the column, the absorbance was measured as a function of time and depth, providing absorbance maps as presented in figure 1. Following recent laboratory investigations, it was considered that each iso absorbance line corresponded to a class of particles. The range of slopes of those lines defined the settling velocity spectrum of the sample. Iso absorbance lines are straight in case of non cohesive sediments (figure 1a), and curved if flocculation occurs (figure 1b). For each line, a flocculation index is defined as the relative variation between surface and bottom slopes (fitted lines in figure 1).

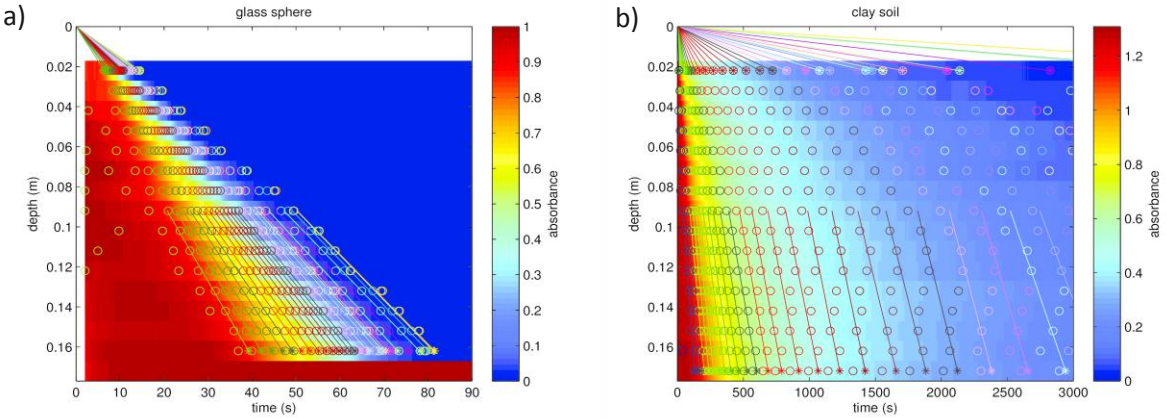

Figure 1: Color-plot of measured absorbance evolution as a function of time and depth: a) glass sphere; b) clay soil suspension.

The tested materials were chosen to be representative of an extensive range of suspensions commonly found in upstream environments: sand, badland, clay soils and organic soils (all representative of freshly eroded materials) and reservoir sediment deposits, tropical mining area river sediment and suspended sediments from alpine rivers (all representative of suspended/resuspended sediments). Tests were conducted after thirty minutes mixing within a 100 l grid-stirred cell. Samples were pumped in the diffusive turbulence flow at a specific depth corresponding to a rate of turbulence of about 7 s^{-1}. The settling measurements deduced from absorbances were compared with standard methods of video analysis of floc size and settling, sediment weighting scale, Andreasen pipette, laser particles sizing, and suspended concentration analysis.

Results

Preliminary tests were conducted with spherical non cohesive particles (glass spheres, figure 1a). The measured settling velocities were consistent with the Stokes' law and the measurement done with LISST-ST at low levels of concentration. At volumetric concentration above 2%, we measured a clear reduction of settling velocity with concentration due to hindered effect. The Flocculation index was zero as expected for non cohesive sediment.

For natural sediments a large spectrum of settling velocities (10^{-2} to 10^{-6} $m.s^{-1}$) were observed. The flocculation index ranged from 0 to 1 for quick settling particles (<1 $mm.s^{-1}$; generally sand or large silts) to 20 for the slow settling particles (clays) (Figure 1b).

Samples prepared within the grid-stirred cell led to concentration around 10$g.l^{-1}$ with strongly hindered settling regimes, generally associated with front and relatively fast en- masse settling velocity. Badland material exhibited the strongest front associated with a settling velocity of 0.2 $mm.s^{-1}$. Riverine and reservoir sediments presented more smoothed fronts associated with settling velocities from 0.5 to 3 $mm.s^{-1}$. The organic soil presented a front comparable with riverine sediments, while clay soil did not lead to front formation.

The comparison of the absorbance data with the pipette and weighting scale settling flux allowed us to assess the advantages and inherent bias existing while calculating settling flux from conservation equations applied to optical measurements. Some specific recommendations have to be considered as optical techniques can underestimate the initial settling velocity and lead to erroneous settling flux calculations

Conclusions

The method discussed allowed for the measurement of settling velocity spectrum and propensity to flocculate for high concentrated solutions (>1g.l). It seems is robust and valid for a large range of sediments types and settlings regimes. The proposed flocculation index allows for the comparison of cohesive properties for different materials, and for the assessment of how settling velocities of high concentration river suspensions may be modified as they begin to settle on flood plains or within reservoirs. Of limitation, the absolute values of the index cannot be directly compared with other flocculation indexes as it is sensitive to the calculated parameters.

The large range of settling velocities distributions observed for the natural materials shows that current modeling efforts may miss valuable information when using only one variable to represent settling velocity. This is particularly relevant when investigating cohesive sediment associated contaminant transport issues where slow settling and flocculating particles may have an important role. The proposed measurement method may allow for an improved understanding of settling flux within high sediment concentration rivers.

Coagulation rates of clay minerals

Jin-Feng Zhang[1*], Qing-He Zhang[1], Jerome P.-Y. Maa[2], Guang-Quan Qiao[1]

[1]State Key Laboratory of Hydraulic Engineering Simulation and Safety, Tianjin University, Tianjin 300072, China
[2]Department of Physical Sciences, Virginia Institute of Marine Science, School of Marine Science, College of William and Mary, Gloucester Point, VA 23062, USA
[*]corresponding author

Introduction

Longitudinal variation of the clay mineral composition in the bottom sediment along an estuary is a commonly observed phenomenon (van Leussen 1994). The diagenesis in clay minerals and different flocculation of various clay minerals are two mechanisms to describe the clay distributions. However, Gibbs (1977) showed that different flocculation is not an important mechanism in the Amazon River. Feuillet and Fleischer (1980) also indicated that the factors of differential settling, flocculation and diagenesis had little or no effects on the different bed sediment mineral composition. They considered the physical mixing of river and marine clay may account for the observed changes in deposited clay mineral along the James River Estuary.

When suspended clay particles first encounter sea water, the expelling static charges among clay particles were diminished because of the salt ions in sea water. Thus, clay particles become easier to attach to each other to form flocs. Effects of salinity on the clay mineral aggregation have been investigated in laboratories and in fields. For example, Whitehouse et al. (1960) performed settling tests with clays in quiescent water at several salinities. The settling velocities for montmorillonite, illite, and kaolinite as a function of the chloride concentration indicated that illite and kaolinite were already flocculation with an increase at the chloride concentration of 2 or 3 ppt, whereas montmorillonite flocculated over a wider chloride range. Qiao et al. (2013) studied the flocculation process of cohesive sediment due to differential settling using the numerical model and concluded that illite was the easiest to form flocs, followed by kaolinite, and montmorillonite was the most unlikely to form flocs. However, Edzwald et al. (1974) considered that montmorillonite coagulated faster than kaolinite which coagulated faster than illite in the stirred-tank reactor. Coagulation experiments conducted using three clays and natural sediment samples in blade and Couette reactors by Gibbs (1983), they concluded that kaolinite was the first to be affected by increasing salinity, followed by illite, and then montmorillonite.

Clay particle dynamics in estuarine waters has been studied by Whitehouse et al. (1960) and Edzwald et al. (1974) with different results because the latter considers the shear coagulation. The effect of turbulence is obviously a major factor (Mietta et al. 2009) for clay mineral coagulation. Hunt (1980) designed coagulation experiments at fluid shear rates of 1/2 to 32 s^{-1} in a rotating cylinder apparatus and found the coagulation rate for kaolinite greater than that for illite, which is greater than that for montmorillonite, but the effect of salinity was not considered. The above conflicting conclusions from earlier studies stimulates this study to have a comprehensive study on the rates of coagulation of various clay minerals by direct numerical simulations which has a wide range of shear rate and salinities.

Methodology

A three-dimensional lattice Boltzmann (LB) model for flocculation processes of fine sediment is adopted. The details of LB method for flocculation process of cohesive sediment in homogenous turbulent flows can be found in Zhang et al. (2013). In this study, we will specifically elaborate the interaction forces between sediment particles. We have analyzed the adhesion of two particles using DLVO theory, a model that accounts for the electrostatic repulsion and van der Waals attractive forces (Zhang & Zhang 2011). Since this model does not include the effect of clay mineral (e.g., montmorillonite, illite, and kaolinite) on cohesion, an extension of the DLVO theory (called XDLVO) that accounts for acid-base interactions (Hoek et al. 2006) is added into the model.

We compute the total XDLVO interaction energy per unit area between two spherical surfaces (separated by a distance *h*) by adding the Lifshitz–van der Waals (LW), Lewis acid–base (AB), and the constant potential electrostatic double layer interaction energy (EL) expressions (Hoek et al. 2006). The total XDLVO interaction energy per unit area between two particles is given by

$$\Phi_T = \Phi_{LW} + \Phi_{EL} + \Phi_{AB} \quad (1)$$

The interaction energies for each individual component are given by Qiao et al. (2013). The effects of clay type on the interaction forces between particles are inflected by the Lifshitz–van der Waals force and Lewis acid–base force.

Results

A series of numerical experiments was performed to test the effect of mineralogy, shear rate and salinity in coagulation of cohesive sediment. Three clay minerals (montmorillonite, illite, and kaolinite), with $\varphi = 5\times10^{-5}$ volume concentration, were used at salinities of 0, 2, 5, 10, 20, and 30 ppt. The oscillated grid turbulence is directly numerical modeled by LB method. Flocculation simulations from low to high shear rates (0 to 32 s^{-1} with an interval of 4 s^{-1}) have been performed. The coagulation rates for various clay minerals are analyzed to illustrate the effect of increasing salinities and shear rates on flocculation processes.

Conclusions

A LB model, fully incorporating interforces of clay minerals through XDLVO forces, for the flocculation processes of cohesive sediment was developed. The simulated results are compared to the experimental results in the previous literature (Edzwald et al. 1974; Mietta et al. 2009).

References

[1] Edzwald, J. K., & O'Melia, C. R. (1975). Clay distributions in recent estuarine sediments. Clays and Clay minerals, 23(1): 39-44.

[2] Feuillet, J. P., & Fleischer, P. (1980). Estuarine circulation: controlling factor of clay mineral distribution in James River estuary, Virginia. *Journal of Sedimentary Research*, 50(1): 267-279.

[3] Gibbs, R. J. (1977). Clay mineral segregation in the marine environment. Journal of Sedimentary Research, 47(1): 237-243.

[4] Gibbs, R. J. (1983). Coagulation rates of clay minerals and natural sediments. Journal of Sedimentary Research, 53(4): 1193-1203.

[5] Hoek, E., & Agarwal, G. K. (2006). Extended DLVO interactions between spherical particles and rough surfaces. *Journal of Colloid and Interface Science*, 298(1): 50-58.

[6] Hunt, J. R. (1980). Coagulation in continuous particle size distributions; theory and experimental verification.

[7] Mietta, F., Chassagne, C., & Winterwerp, J. C. (2009). Shear-induced flocculation of a suspension of kaolinite as function of pH and salt concentration. *Journal of colloid and interface science*, 336(1): 134-141.

[8] Qaio, G. Q., Zhang, Q.-H & Zhang, J.-F. (2013). Lattice Boltzmann model of cohesive sediment flocculation simulation based on the XDLVO theory. *Journal of Tianjin University* (*Science and Technology*), 46(3): 232-238 (in Chinese).

[9] van Leussen, W. (1994). Estuarine macroflocs and their role in fine- grained sediment transport. Ph.D. Thesis, University of Utrecht, The Netherlands.

[10] Whitehouse, V. G. , Jeffrey, L. M., & Debrecht, J. O. (1960). Differential settling tendencies of clay minerals in saline waters, *Clays Clay Miner*., 8: 1-79.

[11] Zhang, J.-F., & Zhang, Q.-H. (2011). Lattice Boltzmann simulation of the flocculation process of cohesive sediment due to differential settling. *Continental Shelf Research*, 31: S94-S105.

[12] Zhang, J.-F., Zhang, Q.-H. & Qaio, G. Q. (2013). A lattice Boltzmann model for the non-equilibrium flocculation of cohesive sediments in turbulent flow. *Computers and Mathematics with Applications*. http://dx.doi.org/10.1016/j.camwa.2013.03.023

Fine-grained sediment dispersal along the Doce River inner continental shelf (eastern Brazilian coast)

E. Godinho, V.S. Quaresma

Geological Oceanography Laboratory, Universidade Federal do Espírito Santo, Brazil

Introduction

The study of terrigenous sediments and driven-hydrodynamic processes are crucial to understand sedimentary regimes along river-influenced continental shelves. Riverine fine sediment dispersal patterns is associated to seasonal changes in river discharge and marine hydrodynamic forcings. Herein, we present the results of field measurements taken along the inner shelf adjacent to the Doce River, northern Espirito Santo, eastern Brazilian coast. This contribution presents preliminary results on the dispersal of riverine fine sediments and spatial distribution of salinity and seabed sediments.

The Doce River discharge varies seasonally, with higher and lower discharges in summer (rainy) and winter periods (dry), respectively. The Doce River shelf is exposed to waves, currents and wind action.

Methodology

Field campaign was undertaken along the inner shelf in order to investigate the physical processes responsible for sediment dispersion adjacent to the Doce River mouth. The data presented here was collected during the rainy season (14 to 17 February 2012). Sampling effort involved water column CTD profiling measuring temperature, salinity and turbidity, and surficial sediment sampling at 41 stations (Fig. 1). A RBR 610 CTD a Van Veen grab were used in the field campaign.

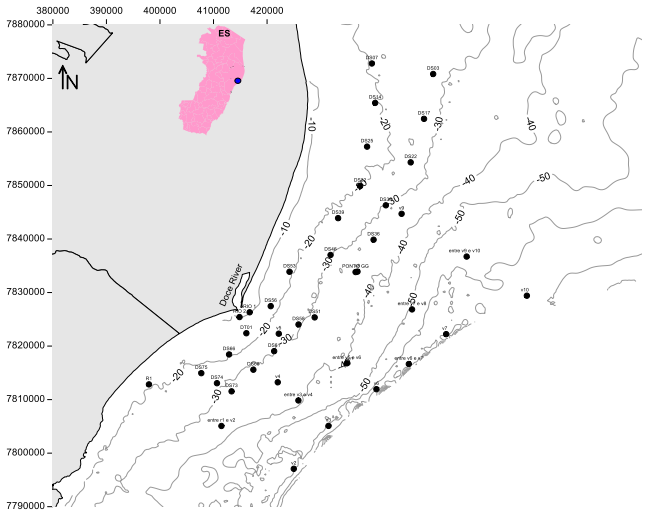

Figure 1 – Map showing the location of the 41 sampling stations. Surficial sediment and CTD data (Temperature, Salinity and Turbidity) were collected.

Results

Results showed that the inner shelf is predominantly muddy, with higher mud contents occurring to the south portion of the river mouth. This trend was followed by turbidity and salinity, showing that dispersion of suspended particulate material from the river plume is directed to the south. These results are in accordance with the findings of Franco (2013). This author recognized, through two sedimentary cores analysis, that fluvial sediments tend to deposit to south of the river mouth.

A superficial lower salinity layer was observed flowing southward, indicating that the dispersion of the river plume. Due to continental shelf position and Coriolis effect, the river plume should be moved to the North, however, that was not observed. During the sampling period, the preferential direction was southward and this is probably related to a consistent Northeast wind-induced stress that occur mainly during summer. The spatial and vertical distribution of salinity and turbidity corroborate with the seabed sediment distribution pattern. A main depocenter southward from the river mouth is driven by seasonal forcing, which are strongly related to high river discharge and summer wind pattern. Sediment accumulation occurs due to fluvial sediment flocculation and depositional processes.

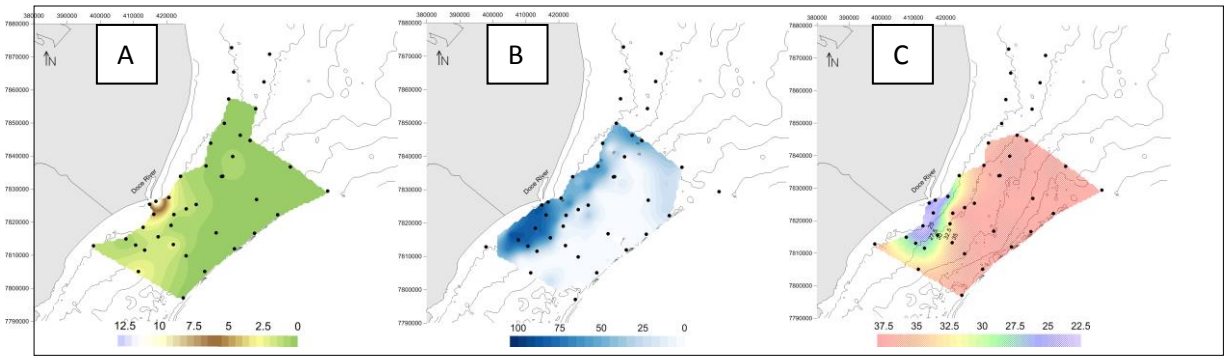

Figure 2 – Spatial distribution of Salinity (A),Turbidity (B) and Mud content (%) (C).

Conclusion

The present study confirms that suspended sediment dispersion, during summer months, is directed to south of the Doce river mouth, where it deposits and accumulates. This is corroborated by salinity, turbidity, and seabed sediment spatial distribution. Low salinity and high turbidity values indicate that the river plume flows to south. The most fine-grained sediment occur at the same place where these salinity and turbidity patterns are observed.

A finite-element numerical model for fluid mud transport

C. L. Hall, R. C. Berger, G. Savant, and W. H. McAnally

Introduction

A finite-element numerical model was developed to predict the transport of fluid mud and interaction with a two-dimensional hydrodynamic model.

Fluid mud is, "a high concentration aqueous suspension of fine-grained sediment in which settling is substantially hindered by the proximity of sediment grains and flocs, but which has not formed an interconnected matrix of bonds strong enough to eliminate the potential for mobility." It is common in estuaries and other coastal zones and may be ubiquitous in waterways, even when not detected by standard sediment measurement techniques. It has been documented in the waterways of Rotterdam, Zeebrugee, Antwerp, Avonmouth, Nantes-St. Nazier, Emden, Savannah, Gulfport, San Francisco, Paramaribo, Bangkok, and Liang Yungang, among others.

Fluid mud is of significance to navigable waterways, since it often requires repeated dredging that produces minor channel improvement, such as the Atchafalaya Bar Channel in Louisiana, and overtaxes placement areas with large volumes of muddy water. It affects water quality and benthic habitat with by burial or by creating anoxic conditions. The issues of engineering significance lead to a need for quantitative numerical modeling of fluid mud formation and transport so that solutions can be rigorously tested.

A numerical model that represents formation, transport, and fate of fluid mud coupled with an existing robust hydrodynamic model can provide a testing platform for design alternatives and their effects on both sedimentation and hydrodynamics**.**

Model Development

The fluid mud model was developed using modified shallow water equations to describe the transport in a viscous fluid mud layer under a water column. Forcing from gravity, shear stress from the overlying water motion, and bottom friction are considered. A finite element formulation was utilized solve the equations of motion. The fluid mud model obtained hydrodynamic forcing information from the existing USACE finite element model, ADH. This model was chosen for its ability to accurately handle hydrodynamic and sediment transport as well as the ability to refine the computational mesh to reduce errors in the solution.

Results

Results from the model were compared to laboratory studies of fluid mud flow on a slope and under shear. These comparisons demonstrated good agreement between model output and lab results. Further application of this model can provide valuable data for sedimentation solution planning for ports and waterways where fluid mud accumulates.

Shelf sediment transport during hurricanes Katrina and Rita

Kehui Xu,[1,2,*] Rangley C. Mickey,[3] Courtney K. Harris,[4] and Robert D. Hetland[5]

[1]Department of Oceanography and Coastal Sciences, Louisiana State University, Baton Rouge, Louisiana, USA.
[2]Coastal Studies Institute, Louisiana State University, Baton Rouge, Louisiana, USA.
[3]College of Science, Coastal Carolina University, Myrtle Beach, South Carolina, USA.
[4]Department of Physical Sciences, Virginia Institute of Marine Science, Gloucester Point, Virginia, USA.
[5]Department of Oceanography, Texas A&M University, College Station, Texas, USA.
[*]Corresponding author: K. Xu, 2165 Energy, Coast and Environment Building, Department of Oceanography and Coastal Sciences, Louisiana State University, Baton Rouge, Louisiana 70803 USA. (kxu@lsu.edu)

Introduction

Within the northern Gulf of Mexico, sediment from the Mississippi and Atchafalaya Rivers is actively building land on the Mississippi Delta, within Atchafalaya Bay, and at the Chenier Plain. The timescales over which, and mechanisms by which sediment travels from these rivers in the coastal ocean are not well understood. Sediment transport flux and direction during extreme storms and floods are poorly defined due to challenges that plague both observing and modeling. This has motivated the development of a three-dimensional hydrodynamic-sediment model for the Texas-Louisiana shelf using the Regional Ocean Modeling System (ROMS) by Xu et al. (2011). This model coupled the hydrodynamic model from Hetland and DiMarco (2008) with the Community Sediment Transport Model (CSTMS) developed by Warner et al. (2008). Results analyzed by Xu et al. (2011) indicated localized fluvial sediment accumulation near the Mississippi Delta as well as southwest of Atchafalaya Bay in the year 1993.

Methodology

After enhancing the model developed by Xu et al. (2011), this study analyzed new modeling results for the year 2005, during which both Hurricanes Katrina and Rita struck the Texas-Louisiana shelf. Unlike the focus of fluvial sediment dispersal by Xu et al. (2011), this study is focused on seabed sediment erosion and deposition during extreme hurricane events. This implementation used improved ocean boundary conditions from Marta-Almeida et al. (2013) based on Hybrid Coordinate Ocean Model (HYCOM). Spatially variable winds from North American Regional Reanalysis (NARR) dataset, updated every three hours, were used to capture spatial and temporal variations of hurricanes over the Texas-Louisiana shelf. Wave Watch 3 (WW3) from the NOAA Environmental Modeling Center provided wave parameters (http://polar.ncep.noaa.gov/waves/download.shtml). A total of six sediment tracers were used in the model: two from the Mississippi River, two from the Atchafalaya River, and two from the seabed. Sensitivity tests of sediment erosion rate and settling velocity were performed, and modeling estimates were compared to radionuclide-based storm-deposit thicknesses (Goni et al., 2007), and sediment accumulation on nearby marsh areas (Tweel and Turner, 2012).

Results

During both hurricanes estimated wave-induced shear stresses dominated wave-current combined shear stresses. Both the highest wave-current combined stresses and the maximum erosional depth on seabed (in the order of 10s cm) were located to the east of two hurricane tracks. Strongest landward winds generally occurred before the hurricanes made landfall, after which winds slowed and veered offshore. During Hurricane Katrina major sediment transport was estimated in the area surrounding the bird-foot Mississippi Delta and the transport was mainly shoreward (See figure on next page). During Hurricane Rita, the estimated maximum erosion occurred on the middle shelf around 20-m isobaths between 93˚W and 90˚W. Seabed sediment type also played a role in sediment transport. Sandy Trinity and Ship Shoals south of Atchafalaya Bay appeared to be more difficult to be eroded during the hurricanes due to their high critical shear stresses and fast settling velocities.

Conclusions

This study showed the episodic nature of sediment transport in the northern Gulf of Mexico and illustrated major hurricanes greatly impact sediment erosion and deposition. In the sensitivity test maximum erosional depth seemed to be more sensitive to erosional rate than settling velocity. Estimated sediment erosion was localized and mainly located along the eastern side of hurricane tracks. During both hurricanes major erosion occurred between the 5-m and 50-m isobaths and net sediment transport flux was landward. Future modeling efforts include the incorporation of seabed consolidation model into this model as well as the application of 1-D hydrodynamics-biological-sediment coupled model (Harris et al., 2013) into 3-D model domain in the northern Gulf of Mexico.

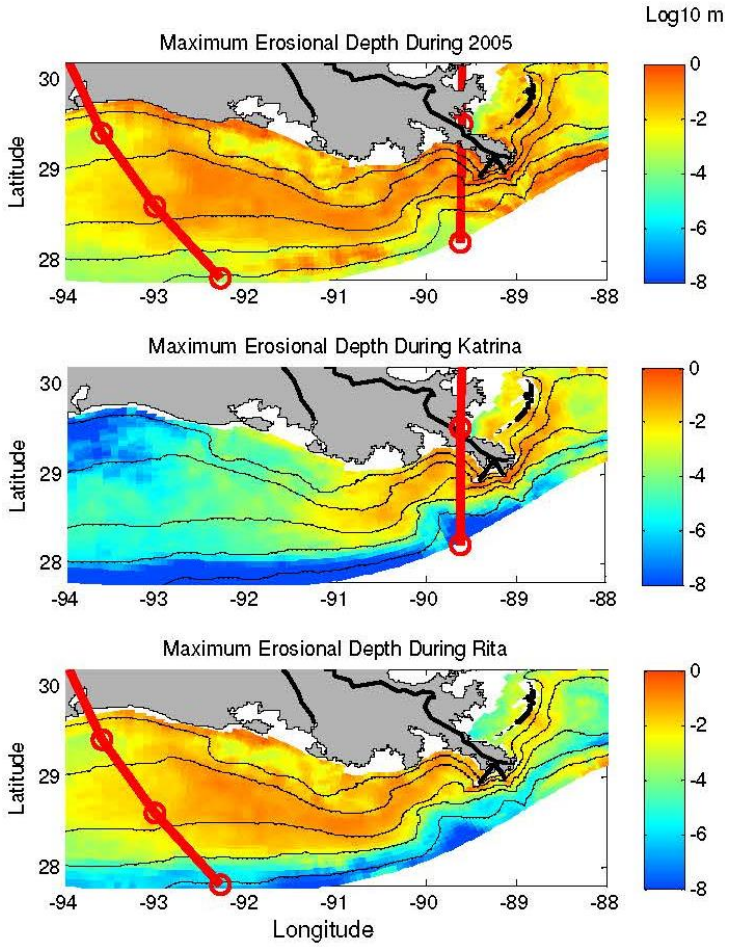

(Top)
Maximum erosional depth (log_{10} m) calculated during the model year 2005;

(Middle)
Maximum erosional depth calculated during Hurricane Katrina (7-day period);

(Bottom)
Maximum erosional depth calculated during Hurricane Rita (7-day period).

Red lines and circles indicate hurricane paths. The above results were based on sensitivity tests using high settling velocity and high erosional rate.

References

Goni, M.A., Alleau, Y., Corbett, R., Walsh, J.P., Mallinson, D., Allison, M.A., Gordon, E., Petsch, S., Dellapenna, T.M. 2007. The effects of Hurricanes Katrina and Rita on the seabed of Louisiana shelf. The Sedimentary Record. Vol. 5. No. 1.

Harris, C.K., Fennel, K., Hetland, R.D. 2013. Effects of resuspension on sediment bed oxygen consumption: a numerical modeling study. American Society of Limnology and Oceanography (ASLO) Aquatic Sciences Meeting, Abstract 11435, New Orleans, LA.

Hetland, R.D., DiMarco, S.F. 2008. How does the character of oxygen demand control the structure of hypoxia on the Texas-Louisiana continental shelf? Journal of Marine Systems 70, 49-62.

Marta-Almeida, M., Hetland, R. D., and Zhang, X. (2013), Evaluation of model nesting performance on the Texas- Louisiana continental shelf, J. Geophys. Res. Oceans, 118, doi:10.1002/jgrc.20163.

Tweel, A.W., Turner, R.E. 2012. Landscape-Scale Analysis of Wetland Sediment Deposition from Four Tropical Cyclone Events. PLoS ONE 7(11): e50528. doi:10.1371/journal.pone.0050528.

Warner, J.C., Sherwood, C.R., Signell, R.P., Harris, C.K., Arango, H.G. 2008. Development of a three-dimensional, regional, coupled wave, current, and sediment-transport model. Computers & Geosciences. 34, 1284-1306.

Xu, K., Harris, C.K., Hetland, R.D., Kaihatu, J.M. 2011. Dispersal of Mississippi and Atchafalaya sediment on the Texas-Louisiana shelf: Model estimates for the year 1993. Continental Shelf Research 31, 1558–1575.

Measuring tide-driven fluid mud transport processes in the Ems estuary

Marius Becker[1], Bryna Flaim[1], Christian Winter[1]

[1]MARUM, Center of Marine Environmental Sciences, Bremen University, Germany.

1. Introduction

The Ems estuary, located between Germany and The Netherlands at the southern North Sea coast, has been regularly deepened and straightened, inducing a change in the hydrodynamic regime. With the net sediment transport being directed upstream, the Ems is now flood-dominated; and significant amounts of sediments are to be dredged each year in order to maintain the nautical depth of the main navigation channel. Suspended sediment concentrations have increased dramatically and exceed the carrying capacity of the flow in large parts of the estuary. Taking into account the abundance of fine-grained cohesive matter, fluid mud layers form at the river bed, which, in turn, influence hydraulic flow properties, such as turbulence and the apparent bed roughness. The process-based understanding of fluid mud dynamics is essential to model and predict mud accumulation and siltation in the Ems estuary, not only regarding the anthropogenic impact, but also in view of the expected changes of environmental boundary conditions, i.e., sea level rise. Significant progress has been made during the past years in terms of the understanding of estuarine systems and the implementation of sediment transport processes in the framework of hydrodynamic numerical models. However, only few studies present detailed measurements of tide-driven fluid mud dynamics, which are required to quantify and parameterize related physical processes in the field.

2. Methods

In November 2010, fluid mud dynamics were measured during four tidal cycles in the Ems estuary at river km 22, operating from the research vessel Senckenberg, which was moored to dolphins aside the navigation channel. The fluid mud body, i.e., the lutocline, was detected by a sediment echo sounder (SES, Innomar). 3 ADCPs (RDI) with different acoustic frequencies were used to determine hydrodynamic parameters and the vertical distribution of suspended sediment concentrations in the upper part of the water column, by backscatter calibration. These continuous profiling measurements were complemented by regular CTD casts, whereas the deployed frame was additionally equipped with an OBS and an ADV.

3. Results and Interpretation

Initial results obtained from SES and ADCP profiles show the continuous entrainment of fluid mud during accelerating flow, and subsequent settling and the reformation of the lutocline during decelerating flow and slack water (Figure 1). Residual suspended sediment transport is strongly flood directed, as highest entrainment rates are found during early flood, where sediments are rapidly mixed and transported to regions of the water column which are characterized by high current velocities. Concerning settling after the flood phase, the lutocline emerges at a height of 1.2 m above the consolidated river bed. During the flood slack water the concentration gradient increases, as indicated by an increase of the acoustic reflector strength, and the thickness of the fluid mud layer below is constant. By contrast, after the ebb phase, a lutocline is detected very close to the river bed. During the ebb slack water the height of the lutocline above the bed increases rapidly, reaching the same height measured during flood slack water. The difference between the end of the flood and ebb phase is thus the location of the maximum concentration gradient, potentially induced by variations of the vertical distribution of turbulence over the vertical.

4. Outlook

The particular differences between ebb and flood regarding entrainment and settling will also be analysed by comparing vertical concentration profiles and the phenomenological description of the lutocline with turbulence parameters obtained from ADV and ADCP.

Acknowledgments

The study is funded through DFG-Research Center/Excellence Cluster, "The Ocean in the Earth System". The Senckenberg Institute and the Federal Waterways Engineering and Research Institute are acknowledged for technical support.

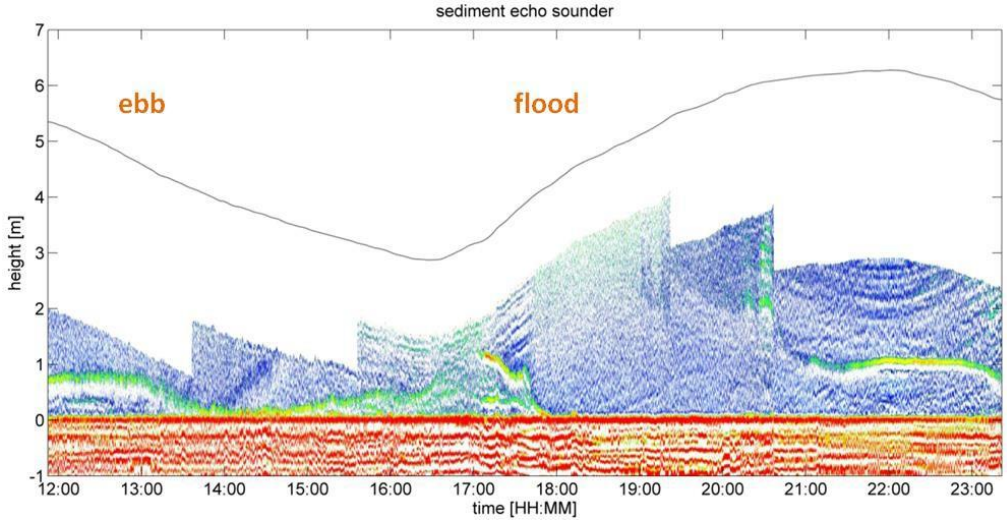

Figure 1: Lutoclines as detected by the sediment echo sounder during one tidal cycle

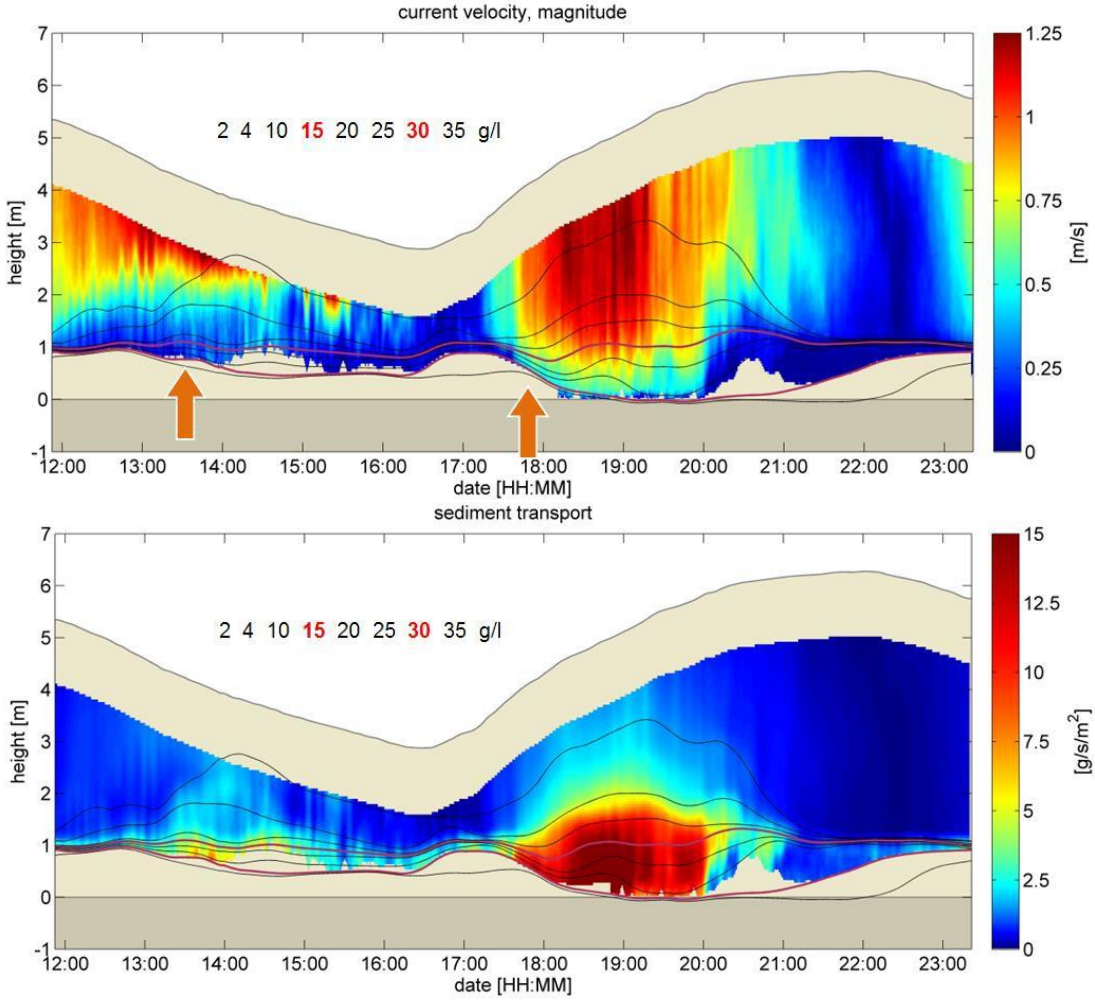

Figure 2: Current velocity magnitude, suspended sediment concentration, and suspended sediment transport during one tidal cycle.

Induced fluid mud flow by ambient current

C. L. Hall and W. H. McAnally (contact author: whmcanally@dsllc.com)

Dynamic Solutions, LLC

Introduction

Laboratory experiments tested the potential for currents flowing over the top of a fluid mud layer to induce flow in the fluid mud.

Fluid mud is, "a high concentration aqueous suspension of fine-grained sediment in which settling is substantially hindered by the proximity of sediment grains and flocs, but which has not formed an interconnected matrix of bonds strong enough to eliminate the potential for mobility." It is common in estuaries and other coastal zones and may be ubiquitous in waterways, even when not detected by standard sediment measurement techniques. It has been documented in the waterways of Rotterdam, Zeebrugee, Antwerp, Avonmouth, Nantes-St. Nazier, Emden, Savannah, Gulfport, San Francisco, Paramaribo, Bangkok, and Liang Yungang, among others.

Fluid mud is of significance to navigable waterways, since it often requires repeated dredging that produces minor channel improvement, such as the Atchafalaya Bar Channel in Louisiana, and overtaxes placement areas with large volumes of muddy water. It affects water quality and benthic habitat with by burial or by creating anoxic conditions. The issues of engineering significance lead to a need for quantitative numerical modeling of fluid mud formation and transport so that solutions can be rigorously tested.

It has been widely observed that fluid mud flows downslope under the effect of gravity. Horizontal flow under the tractive force of the overlying water column has been hypothesized, but not well demonstrated.

Experiments

The experimental apparatus consisted of a 15 m long, 30 cm wide, and 15 cm deep tilting flume with a 15 cm deep depression at the flume midpoint to contain fluid mud, shown in Figure 1. Sodium bentonite suspensions at concentrations ranging from 7 to 35 g/L were placed in the flume depression and the overlying water speed was gradually increased from zero to 3.8 cm/sec during each experiment. Measurements consisted of flow depth and speed, pore pressure and total pressure within the fluid mud layer, and photographic recording of the fluid mud layer.

Figure 5. Tilting flume with depression.

Results

The fluid mud layer began to flow downstream and form interfacial waves at a overlying water flow speed of 0.5 cm/sec. Flow speed of the fluid mud at the interface was about 7% of the mid-depth water flow speed. At higher flow speeds the fluid mud flowed out of the depression and downstream in the flume as a distinct layer beneath the overlying water flow. Non-breaking interfacial waves formed on the fluid mud and propagated downstream as shown in Figure 2.

Figure 6. Interfacial waves at the water-fluid mud interface.

As water velocities increased to 2 cm/sec and greater, the interfacial waves began to break and entrain fluid mud into the overlying flow, confirming earlier experiments.

The experimental results confirmed that water flow over a fluid mud layer can induce flow within the fluid mud and will serve as validation data for a numerical model of fluid mud transport that is underway.

Application of a fluid mud transport model to simulation of sediment dynamics during storm event in Tokyo Bay

Yasuyuki NAKAGAWA[1*], Kazuo NADAOKA[2], Hiroshi YAGI[3], Yasuo NIHEI[4], Akihiro KIMURA[5], Youji KUBOTA[5] and Minoru YOSHIDA[6]

[1] Port and Airport Research Institute, 3-1-1 Nagase, Yokosuka 239-0826, JAPAN
[2] Tokyo Institute of Technology, 2-12-1 Ohokayama, Meguro-ku, Tokyo 152-8550, JAPAN
[3] National Research Institute of Fisheries Engineering, 7620-7 Hasaki, Kamisu 314-0408, JAPAN
[4] Tokyo University of Science, 2641 Yamazaki, Noda, 278-8510, JAPAN
[5] Hydro-soft Technology Institute Co. Ltd., 1-7-4 Minami-Horie, Nishi-ku, Osaka, 550-0015, JAPAN
[6] Port and Airport Technical Survey Yokohama Office, Ministry of Land, Infrastructure, Transport and Tourism, 1-2 Yamauchi, Yokohama 221-0054, JAPAN

Introduction

Very soft mud with high water content over 400 % is prevailing off Haneda in the north west of Tokyo Bay and its behavior is crucial for the environment around the water area. The fine sediment transport processes of such muddy sediments were modeled considering vertical profiles of mud concentration near the bottom surface. Using the Bingham fluid model, analytical solution for horizontal mass flux in the fluid mud layer was derived in the previous study. The present study shows a numerical simulation with application of the fluid mud model to an extreme flood and storm event in Tokyo Bay. External forces such as current and waves were calculated with a 3-D circulation model (POM) and wind wave model (SWAN), respectively, and numerical results were validated through the comparison with field observed data.

Methodology

The horizontal mass flux, $\mathbf{q}_m$, in the fluid mud layer is derived as Eq. (1) (Nakagawa et al. 2012), where Bingham fluid model is applied considering the vertical profile of the mud concentration, C_m, expressed by Eq. (2) (Foda et al., 1993),

$$\mathbf{q}_m(x,y,t) = \int_{-h_y}^{0} C_m(x,y,z,t)\mathbf{u}_m(x,y,z,t)dz = \frac{\mathbf{u_m}}{|\mathbf{u_m}|}\frac{D^2}{\mu}\left[\left(|\boldsymbol{\tau}_b| - \alpha_0\right)\left(\frac{1}{2}C_0 h_y'^2 + \frac{16}{45}\Delta C h_y'^{\frac{9}{4}}\right) - \alpha_0\alpha_1\left(\frac{4}{9}C_0 h_y'^{\frac{9}{4}} + \frac{8}{25}\Delta C h_y'^{\frac{5}{2}}\right)\right] + \frac{\mathbf{u_m}}{|\mathbf{u_m}|}\frac{D^2}{\mu}\left[-\alpha_0\alpha_2\left(\frac{2}{5}C_0 h_y'^{\frac{5}{2}} + \frac{16}{55}\Delta C h_y'^{\frac{11}{4}}\right) - \alpha_0\alpha_3\left(\frac{4}{11}C_0 h_y'^{\frac{11}{4}} + \frac{4}{15}\Delta C h_y'^{3}\right)\right] \quad (1)$$

$$C_m(z) = C_0 + \Delta C\left(-z/D\right)^{0.25} \quad (2)$$

where τ_b is the shear stress on the mud, μ is the dynamic viscosity of the mud and h_y is the yield depth which is determined by the vertical profile of yield strength in the mud layer. The yield strength can be related with the mud concentration (Van Kessel and Kranenburg, 1996). C_0 is the concentration at the top of the fluid mud layer and ΔC represents an increase in the concentration at the arbitrary depth at $-D$ from the surface of the mud layer as shown in **Fig. 1**.

The fluid mud model was applied to numerical simulations of dynamical sediment transport event under an extreme flood and storm condition in Tokyo Bay in Sept. 2007 with the passage of a typhoon, where field monitored data are available for the validation of the model result. Tidal current was calculated for the estimation of bottom shear stress with a 3-D circulation model (POM) considering fresh water discharge through the main rivers and wind stress. Bottom shear stress due to wave was calculated based on the numerical results of wave field simulated by the wave model (SWAN). The distributions of fluid mud flux in space and time were simulated under the combined bottom shear stress due to the current and wave during the storm event.

Results and Conclusion

Spatial distribution of water content in the bay is shown in **Fig. 2(a)**, which is based on the sediment analysis of samples taken before the storm around the site. The model parameters for the mud concentration profiles in Eq. (2) were determined with consideration of the horizontal water content distribution and vertical profiles observed in the core sample. Numerical result of simulated distribution of fluid mud flux is shown in **Fig. 2(c)**, which is derived by the bottom shear stress due to current and wave indicated in **Fig. 2(b)**. The south-west ward transport of mud is prominent in the higher water content mud area off Haneda, coinciding with the near-bottom suspended sediment flux observed at the monitoring station (Nakagawa et al. 2011).

References

Foda, A., Hunt, J. R., and Chou, H-T. (1993). A nonlinear model for the fluidization of marine mud by waves. *Journal of Geophysical Research*, Vol..98, No.C4, 7039-7047.

Nakagawa, Y., R. Ariji, K. Nadaoka, H. Yagi, K. Shimosako and K. Shirai (2011) : Field measurement of erosion and deposition processes of muddy sediment during storm event in Tokyo Bay, Proc. of Coastal Sediments'11, ASCE, pp.2043-2414.

Nakagawa, Y., K. Nadaoka, H. Yagi, R. Ariji, H. Yoneyama and K. Shirai(2012): Field measurement and modeling of near-bed sediment transport processes with fluid mud layer in Tokyo Bay, Ocean Dynamics, , Volume 62, Issue 10-12, pp 1535-1544, DOI 10.1007/ s10236-012-0570-4

Van Kessel, T. and Kranenburg C. (1996). Gravity current of fluid mud on sloping bed. *Journal of Hydraulic Engineering*, Vol.122, No.12, 710-717.

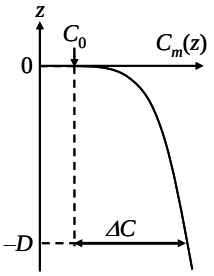

Fig-1 Approximation of sediment concentration profile in fluid mud layer

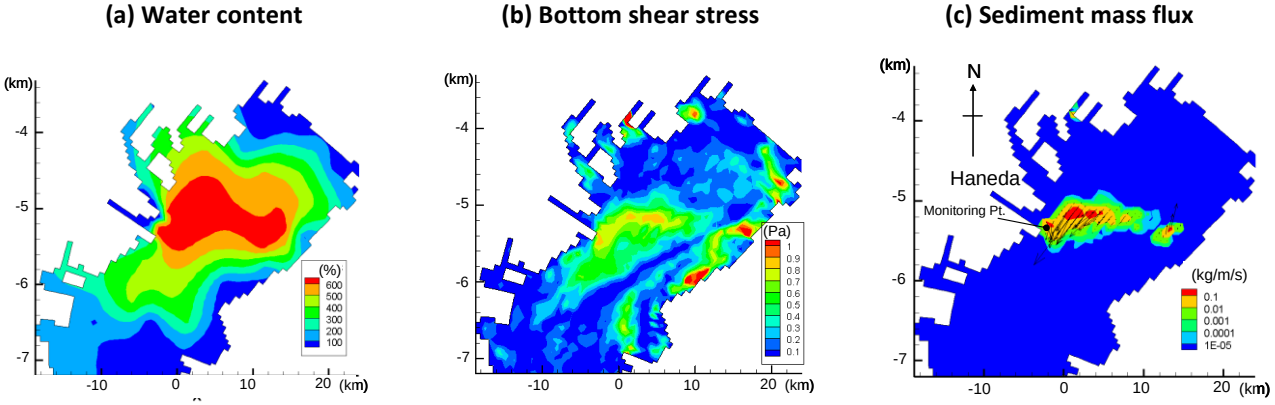

Fig-2 Water content distribution (a) for numerical simulation and computed results of bottom shear stress (b) and fluid mud mass flux (c)

Onsite particle size characterization of fluid mud from Atchafalaya Bay, Louisiana

Xiaoling Tan[1,*], Yoko Furukawa[2], Allen H. Reed[2], and Guoping Zhang[1]

[1]Department of Civil and Environmental Engineering, Louisiana State University, Baton Rouge, LA 70803, USA
[2]Naval Research Laboratory, Stennis Space Center, MS 39529, USA
[*]Corresponding author, xtan3@lsu.edu.

Abstract

Atchafalaya River forms at the confluence of the Red River with the Mississippi at Old River and empties into the Gulf in Atchafalaya Bay, which is building up a new delta in the bay as well as the only naturally gaining ground in Louisiana coastline (Rouse *et al.*, 1978). In order to better understand how the discharge from Atchafalaya River distributes as well as the transport behavior of suspended cohesive sediment, fluid mud samples, predominantly composed of cohesive sediments, organic matter, and interstitial water, were collected on seafloor surface from and beyond the Atchafalaya Bay. The sampling stations (as shown in Fig. 1) are from the area of downdrift sediment recipients from Atchafalaya Bay in Chenier plain (Wells & Kemp, 1981).

Fig. 1. Selected sampling sites in Atchafalaya Bay of the Northern Gulf of Mexico.

For each selected site, the fluid mud sample was collected via a nepheloid layer sampler. Briefly, a funnel was lowered to immediately above the sediment-water interface to capture the mud via its gentle suction. Then, the sample was stored in Nalgene bottles until the particle size distribution (PSD) was characterized by a Cilas particle size analyzer (Tan *et al.*, 2012), which was conducted within several hours after sampling. The onsite characterization aims to minimize the influence of physical disturbance and chemical reactions due to sample storage, handling, and transportation, and hence the PSD and composition analysis may be considered representative of the in-situ conditions. Statistical deconvolution of the PSD curves by a well- developed routine was applied to study the multimodality and composition variations of the sediments. Other basic parameters of the sampling sites, including pH, salinity, depth, bottom current magnitude, total organic carbon (TOC), have also been measured for the sediment property analyses.

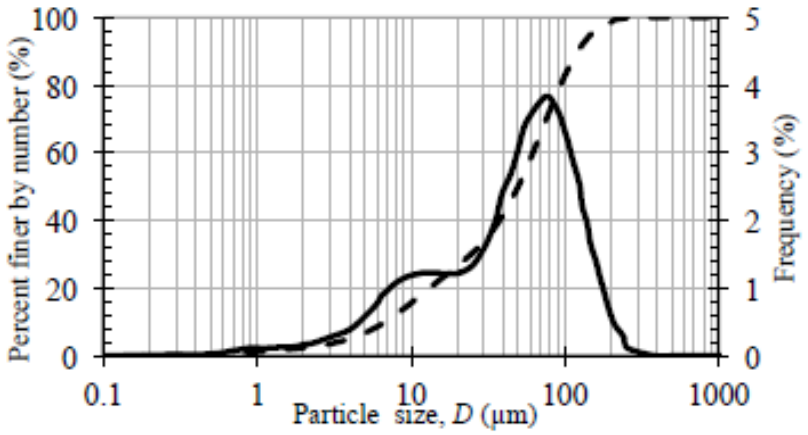

Fig 2. Particle size distribution of fluid mud from a selected sampling site.

Results indicated that particle size of the fluid mud ranges from ~0.1 μm to as large as 1000 μm, and can be divided into four discrete particle groups, primary particles (~0.1 to 2.5 μm), flocculi (10-20 μm), microflocs (50-200 μm), and macroflocs (>200 μm) (Lee *et al.*, 2012), whose compositions generally vary with sampling location. Fig. 2 shows example PSD curves of a collected fluid mud sample. For all the sampling sites, the pH, salinity, TOC, and bottom current magnitude are all different from each other, ranging from 8.2-8.7, 14-32 PSU, 0.5-2.3 wt.%, and 0.18-0.82 m/s, respectively. In general, the particle size and fraction of flocs increases with salinity, which is attributed to the double layer compression induced flocculation. Further multivariant statistical analysis was also conducted to investigate the relationship between the PSD and all the environmental variables.

References

Lee, B. J., Fettweis, M., Toorman, E. & Molz, F. J. (2012) Multimodality of a particle size distribution of cohesive suspended particulate matters in a coastal zone. *Journal of Geophysical Research–Oceans,* **117.**

Rouse, L. J., Roberts, H. H. & Cunningham, R. H. W. (1978) Satellite observation of the subaerial growth of the Atchafalaya Delta, Louisiana. *Geology,***6,** 405–408.

Tan, X., Zhang, G., Yin, H., Reed, A. H. & Furukawa, Y. (2012) Characterization of particle size and settling velocity of cohesive sediments affected by a neutral exopolymer. *International Journal of Sediment Research,* **27,** 473–485.

Wells, J. T. & Kemp, G. P. (1981) Atchafalaya mud stream and recent mud flat progradation--Louisiana Chenier Plain. *Aapg Bulletin---American Association of Petroleum Geologists,* **65,** 1689–1690.

Field testing, laboratory testing and numerical modeling of the effect of spillage on the environment in the Fehmarnbelt

Klavs Bundgaard[1], Ulrik Lumborg[1], and Flemming Møhlenberg[1]

[1]DHI, Agern Allé 5, DK-2970 Hørsholm, Denmark

Introduction

Femern A/S is planning and designing a fixed link across the Fehmarnbelt between Denmark and Germany. Fehmarnbelt is located in the Belt Sea of the western Baltic Sea. Two solutions are considered. A cable stayed bridge and an immersed tunnel. See Figure 1.

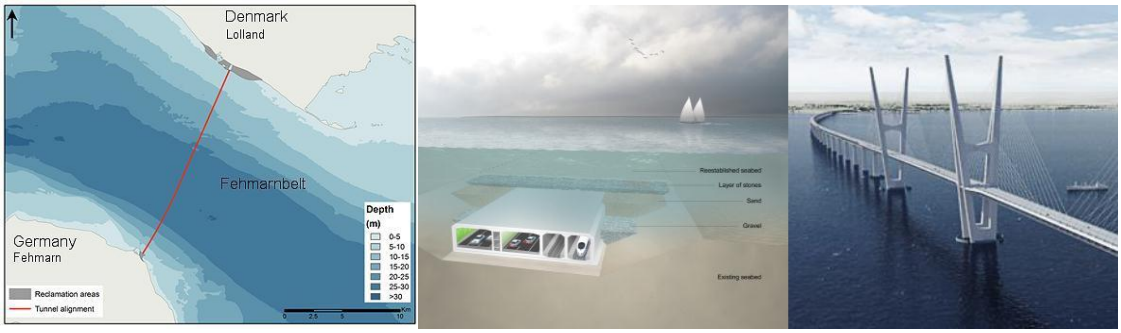

Figure 1. Overview of the proposed fixed link between Denmark and Germany.

One important part of this work is to prepare an Environmental Impact Assessment Statement (in Denmark a VVM; and in Germany a UVS) in order to get approval of the project by the national authorities in the two involved countries. Among other things, the approval documents are based on technical background studies describing the environment of the area which may be impacted by the project (baseline descriptions) and assessing the expectable impacts (impact assessment). One thing being crucial at the site is the shadowing effect of spilled dredged bed material. This abstract describes some of the challenges and solutions met during the numerical model study for the EIA. The description comprises of both the numerical challenges and the challenges in terms of getting sufficient input data for the study as well as the coupling between spilled sediments and marine benthic biology. The seabed in the Fehmarnbelt is variable in terms of sediment types. It consists of clay till, Paleocene clay, late glacial clay, sand, and silt. In total 40% of the seabed consist of sediments with a diameter less than 64 µm. These different sediment types will all be dredged at different times in the project and some of them with different dredging methods. The total dredging volume is 55.8 mill m^3. The first challenge in this project is to gather enough knowledge on the location, amount and behavior of each sediment type to put together a six-year dredging simulation that represents the right timing for the dredging operations as well as the right spill amounts for each soil type and the right settling and light dampening behaviors for each sediment type. The second challenge is to find a way to run the model with sufficient resolution to resolve the plumes over a period of six years.

Methodology

In order to meet the first challenge a test program was setup for the purpose of determining a way to predict sediment settling velocities and floc size distributions in the dredge plume based on laboratory tests on the actual soil. The test series included laboratory testing for physical properties and settling velocities of each sediment type as well as two full scale field tests for plume behavior, time scale and amount of flocculation. Based on these tests relations were established to determine settling velocity distributions for each soil type.

The results were to be used for assessing possible biological impacts. For this there are two key parameters which are sediment coverage and light dampening. The light dampening is dependent on the level of flocculation, i.e. the grain size as well as floc shape, and sediment color. A series of laboratory and field tests were done using various measuring techniques to establish a relation between light dampening and the individual grain sizes. By using the dredging plans from the client a way to model six consecutive years of dredging including dredging, backfilling and reclamation activities was developed. Based on the relations achieved during the field and laboratory tests simulations on the effects of sediment spillage on flora, fauna and birds were done.

Results

Large scale field tests are a logistical challenge that depends on a lot more than just good planning. However, during the field tests and the laboratory tests estimates of flocculation response times, estimated levels of flocculation, estimates of floc densities, and relations between light dampening coefficients and floc sizes were established. Among other findings results showed that flocculation was a relatively slow process that did not reach equilibrium for several hours after dredging (Figure 2). Tests also showed an increase in floc size of up to a factor 15 over a period of 1.5 hours in the dredging plume with a corresponding decrease in the floc density.

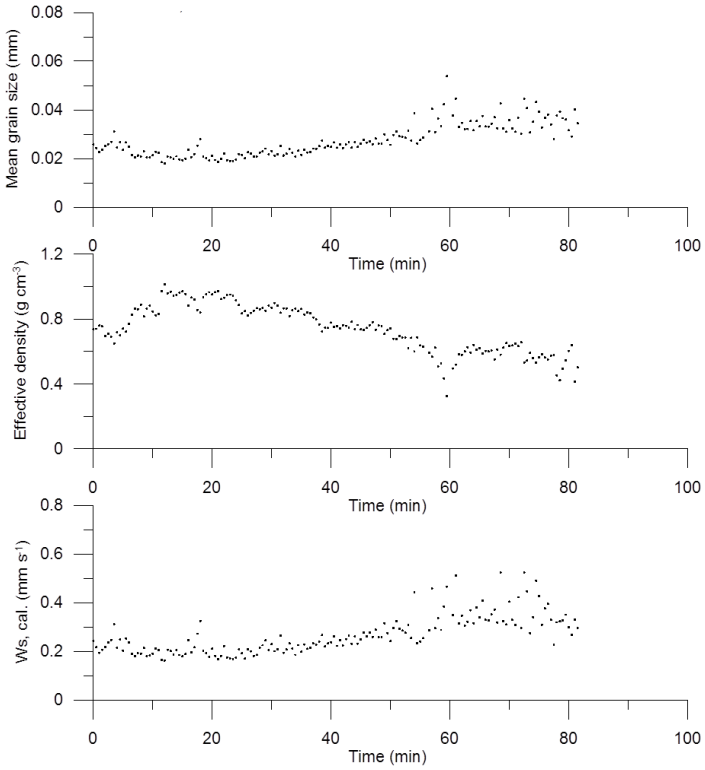

Figure 2. Development of flocculation levels from a LISST-100 floating freely in a sediment plume.

Tests showed that the actual grain (floc) size distribution is extremely important for determining light dampening and that it is the smallest flocs that determine the majority of the light dampening.

The field and laboratory tests formed the basis for an extremely complex 3D numerical model of hydrodynamics, sediment dynamics, and water quality.

Acknowledgment

The authors wish to thank Femern A/S for letting us present data gathered during the project. The authors also acknowledge Dr. Thorbjørn Joest Andersen and the University Of Copenhagen for their help and support during the field tests.

Effect of diatoms on flocculation of suspended bed-sediments in a large shallow lake: Consequences for ecology and sediment transport processes

M. A. de Lucas[1], D. Sarpe [3] and J. C. Winterwerp[1,2]

[1]Environmental Fluid Mechanics, Delft University of Technology, 2628CN, Delft, The Netherlands, m.a.delucaspardo@tudelft.nl
[2]Sediment Transport and Morphology, Deltares, 2629HD, Delft, The Netherlands
[3]Netherlands Institute of Ecology (NIOO) 6700 AB Wageningen, The Netherlands

Introduction

The Markermeer is a large man-made fresh water lake located in the centre of The Netherlands. Together with the northern IJsselmeer is the largest fresh water reservoir of Europe. This area is known as the IJselmeer Region. During the last decades, the lake has experienced a decrease in its ecological values. [*Noordhuis & Houwing, 2003; van Eerden & van Rijn, 2003*]. This ecological decline has been attributed to high turbidity levels and sediment transport processes in the lake [*van Duin, 1992; van Kessel et al, 2008*]. However, turbidity levels over the years cannot be fully explained by occurrence of storms and associated re-suspension events. On the other hand, the species of diatoms present in the lake have changed over the last decades as a result of measures to reduce nutrients in the lake. The current overall chlorophyll concentration varies over the year in a way that is not understood. Therefore we hypothesize that interactions between lake's diatoms and suspended bed-sediments are affecting sediment transport processes and ecology.

Cohesive sediments and algae can form aggregates [*Verspagen et al, 2006*]. In fact, previous research has confirmed the existence of large floc aggregates during diatoms bloom season [*van der Lee, 2000; Mikkelsen 2002*]. Furthermore, seasonal changes in settling velocities of fines have been reported [*Sanford et al, 2001*] and attributed to seasonal variations in diatom concentration [*Mikkelsen, 2002*]. Therefore an effect of diatoms in floc size and structure is suggested. Further to these observations Verney et al [*2009*] presented a detailed study quantifying the influence of diatom blooms on the growth rate of flocs (at an specific turbulence level). The aim of the current study is to investigate the effect of specific species of diatoms on the flocculation of suspended bed-sediments over a range of turbulence levels. In the study equilibrium floc sizes and turbidity of the suspension for each of the studied turbulence levels are determined. Moreover the effect of suspended bed-sediments on the diatoms configuration in the water column is addressed as well. A final goal of the study is to contribute to the overall understanding of sediment transport processes and ecology in the lake.

Flocculation of suspended sediments is studied through a set of laboratory experiments, yielding: small scale flocculation experiments in a jar and large scale flocculation experiments in a settling column. In the small scale experiments, the flocculation behavior of suspended bed-sediments and the induced turbidity is first studied. Later the behavior of two species of algae in the jar test is analyzed. Finally sediments from the bed are mixed with diatoms, and the effects of their co-existence in flocculation processes are studied. In the large scale experiments a mixture of bed sediments and one species of algae is studied. Here the main focus is on the effect of diatoms on the settling velocity of suspended bed-sediments.

Methods

Small scale flocculation experiments are performed in mixing jars. The turbulence field in the jar is induced by a rotating paddle, and is characterized by the turbulence shear rate G. An average value for G in the jar can be approximated with:

$$\log G = 0.849 + 1.5 \log(60nf),$$

where nf is the stirring frequency of the paddle in rotations per second [*KIWA, 1976*]. The small scale experiments consist of studying the equilibrium floc size as a function of G in the jar. For every studied sediment type a sequence of six steps in G is applied. Values of G range from 65 s^{-1} to 8 s^{-1}.
Floc size distribution of suspended sediments is measured with a Malvern Mastersizer 2000. Malvern also measures other parameters like sample obscuration and volume concentration of sediments. Suspended sediments are sampled from the mixing jars and pumped to the Malvern. The pump discharge for sampling is selected to avoid break-up of flocs during sampling and pumping, and so is the interval between measurements and the sampling pipes length.

Large scale flocculation experiments have been performed in the settling column described in Maggi [*2005*] and Mietta [*2010*]. Sediments settle through the 5 m high settling tube, where flocculation is induced by the turbulence field created by an oscillating grid. The magnitude of the turbulence field is a function of the frequency of the grid fg: $G = 83.72 fg$ [s^{-1}] [*Maggi, 2005*]. Suspended sediments are sampled from the lowest section of the settling tube. Sediment concentration is

measured in the lowest section of the settling column as well. The measuring set-up is formed by a rectangular PVC prism, a camera, a ground-glass diffuser, and a light source. Suspended sediment particles are injected into the PVC prism, where they are illuminated from the light source. Illumination is not direct, but through the ground-glass diffuser. The camera acquires the shadow image of the particles. Images are post-processed with a Matlab algorithm, yielding FSD graphs. The analysis of two consecutive images allows determining the settling velocity. Davis7-software by LaVision is used to determine settling velocities. Davis7 calculates settling velocities with a PIV+PTV hybrid approach, where PIV is performed as a first step and the result of the PIV is later used as first estimator for the PTV.

Results and Discussion

Our results from the small scale experiments show that, for suspended bed-sediments, equilibrium floc sizes follow the Kolmogorov micro-scale. However, settling events at the lowest turbulence field are registered in some cases. This is caused by the limited residence time in the jar set-up. Furthermore the obscuration measured with the Malvern decreases for increasing floc sizes. The experiment with the algae diatoms in the jar reveal much lower obscuration levels than for bed sediments, as well as the ability of the diatoms to stay in the water column independently of the magnitude of the turbulence field. When combined, suspended bed-sediments and diatoms produce a higher obscuration than any of the individual sediment fraction independently. This increased obscuration is not equal to the sum of the individual obscurations caused by each sediment fraction. Moreover obscuration increases for increasing floc sizes in some cases, which suggests a floc structure different from the case of suspended bed-sediments. These observations suggest aggregation of bed sediments and diatoms when subjected to a turbulence field. These organic-inorganic aggregates attain different equilibrium floc sizes than its individual components, as quantified with the current study. Furthermore, the co-existence of bed-sediments and diatoms in the water column resulted, in some other cases, in settling of the complete diatoms population from the suspension. The latter does not occur when diatoms are alone in the water column, which was found for all turbulence levels.

The increased turbidity caused by the co-existence of bed sediments and diatoms at the water column may be used to complete the analysis of the historical turbidity levels in the study-site. The turbidity regime is a function of the interaction of suspended bed-sediments with local species of algae. Furthermore it has been shown that algae can settle as a result of its interaction with suspended bed-sediments, which affects the nutrients balance in the lake.

The large scale experiments also revealed an effect of aggregation between diatoms and minerals on the settling velocity of flocs. Characterization of settling velocities with and without diatoms is achieved. Finally several of the images recorded by the measuring set-up confirms the existence of flocs with an elongated shape, different than the standard shape shown by inorganic flocs.

Conclusions

Suspended bed-sediments and algae can flocculate in fresh-water environments. The resulting aggregates differ from the original aggregates in light-absorption and light-diffraction properties, shape, structure, and settling velocities. All these differences have been quantified over the current study. Finally it can be concluded that studying the characteristics of organic-inorganic aggregates as a function of environmental conditions like turbulence level and seasonal variations of algae provides relevant information for a proper understanding of sediment transport processes and ecology.

References

Noordhuis R, Houwing EJ (2003) Afname van de Driehoeksmossel in het Markermeer. RIZA rapport 2003.016.

van Kessel T, de Boer G, Boderie P (2008) Calibration suspended sediment model Markermeer. Deltares report Q 4612.

van Eerden M, van Rijn S (2003) Redistribution of the Cormorant population in the Ijsselmeer area. CRGB 5: 33 - 37.

van Duin E H S (1992) Sediment transport, light and algal growth in the Markermeer—a two dimensional water quality for a shallow lake. Ph.D. thesis, Wageningen University.

Maggi. F. Flocculation dynamics for cohesive sediments. Ph.D. Thesis, TU Delft press, 2005.

Mietta. F. Evolution of the floc size distribution of cohesive sediments. Ph.D. Thesis, TU Delft press, 2010.

KIWA. Bekerglasproef voor coagulatie. 1. mengtijden en g-waarden. 1976.

Verspagen J. M. H., Visser P. M., Huisman J., (2006) Aggregation of clay cuases sedimentation of the buoyant cyanobacteria Microcystis. Aquatic Microbial Ecology.

Van der Lee (200) Temporal variation of floc size and settling velocity in the Dollard estuary. Continental self-research.

Mikkelsen O A (2002). Examples of spatial and temporal variations of some fine-grained suspended particle characteristics in two Danish coastal water bodies. Oceanologiga Acta.

Sanford L. P., Suttles S. E., Halka J. P. (2001) Reconsidering the physics of Chesapeake Bay Estuarine Turbidity Maximum. Estauries. Reconsiderin

Verney R, Lafite R.,Brun-Cottan J.C. (2009) Flocculation Potential of Estuarine Particles: The Importance of Environmental Factors and of the Spatial and Seasonal Variability of Suspended Particulate Matter

River discharge related changes of the Weser ETM

Frank Kösteres[1] and Iris Grabemann[2]

[1]Federal Waterways Engineering and Research Institute, Hamburg, GERMANY Email: frank.koesters@baw.de
[2]Helmholtz-Zentrum Geesthacht, GERMANY Email: iris.grabemann@hzg.de

1. Introduction

In the Weser estuary (Fig. 1), regions of high sedimentation exist in the mixing zone which require dredging to maintain shipping feasibility. These regions are closely linked to the estuarine turbidity maximum (ETM). It is known from previous studies that the position of the ETM varies together with the mixing zone forced by river discharge variations [1] and changes in the temporary sediment sources are expected to occur. In this study an attempt is made to calculate the sediment inventory of the ETM for different river discharge situations based on simulations using a three-dimensional numerical model and based on time series measurements along the estuary.

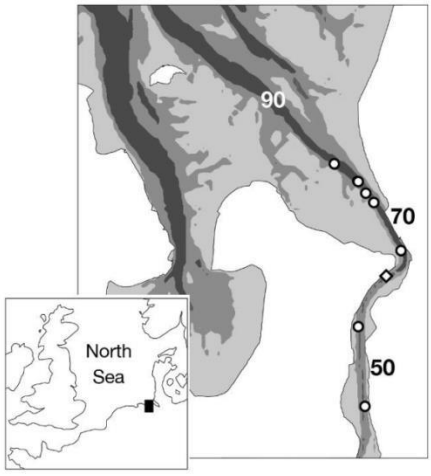

Figure 1: Map of the Weser estuary. The numbers show the distance in along-stream direction, starting from a weir as tidal boundary (km -5). The dots represent the locations of measurements.

2. Methods

The three-dimensional numerical model of the Weser estuary is based on the method UnTRIM [2] using an unstructured grid in the horizontal to provide a good representation of the complex topography. Transport of suspended particulate matter (SPM) is modeled by coupling UnTRIM with the SediMorph model [3] to take into account sediment deposition and resuspension of three different sediment size classes. The model was applied for different river discharge situations and the position of the ETM and its longitudinal extension were determined according to varying river discharge.

Long-term near surface measurements of turbidity and salinity were analyzed at up to 9 stations along the estuary together with a few short-term measurements (a few weeks) in two to three water depths (measurement data obtained from German Waterways and Shipping Administration of the Federal Government). Empirical relationships between river discharge, tidally averaged salinity, turbidity and characteristic intra-tidal SPM patterns [1] were used to estimate the tidally averaged position of the ETM and its longitudinal extension. The results of both methods, modeling and measurements, were used to roughly estimate the temporal ETM inventory for different discharge situations.

3. Results and Discussion

The turbidity measurements used here corroborate previous results [1] with respect to changes of ETM position and its longitudinal extension with varying river discharge (Figure 2a). For low river discharge (120±20 m³/s) the tidally averaged position of the ETM reaches downstream up to approximately km 60. For high river discharge (1000±100 m³/s) an ETM can occur seaward of about km 63. The simulations show similar results for the river discharge situations investigated here concerning the ETM position (compare Figures 2a and 2b). For medium and high river discharge the centre of the ETM is at about the same position along the river axis. For low river discharge situations the model predicts an ETM slightly further downstream. Even though the ETM position and SPM concentration are similar in model and measurements, they differ in details (Figure 2b). The results suggest that the sediment inventory is of comparable size for the river discharge situations chosen.

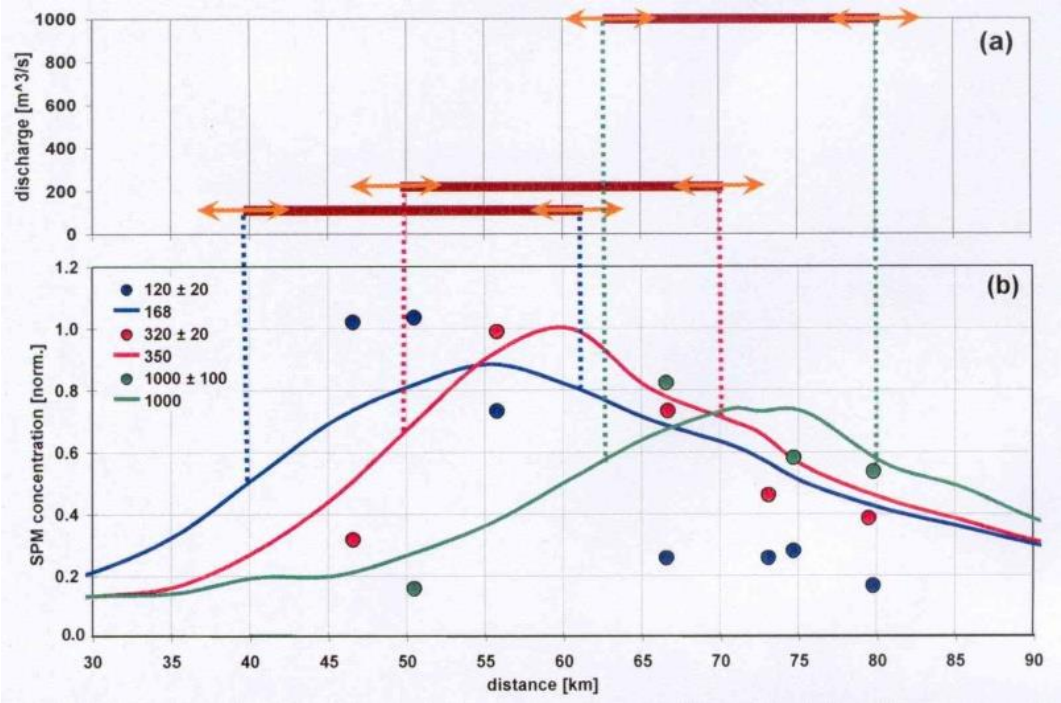

Figure 2: (a) ETM position for different river discharge situations as obtained from turbidity measurements. The horizontal axis denotes the along-stream distance as shown in Figure 1. (b) Tidally averaged, normalized SPM from model results (solid lines) and measurements (dots).

4. Conclusions

Determining the position of the ETM from turbidity measurements as a qualitative measure seems to be reliable but inferring representative values of the SPM concentration is still limited by a number of uncertainties. The numerical model delivers a more complete set of information on the sediment distribution, but is influenced by the model parameters chosen such as the sediment fractions modeled and the choice of sinking velocities. Despite the uncertainties, the similarity between model and measurements yields some confidence in the approaches taken.

5. References

[1] Grabemann, I. and Krause, G. (2001). On different time scales of suspended matter dynamics in the Weser estuary. *Estuaries*, 24(5), 688-698.

[2] Casulli, V. and Zanolli, P. (2002). Semi-Implicit Numerical Modeling of Non-Hydrostatic Free-surface Flows for Environmental Problems. *Mathematical and Computer Modeling*, 36, 1131–1149.

[3] Malcherek, A., Piechotta, F. and Knoch, D. (2005) Mathematical Module SediMorph, Technical report, Federal Waterways and Engineering Institute.

Effects of mud in the sediment budget of the Western Scheldt

Gerard Dam[1], Jelmer Cleveringa[2], Mick van der Wegen[3]

[1]UNESCO-IHE / Svašek Hydraulics, dam@svasek.com
[2]Arcadis, jelmer.cleveringa@arcadis.nl
[3]UNESCO-IHE / Deltares, m.vanderwegen@unesco-ihe.org

The Western Scheldt estuary is located in the south-west of the Netherlands. It is the gateway to the Port of Antwerp. The bed of Western Scheldt consists mainly of sand, although in intertidal areas and parts of secondary channels mud can be found. In the estuary sediment import from the sea followed from several sediment budget studies, as indicated in the left part of Figure 1. In previous studies the import was attributed to the sand fraction alone, because the volumetric contribution of mud to the sediment balance was thought to be negligible. The combined analysis of data on the sediment composition and budget in our study shows that the net sediment transport actually consists of a distinct sand and mud contribution: as the import of mud from the sea is larger than the total sediment import, an export of sand has to take place at the mouth of the estuary. Figure 2 shows the difference in transport patterns of sand and mud. Reinterpretation of historic sediment budget studies suggests that this import of mud and export of sand already occurred from at least 1860 onwards.

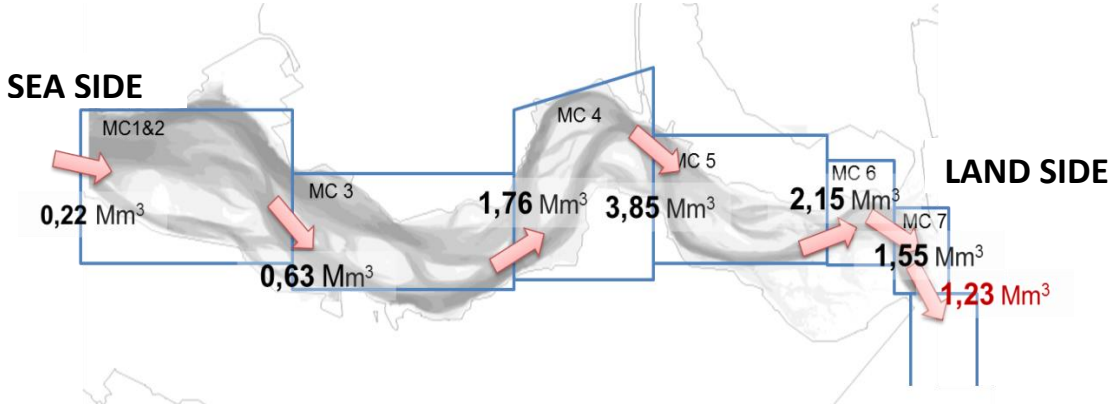

Figure 1: Total sediment balance of the Western Scheldt.

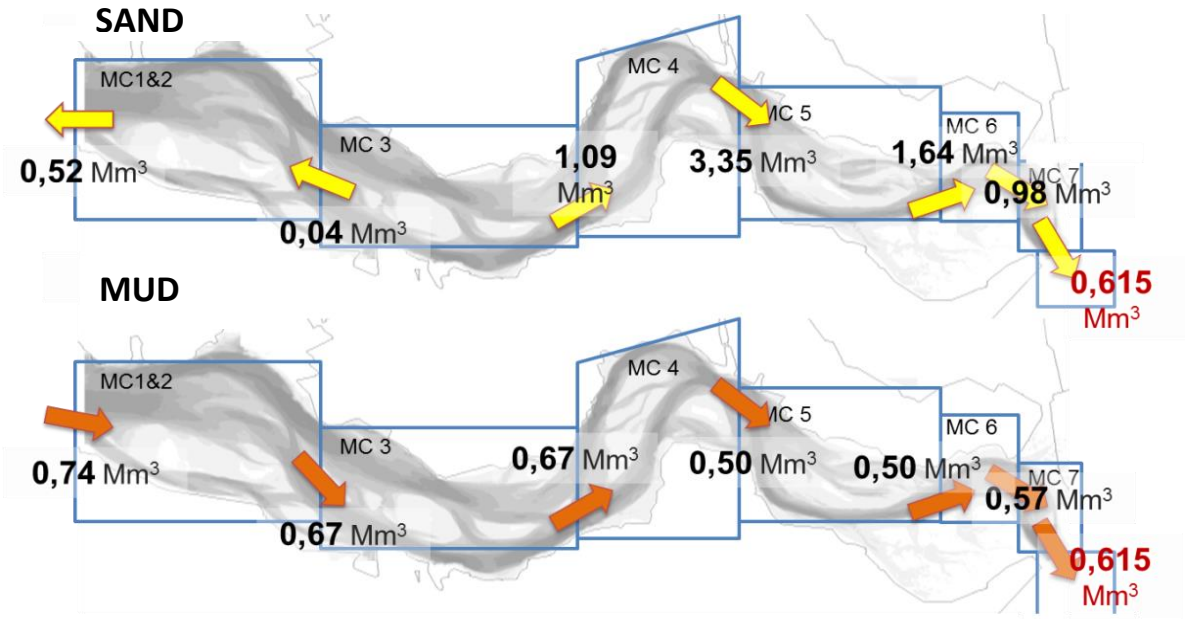

Figure 2: Sand and mud balance of the Western Scheldt.

Assumptions had to be made, for instance with respect to the representative quality of the data on the sediment composition, but a sensitivity analysis shows that the net transport directions of the sand and mud fractions hardly change.

The distinct pattern of import of mud and export of sand is reproduced by a process-based sand-mud model of the estuary. Almost all process-based models using a sand fraction only predicted an export of sand. Previously this was interpreted as an error of the models because it did not match the import that followed from sediment budgets. With the new information on import of mud and export of sand, in retrospect the sand models were reproducing the net direction of the sand export correctly.

The distinct import/export behaviour of sand and mud provides new insights for the management of the estuary. The sediment budget of the estuary is a key indicator for the condition of the estuary. Maintaining a healthy balance between sand and mud may aid to the development of the Scheldt estuary.

Sediment transport characteristics in the Elbe estuary for different morphological states

Holger Weilbeer[1*] and Ariane Paesler[2]

[1]Federal Waterways Engineering and Research Institute (BAW), Wedeler Landstr. 157, 22559 Hamburg, Germany. Email: holger.weilbeer@baw.de
[2]Federal Waterways Engineering and Research Institute (BAW), Wedeler Landstr. 157, 22559 Hamburg, Germany. Email: ariane.paesler@baw.de

Introduction

The Elbe estuary is a very important German waterway. Its mouth is situated in the south-east of the German Bight, with the weir in Geesthacht defining the tidal limit. The entire length from the weir to the mouth, which has a width of approximately 15 km, is more than 160 km. Over the centuries, the Elbe estuary has been modified several times to the changing requirements of maritime traffic. Furthermore a range of measures such as the construction of the weir in Geesthacht, the cut-off of tributaries, the backfill of harbour basins, as well as diking and poldering were carried out during the past 50 years. Today the morphology of the Elbe estuary is characterised by a deep fairway leading to the Port of Hamburg and a complex system of islands, tributaries and branches in the landward section of the estuary as well as extensive tidal flats and tidal creeks in the seaward section.

The anthropogenic measures have given rise to changes in hydrodynamic (tidal asymmetry) and sediment transport processes (tidal pumping), and the fairway has to be maintained by dredging in order to guarantee the safety of the shipping traffic. In this study changes of the hydrodynamics and sediment transport regime in the Elbe estuary are investigated. The development of this estuary in the last decades must be understood e.g. in order to find solutions for recent sediment management problems and to improve the hydrological and ecological system all in all.

Method

Hydrodynamics and sediment transport characteristics are investigated by use of different numerical models. The models were calibrated and validated for different hydrological conditions and for different morphological states (2006 and 2010). In next steps different bathymetries of the Elbe estuary representing the bathymetry to that time (1970, 1997 and 1999) are computed with the same model and the same hydrological conditions. Hydrodynamics and sediment transport of these model runs are analyzed and compared to each other. In that way changes caused by different morphological states can be determined. This method can also be used to evaluate measures which are planned for the future.

First model runs were performed with the classical UnTRIM hydrodynamic and suspended transport model (Casulli&Walters, 2000). In addition an advanced version of the model code (UNTRIM^2) is used. In this version the model bathymetry is defined with sub grid resolution (Casulli, 2008). Sub grid resolution can be much finer compared to the resolution of the computational grid. Bathymetry can be prescribed independent of computational grid resolution. Dry and wet areas can be prescribed in great detail. Thus comparable accuracy with respect to bathymetry can be achieved at much lower CPU cost using sub grid technology, compared to a full discretization of bathymetry with the classical grid approach.

Results

Figure 1 shows as an example of this analysis the net transport of suspended sediment concentrations in the Elbe estuary. A positive value of net transport indicates a net transport upstream. The model runs consider a rather low head water discharge of 350m³/s. A distinct sediment transport in flood direction is predicted, at least upstream to turbidity zone. The transport in upstream direction is more pronounced in recent topographies with a deeper fairway. Owing to these transport characteristics fine sediments accumulate in a long-term development in this part of the Elbe and lead to an increase in the amount of maintenance dredging.

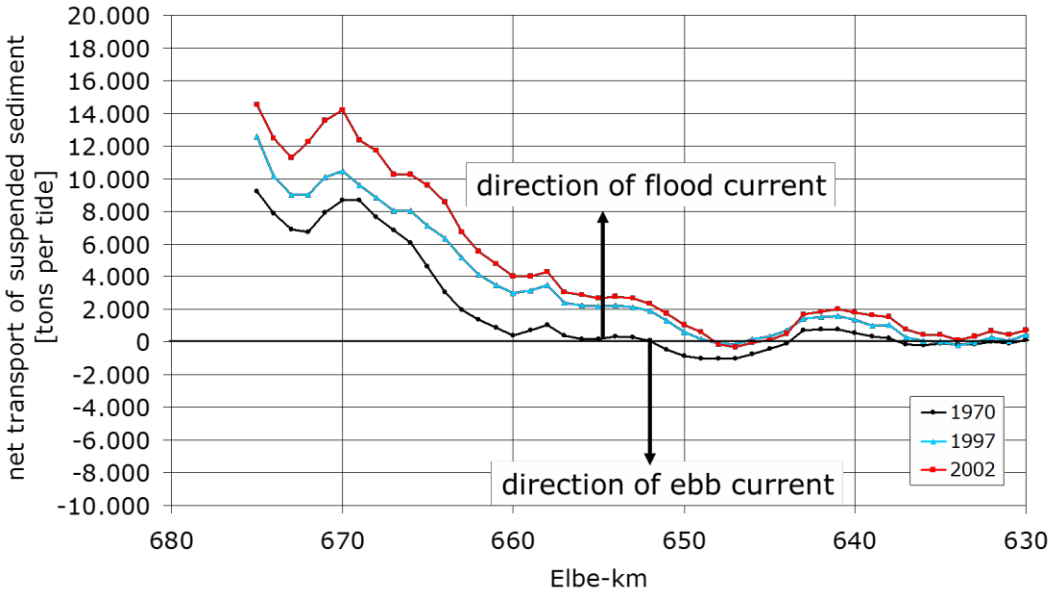

Figure 1: Calculated net transport of suspended load in the Elbe estuary for different morphological states.

References

Casulli, V., Walters, R.A., 2000. An Unstructured Grid, Three-Dimensional Model based on the Shallow Water Equations. *International Journal for Numerical Methods in Fluids*, 32:331-348.

Casulli, V. (2008), *A high-resolution wetting and drying algorithm for free-surface hydrodynamics*, International Journal for Numerical Methods in Fluids, Volume 60, Issue 4, pages 391 - 408.

A 3D numerical investigation of fine sediment transport in the oscillatory bottom boundary layer – turbulence modulation by sediments

X. Yu[1], C. E. Ozdemir[2], Z. Cheng[1], T.-J. Hsu[1] and S. Balachandar[3]

[1]Center for Applied Coastal Research, University of Delaware
[2]Applied Ocean Physics & Eng., Woods Hole Oceanographic Institution
[3]Mechanical & Aerospace Eng., University of Florida

Introduction

To predict hydrodynamic dissipation and fate of fine sediments in the coastal environments, it is critical to quantify the state of muddy seabed. It is well established in the literature that the sediment-induced density stratification plays an important role fine sediment transport. Ozdemir et al. (2010, *J. Fluid Mech.*, 665, 1–45) revealed four different flow regimes of oscillatory bottom boundary layer (OBBL) laden with fine sediments at Stokes Reynolds number 1000: (1) a well-mixed sediment concentration with no modulation of turbulence in very dilute flow, (2) the formation of lutocline in moderate concentration, (3) nearly laminar or (4) complete laminarized bottom boundary layer with high sediment load. Recently, we further investigated the interplay between the sediment-induced density stratification and the enhanced effective viscosity through a simple Newtonian rheological model in determining the collapses of turbulence and the onset of laminarization. It is also well-known that once flow turbulence is annihilated, hindered settling effect becomes very important in the formation of fluid mud. In this study, the hindered settling effect is also investigated along with the higher-order inertial effects, which may be non-negligible when fine sediments transport as flocs.

Method

We consider fine sediment with settling velocity of 0.5~1 mm/s. Typical wave condition of muddy continental shelf is of oscillatory velocity amplitude of no more than 0.6 m/s and wave period of 6~10 sec. The resulting Stokes Reynolds number of OBBL is of no more than 1000. Hence, the wave boundary layer is not fully turbulent and the transitional nature of turbulent flow must be considered. On the other hand, existing computational resource allow us to resolve all the scales of 3D carrier flow turbulence without the need for a turbulence closure. Moreover, we estimate the Stokes number $St=\tau_p/\tau_l$, where τ_p is the particle response time and τ_l is characteristic fluid timescale, to be only 0.03 for un-flocculated silt particles or 0.3 for flocs of fractal dimension of 2.0. Therefore, the Equilibrium approach can be applied, where particle velocity can be calculated algebraically as the sum of the fluid velocity, the settling velocity and an asymptotic expansion in terms of Stokes number (Balachandar & Eaton 2010, *Annu. Rev. Fluid Mech.*, 42, 111–133). As sediments become concentrated, inter-particle interactions can increase the flow viscosity. As a first step, we consider simple Newtonian rheological models, where the fluid viscosity increases with floc volumetric concentration.

We idealized the bottom wave boundary layer by considering the statistically-averaged flow velocity and sediment concentration to be fully-developed in both spanwise and streamwise directions. In the vertical direction, two walls are located at the bottom and the top of the domain. A hybrid high accuracy 3D numerical scheme, which uses Fourier expansions in the fully developed directions and a 6^{th}-order compact finite difference scheme in the vertical direction, is implemented to efficiently resolve all the turbulence scales, and the interaction between the fluid phase and the sediment phase.

Results

Continuing the work of Ozdemir et al. (2010) where the transition between flow regimes is only considered to be due to sediment-induced density stratification, here we present simulation results of two cases to demonstrate turbulence modulation can be also caused by enhanced viscosity. Case 1 is of OBBL

without sediment at Stokes Reynolds number of 1000 (not shown). Case 2 represents a scenario of regime II with the formation of lutocline caused by sediment-induced density stratification only. Case 3 further includes enhanced viscosity via rheological stress. Using λ_{ci} to visualize turbulent coherent structures (Figure 1), it is evident that turbulence is less intense during flow peak (see (a2)) when enhanced viscosity is included. Comparing (a2) to (a1), turbulent coherent structures are more organized and aligned with less small and chaotic motions. However, turbulent vortex structures for both cases are more similar during flow reversal (compare (b1) and (b2)). Further analyses suggest that the averaged streamwise flow velocity for case 2 under flow peak does not have a logarithmic region, suggesting the onset of laminarization due to enhanced viscosity. During the conference, more discussions on turbulence modulation will be presented, including the higher order inertia effect, which is more appropriate for flocs. More importantly, hindered settling effect will be included in the simulations which allow us to further simulate the formation of fluid mud after the onset of laminarization.

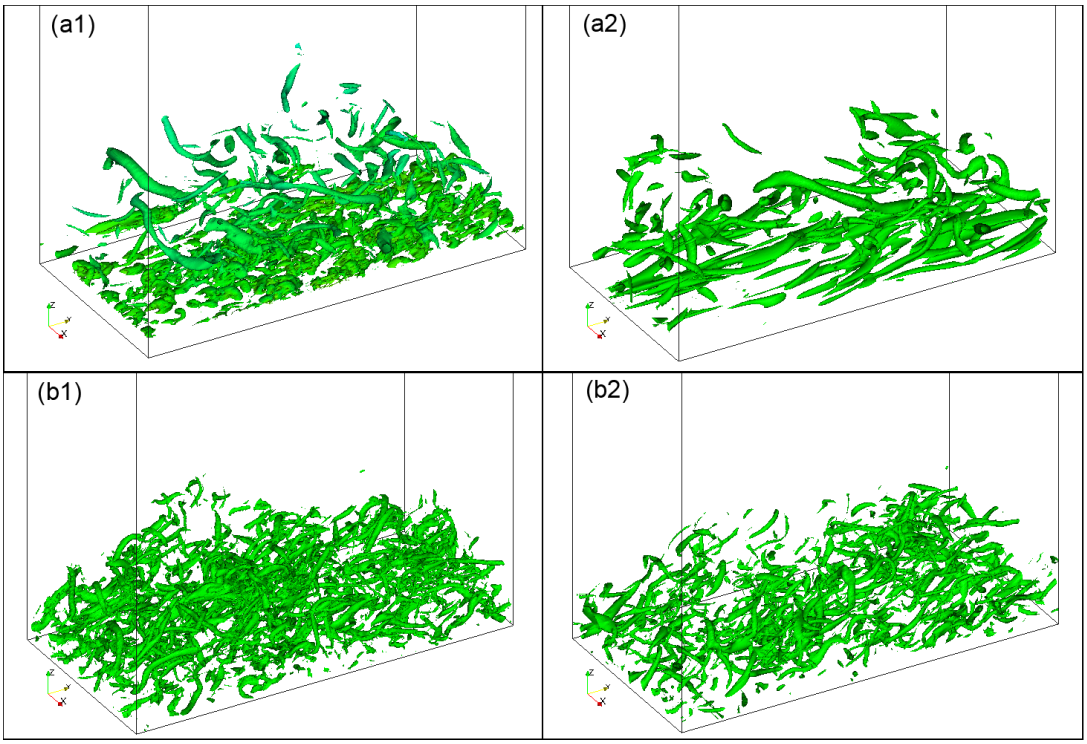

Figure 1: (a1) Turbulent coherent structures under flow peak without considering rheology and (a2) with Einstein's rheology. Turbulent coherent structures are identified by λ_{ci} method. (b1) Turbulent coherent structures under flow reversal without considering rheology and (b2) with Einstein's rheology.

Sediment remobilization by wind, waves, and currents during meteorological frontal passages in a shallow, micro-tidal bay

Joe Carlin, Guan-Hong Lee, Tim Dellapenna, Paul Laverty

Sediment transport in the bays and estuaries of the Northern Gulf of Mexico can be significantly impacted by episodic meteorological events. This study investigated the impact of cold fronts on the seabed of the shallow (~ 2 m), micro-tidal Galveston Bay located along the Texas coast in the northwestern Gulf of Mexico. Two instrument deployments, which included an Acoustic Doppler Velocimeter (ADV), Acoustic Wave and Current meter (AWAC), CTD with Optical Backscatter Sensor (OBS), and sonar altimeter; collected flow and suspended sediment concentration data during two separate cold front passages. Results show that wind stresses increased as a result of the frontal passage, where wind speed had increased following the shift in wind direction from the south/southeast to the north/northwest. This also resulted in a 2-3 fold increase in near-bottom current speeds, and waves in the bay. Sediment resuspension was induced due to enhanced shear velocities near the bed caused by waves generated in the bay. These results show that sediment resuspension requires wind stresses strong enough, and from the proper direction to generate waves. Therefore sediment remobilization does not occur throughout the frontal passage, but rather at discrete times when the proper conditions persist. Maximum sediment resuspension observed occurred after the front had passed through the area. During this period an order of magnitude increase in suspended sediment concentrations were measured. In this micro-tidal bay, with a negligible freshwater discharge, where cold fronts impact the area on average 30-40 times a year, the cumulative effect of these events may represent the dominate mechanism for sediment transport in this bay, and similar bays throughout the region.

Modeling sediment transport processes in Mobile Bay, Alabama, US

Earl J. Hayter, Raymond S. Chapman, Mary E. Anderson, Mary A. Cialone, Phu V. Luong,
S. Jarrell Smith, and Joseph Z. Gailani

U.S. Army Corps of Engineers, Engineer Research and Development Center, 3909 Halls Ferry Road, Vicksburg, MS 39180 USA

Introduction

The Mobile District of the U.S. Army Corps of Engineers (USACE) began thin layer placement (TLP) of dredged material in Mobile Bay (MB) in April, 2012. TLP has not been used within Mobile Bay for decades. This in-bay TLP operation provided the U.S. Army Engineer Research and Development Center (ERDC) a monitoring opportunity to quantify evolution of the TLP deposits. The goal of this monitoring was to provide technical evidence to support thin layer placement as an acceptable practice for dredged material management in MB over the long-term. Best management practices for in-bay placement and to quantify exposure estimates of dredged material to surrounding receptors such as submerged aquatic vegetation can be supported by a mixed sediment transport model for the Bay. This presentation will describe a three-dimensional (3D) hydrodynamic and sediment transport model of Mobile Bay to quantify the resuspension and far-field fate of TLP deposits.

Methodology

The three-dimensional surface water modeling system, LTFATE, which is a 3D curvilinear grid hydrodynamic and sediment transport model, was used to simulate the hydrodynamics, salinity, temperature, and sediment transport in the model domain which stretches from Pensacola Bay, FL to Lake Ponchartrain, LA (see Fig. 1). The model domain is divided into 64 separate grids (or blocks) where each grid is assigned to a separate CPU (Luong and Chapman, 2009). An existing 2D Advanced Circulation Model (ADCIRC) (Luettich et al., 1992) of the Gulf of Mexico was run to generate the seaward hydrodynamic boundary conditions for the LTFATE Multi-block model. Other driving forces used in the LTFATE hydrodynamic model were river inflows, spatially variable winds and atmospheric pressure, radiation stresses calculated by the STWAVE model (Smith et al., 2001), and Coriolis acceleration. Measured velocities and salinities at different locations in Mobile Bay were used to calibrate and validate the hydrodynamic model in LTFATE.

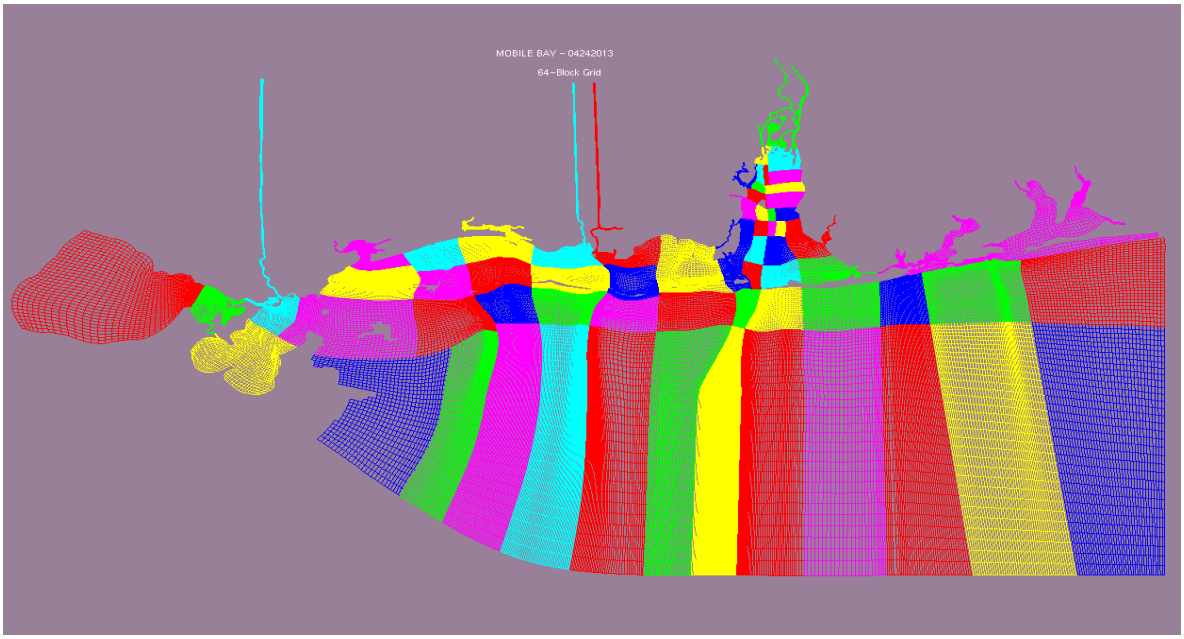

Fig. 1 64-Block LTFATE Model Domain

The sediment transport model included in LTFATE is a modified version of the SEDZLJ mixed sediment transport model developed by Jones and Lick (2001). This model is capable of simulating the transport of both cohesive and noncohesive sediment, and represents the processes of settling, deposition, erosion, bedload transport of noncohesive sediment, bed armoring, consolidation of fine-grain dominated sediment beds, and formation and movement of fluid mud. Sediment data collected and analyzes performed that were used in LTFATE included the following: a) measurements of cohesive sediment settling velocities were made using the Particle Imaging Camera System (PICS) (Smith and Friedrichs, 2011); b) sediment cores collected throughout Mobile Bay were used to perform SEDFLUME tests; c) SEDFLUME tests of consolidating reconstituted sediment cores of the TLP sediment were performed; and d) SSC measurements made over a two-week field study in proximity to the areas where the TLP were performed. The results from the SEDFLUME tests were used to determine the critical shear stresses for resuspension and gross erosion rates of both the native and TLP sediments with depth, while the SSC measurements were used to verify model predictions of SSC under different forcing conditions. Historic navigation channel infilling data were used to calibrate the native bed sediment transport component of the model. For this modeling, LTFATE was run in the morphologic mode, i.e., changes in bed elevations due to net erosion and/or deposition were used in the next time step to update the hydrodynamics.

Results

The LTFATE model was used to simulate sediment transport of native and TLP sediments for four months during average conditions (Feb – May 2010), as well as during the following two storms that impacted Mobile Bay: Hurricane Gustav (August 2008) and Hurricane Ida (November 2009). Three alternative TLP scenarios were modeled for these simulation periods. The long-term fate of the TLP sediments was determined during each of these model simulations for all three alternatives. The results from these simulations will be presented.

References

Jones, C.A. and W. Lick, 2001. SEDZLJ: A Sediment Transport Model. Final report. University of California, Santa Barbara, California. May 29, 2001.

Luettich, R.A., Jr., J.J. Westerink, and N.W. Scheffner. 1992. "ADCIRC: An Advanced Three-Dimensional Circulation Model for Shelves, Coasts, and Estuaries," Technical Report DRP-92-6, U.S. Army Engineer Waterways Experiment Station, Vicksburg, MS.

Luong, P. V., and R.S. Chapman, 2009. "Application of multi-block grid and parallelization techniques in hydrodynamic modeling." DoD High Performance Computing Modernization Program: User Group Conference (HPCMP-UGC), San Diego, CA.

Smith, S.J., and C.T. Friedrichs. 2011. Size and settling velocities of cohesive flocs and suspended sediment aggregates in a trailing suction hopper dredge plume. Continental Shelf Research. 31: S50-S63.

Smith, J. M., A.R. Sherlock, and D.T. Resio, 2001. "STWAVE: Steady-state spectral WAVE model: User's manual for STWAVE Version 3.0," Supplemental Report ERDC/CHL SR-01-1, U.S. Army Engineer Research and Development Center, Vicksburg, MS.

Krone deposition equation and significance of floc aggregation

Ashish J. Mehta[1], Andrew J. Manning[2] and Yogesh P. Khare[1]

[1] College of Engineering, University of Florida, Gainesville, FL 32611, USA
[2] School of Marine Science & Engineering, University of Plymouth, Drake Circus, Plymouth, Devon, PL4 8AA, UK

For modeling the rate of deposition of cohesive flocs in estuaries the Krone equation is extensively used. It was derived from flume experiments on sediment from the San Francisco Bay, and is applicable to low suspended sediment concentration environments in which shear-induced aggregation – the growth and breakup of flocs – has a limited role. It is shown that the use of this equation can lead to substantially erroneous estimates of the mass deposition flux at typical estuarine concentrations.

Krone's own experimental data permit the development of a more general equation accounting for the effects of concentration and turbulent shear rate on aggregation. This is dramatically observed in a deposition test in which a wire mesh was inserted in the flow to change turbulent shear and increase deposition.

We note however, that even with the inclusion of aggregation in the general equation, field-based observations from San Francisco Bay suggest that typical flumes generally do not meet the scaling requirements for field application of laboratory data. Thus, even though the Krone equation should be eschewed in favor of the general equation, interpretations of model-predicted deposition rate must not be accepted without robust field-based verification.